SRR-CWDA-2018-00025
Revision 2

Air Pathway Release Model for the Saltstone Disposal Facility Performance Assessment

February 2019

Prepared by: Savannah River Remediation LLC
Waste Disposal Authority
Aiken, SC 29808

Prepared for U.S. Department of Energy Under Contract No. DE-AC09-09SR22505

APPROVALS

Author:

Barry Lester
WDA Assessments
Savannah River Remediation LLC

2/5/2019
Date

Ben Dean
WDA Determinations
Savannah River Remediation LLC

2/5/2019
Date

Technical Review, per S4-ENG.51:

Steven Hommel
WDA Assessments
Savannah River Remediation LLC

2/5/2019
Date

Management Review:

Kent Rosenberger
WDA Assessments, Manager
Savannah River Remediation LLC

2/5/2019
Date

TABLE OF CONTENTS

LIST OF FIGURES

LIST OF TABLES

ACRONYMS/ABBREVIATIONS

APR	Air Pathway Release
ARP	Actinide Removal Process
DDA	Deliquification, Dissolution, and Adjustment
DLL	Dynamic Link Library
DSS	Decontaminated Salt Solution
GCL	Geosynthetic Clay Liner
HDPE	High Density Polyethylene
LHS	Latin Hypercube Sampling
MCU	Modular Caustic Side Solvent Extraction Unit
MOP	Member of the Public
PA	Performance Assessment
SDF	Saltstone Disposal Facility
SDU	Saltstone Disposal Unit
SWPF	Salt Waste Processing Facility
WDA	Waste Disposal Authority

1.0 INTRODUCTION

Waste Disposal Authority (WDA) has initiated work to support an update to the Saltstone Disposal Facility (SDF) Performance Assessment (PA) (SRR-CWDA-2009-00017). The update to the PA will address changes in construction details, size, and locations of existing and planned-future Saltstone Disposal Units (SDUs) (i.e., concrete vaults used for containing low activity waste). The updated SDF PA shall also incorporate new data developed through ongoing research activities and apply updated disposal inventories based on disposal operations. As part of the PA effort, models shall be developed to evaluate the release of radionuclides from SDUs, and contaminant transport through groundwater pathways and through air pathways. Finally, resulting concentrations from transport models will be used to evaluate the potential risks imposed on members of the public (MOPs).

This report documents the update to the Air Pathway Release Model (referred to herein as the SDFAPR Model) for the update to the SDF PA. The SDFAPR Model was developed using GoldSim simulation software. GoldSim is an object oriented, probabilistic modeling software designed to evaluate parameter sensitivity and the influence of parameter uncertainty. Within the SDFAPR Model, GoldSim simulates the potential for migration of radionuclides released to the atmosphere that are presently (or will be) disposed at the SDF.

Version 1 of this SDFAPR Model, as documented within this report, was developed to evaluate the release of radionuclides from SDUs to the atmosphere. Specifically, it is designed to provide the surface flux which can be used as in input to an atmospheric transport model for evaluating the degree of attenuation associated with air-pathway transport to the site boundary and 100-meter compliance boundary. Peak atmospheric concentrations calculated at the site boundary and 100-meter compliance boundary will be used to evaluate peak doses at the boundaries.

This report discusses the approach taken in the development of the model including the use of the GoldSim software, the organization of the model, and the basic processes simulated. [GTG-2017a] The previous modeling was conducted using PORFLOW. [SRR-CWDA-2009-00017] This document also presents a compilation of the data used in the SDFAPR Model.

1.1 Quality Assurance

Development of this report and supporting analyses are subject to the QA program and requirements as defined in Manual S4, Procedure ENG.51 – *Verification and Checking of Technical Documents*.

2.0 MODEL DEVELOPMENT

This section describes the details of the development of the SDFAPR Model. The model is designed to evaluate the air-phase transport of potentially volatile radionuclides. Conceptually, these radionuclides are dissolved in interstitial water found within the pores of the saltstone waste form. Once dissolved, the radionuclides may be released to the accessible environment (the atmosphere) via diffusion through the saltstone monolith, the sand overlying the SDU roof, and the closure cap barriers.

For the air pathway analysis, several gaseous-phase radionuclides can be evaluated by the SDFAPR Model. The radionuclides evaluated by the SDFAPR Model for gaseous-phase flow include: C-14, Cl-36, H-3, I-129, Rn-222, Se-79, Sb-125, Sb-126, Sn-126, and Tc-99. The 10 radionuclides are the same set as evaluated in the earlier PORFLOW air pathway model. Their selection is discussed in the 2009 SDF PA. [SRR-CWDA-2009-00017] Note that although Sb-125 and Sb-126 are not found in the present inventories included in the model, they are included for consistency with the earlier PORFLOW model. [SRNL-STI-2008-00447 and SRR-CWDA-2009-00017] Because the release of radon from the SDUs will be strongly controlled by ingrowth from parent radionuclides found in the saltstone, seven parent radionuclides are included in the model. These parent radionuclides include Cm-246, Pu-242, Pu-238, U-238, U-234, Th-230, and Ra-226.

All inputs used within this report are based on past SDF modeling and are used for model validation purposes. As such, these inputs are subject to change to better reflect the latest available information. For example, the final inventory values for use in an upcoming revision to the SDF PA have not yet been determined.

The SDFAPR Model was developed using GoldSim (Version 12.0), which is a graphics-based object-oriented computer program designed to carry out dynamic, probabilistic simulations. [GTG-2017a] GoldSim contains contaminant and radionuclide transport modules that can be used to develop software for probabilistic or deterministic simulations of the release of contaminants from engineered barriers, and the fate and transport of contaminants through natural barriers. GoldSim's contaminant and radionuclide transport modules, approximate contaminant or radionuclide transport processes analytically (or semi-analytically) using pipe elements (or networks of pipe elements) or numerically using networks of mixing cells (cell pathway elements). [GTG-2017b]

In probabilistic mode, the model uses a Monte Carlo method, randomly selecting a set of input data from probabilistic distributions of various parameters describing the system being modeled. [GTG-2017a] GoldSim also allows the user to select an alternative approach, Latin Hypercube Sampling (LHS), in which the parameter-specific probabilistic distributions are each divided into bins of equal probability and the median in each bin (or a randomly sampled value from within each bin) is selected for each realization (sampling). [GTG-2017a] For each realization of a Monte Carlo or LHS data sampling, the SDFAPR Model is designed to calculate doses along a 100-meter boundary surrounding the disposal units at the SDF and at the site boundary. The doses can be calculated from radionuclide concentrations generated by the model.

The conceptual model used in the SDFAPR Model is consistent with that used to develop the Air and Radon Pathway Model for the 2009 SDF PA (SRR-CWDA-2009-00017), as described in *Air and Radon Pathway Modeling for the Saltstone Disposal Facility* (SRNL-STI-2008-00447), with some improvements. Specifically, several options are now included to allow for a more rigorous evaluation of diffusive air-phase transport described below.

The implementation of the model also differs from that used in the 2009 SDF PA. Previously, the Air and Radon Pathway Model for the 2009 SDF PA was developed using PORFLOW software, using a finite element structure. For this new SDFAPR Model, the implementation within GoldSim incorporates strings of GoldSim cell-pathway elements (mixing cells), linked in series.

2.1 Conceptual Model for the SDFAPR

The SDFAPR Model simulated the four SDU-types found in the SDF:

- SDU 1, a 100-foot by 600-foot rectangular vault,
- SDU 4, a 200-foot by 600-foot rectangular vault,
- 150-foot diameter cylindrical vaults (representing SDUs 2A, 2B, 3A, 3B, 5A, and 5B), and
- 375-foot diameter cylindrical vaults (representing SDUs 6, 7, 8, 9, 10, 11, and 12).

Figure 2.1-1 shows the present locations of constructed and under-construction SDUs, as well as the assumed locations for future SDUs (SDUs 8 through 12) within the layout of the SDF. Note that these locations are subject to change.

For the release and transport calculations, the model utilizes a submodel contained within a set of nested looping containers. This allows the model to run through the complete set of 15 SDUs in looping mode, using the appropriate string of cell-pathway elements for each SDU based on the SDU-types. The model can also simulate a subset of SDUs or individual SDUs in a simulation.

Saltstone is made from a dry mix of blast furnace slag, fly ash, and cement. However, variations in the saltstone properties may occur due to differences in the processing of the waste component: the decontaminated salt solution (DSS). As such, there are three types of saltstone considered within this model, each identified by the applicable processing approach:

1) Deliquification, Dissolution, and Adjustment (DDA),
2) Actinide Removal Process/Modular Caustic Side Solvent Extraction Unit (ARP/MCU), and
3) Salt Waste Processing Facility (SWPF).

Once the DSS is mixed with the dry feeds, it forms into a pumpable grout. This grout is pumped into the SDUs where it cures into the saltstone waste form. Upon completion of disposal operations for each SDU, it is expected that any remaining void spaces within the SDUs will be filled with a "clean cap grout." Like saltstone, the clean cap grout material will also be made with blast furnace slag, fly ash, and cement, however, it will use uncontaminated water in lieu of the DSS. [SRR-CWDA-2009-00017]

Figure 2.1-1: Saltstone Disposal Facility Layout

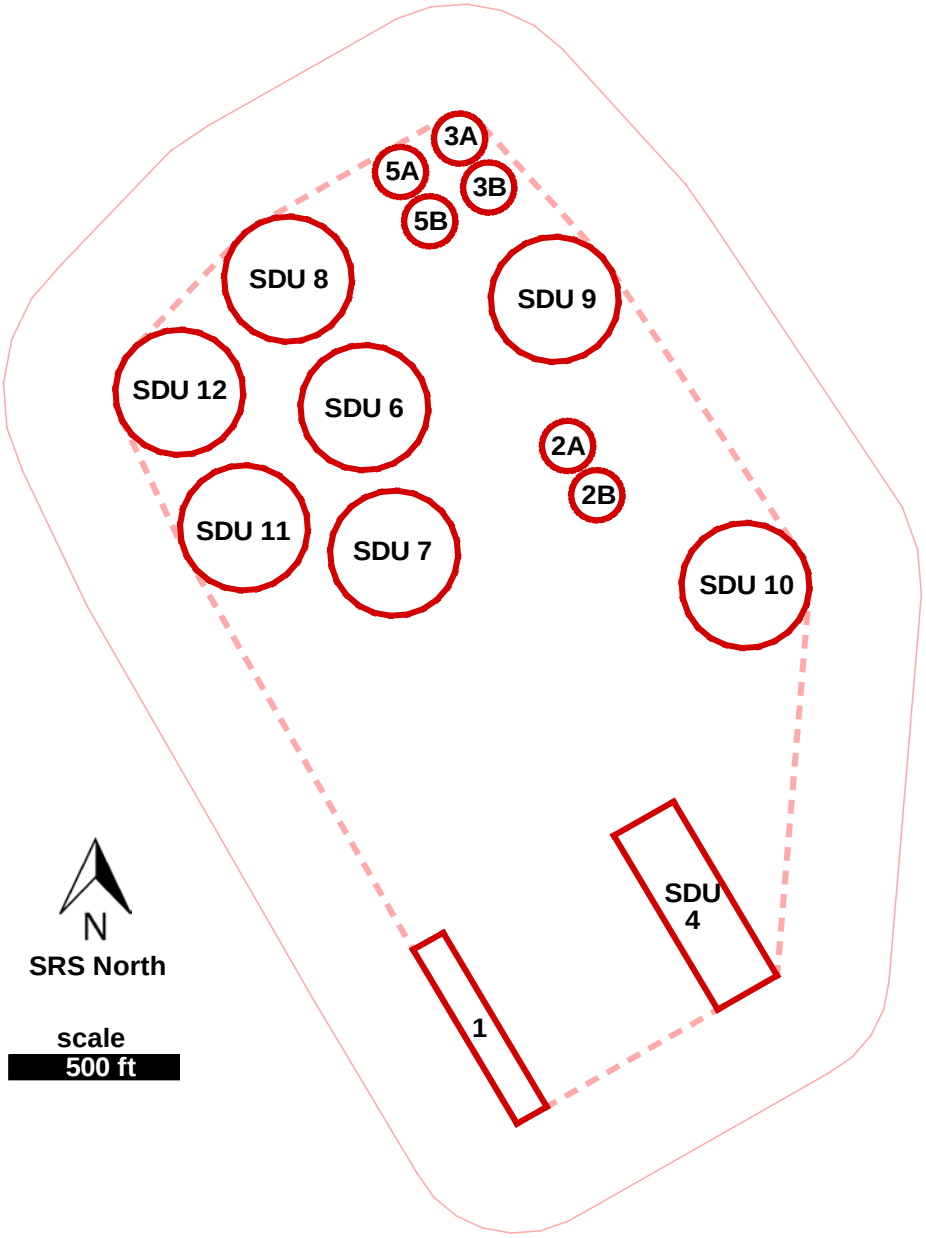

Note: Modified from G-AES-S-00004

Once all SDUs have been filled, soil will be used to backfill around the SDUs and a closure cap will be installed. The multi-layered, engineered closure cap (and the material properties for each layer) is described in the *Saltstone Disposal Facility Closure Cap Concept and Infiltration Estimates* (WSRC-STI-2008-00244). While the erosion barrier layer of the closure cap will be covered by 30 inches of additional backfill, 6 inches of top soil, and a vegetative cover (Figure 2.1-2), the SDF APR Model conservatively assumes that the erosion barrier layer will be the top-most layer (i.e., the overlying layers are not credited).

Figure 2.1-2: SDF Conceptual Closure Cap Layers

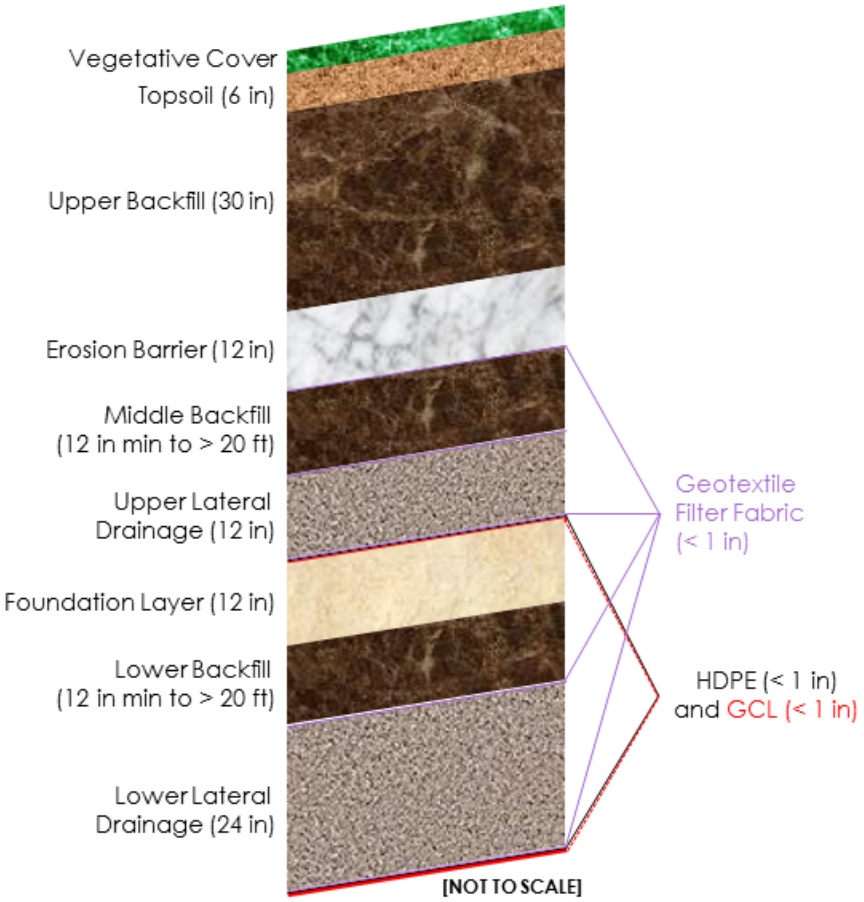

The GoldSim-based SDFAPR Model, comprised of the saltstone monolith, the SDU roof, and the closure cap, applies conservative assumptions to evaluate an upper-bound to the release of volatile radionuclides transported through the air phase and released to the atmosphere. The GoldSim model replaces a PORFLOW model which provided the same functionality for the 2009 SDF PA (SRR-CWDA-2009-00017, SRNL-STI-2008-00447). The flux of radioactive gases through the SDUs and closure cap to the land surface was evaluated for the closure configuration presented in SRNL-STI-2008-00447 (see also the *Saltstone Disposal Facility Closure Cap Concept and Infiltration Estimates*, WSRC-STI-2008-00244).

Based on conservative assumptions, volatile radionuclides within saltstone monoliths can be simulated as diffusing upwards into the air-filled pore space of the overlying materials, similar to simulations from the 2009 SDF PA PORFLOW model (SRR-CWDA-2009-00017, SRNL-STI-2008-00447). Within GoldSim, the SDFAPR Model applies a more rigorous approach for handling diffusive transport in the air phase. GoldSim allows for radionuclide partitioning into solid phases within the SDFAPR Model. The model can also consider partitioning of the radionuclides between an immobile water phase and mobile air phase in the partially saturated material above saltstone. In addition, the mass releases can be evaluated over a one-meter squared area to approximate a point source or over the full top-surface area of the SDU to represent the true area of release (vertical release only).

Radionuclides released at the land surface would be subject to fluctuations in atmospheric pressure which could influence their release. As with the PORFLOW model used for the 2009 SDF PA, the GoldSim-based SDFAPR Model assumes that fluctuations in atmospheric pressure at the land surface that could induce small pulses of air movement into and out of the shallow soil profile (over relatively short periods of time) will have a zero-net effect when averaged over longer time periods (SRNL-STI-2008-00447). Thus, advective transport of radionuclides in air-filled soil pores is not considered to be a significant process when compared to air-phase diffusion.

The components of the closure cap from land surface downwards include a top soil layer, an upper backfill layer, an erosion barrier layer, a geotextile fabric, a middle backfill layer, a geotextile fabric, an upper lateral drainage layer, a geotextile fabric, a high-density polyethylene (HDPE) geomembrane, a geosynthetic clay liner (GCL), a foundation layer (backfill with bentonite admix), a lower backfill layer, a geotextile filter fabric, and a lower drainage layer (WSRC-STI-2008-00244). As a conservative assumption, the geotextile fabrics, the HDPE geomembrane, and the GCL are excluded from this analysis. Including the HDPE geomembrane and the GCL would be expected to significantly reduce gaseous flux at the land surface. The HDPE geomembrane would have very low gaseous diffusion coefficients and the GCL would have very little air-filled porosity, since it would be at or near saturation (SRNL-STI-2008-00447). The top soil layer and the upper backfill layer are also excluded from the analysis, since they are located above the erosion barrier and their influence could be negated by erosion. For the purposes of this analysis, it is assumed that SDU and closure-cap structural components situated below the top of the erosion barrier remain intact for the duration of the simulation.

2.1.1 Summary of Key Air and Radon Pathways Assumptions

The following are the key air and radon pathways analysis assumptions associated with each disposal unit simulation (SRR-CWDA-2009-00017):

- The waste in SDU 1 can be represented by either DDA or ARP/MCU saltstone,
- The waste in SDU 4 can be represented by either DDA or ARP/MCU saltstone,
- The waste in the 150-foot diameter and 375-foot diameter SDUs disposal units can be represented by SWPF saltstone,
- The clean cap grout (i.e., uncontaminated grout used to fill void spaces above the saltstone) within each disposal unit has the same material properties as saltstone,
- Exclusion of the top soil, upper backfill, HDPE geomembrane, and GCL layers of the closure cap make the model more conservative,
- Exclusion of all geotextile fabrics has no impact on the model, and
- The final closure cap is assumed to remain physically stable below the top of the erosion barrier for the duration of the simulation.

2.1.2 Measures Implemented to Ensure Conservative Results

In this analysis, several conservatisms imposed in support of the 2009 SDF PA (SRR-CWDA-2009-00017, SRNL-STI-2008-00447) continue to be imposed to maintain defensibility. These include:

- The use of boundary conditions that force the volatile radionuclides to move upward from the waste disposal zone to the land surface. This precludes the gaseous radionuclides diffusing sideways and downward in the air-filled pores surrounding the saltstone monolith; effectively increasing the flux released into the atmosphere at the land-surface.
- Not taking credit for the removal of radionuclides by pore water moving vertically downward through the model domain. This mechanism would likely remove some dissolved radionuclides, and therefore its omission has the effect of increasing the estimate of instantaneous radionuclide flux at the land surface.
- Exclusion of the HDPE geomembrane and the GCL. Inclusion of these materials in the model would significantly reduce the gaseous flux at the land surface due to their material properties (i.e., low air-filled porosity and/or low effective gaseous diffusion coefficient).
- Exclusion of the cover materials above the erosion barrier (i.e., top soil and upper backfill layers). Excluding these materials shortens the diffusion pathways and could increase the flux at the land surface.
- Use of the minimum closure cap thicknesses in the model.

2.2 Mathematical Model for the SDFAPR

The governing equations for and basic structure of the air-phase diffusive transport within the GoldSim software system are described in this section.

2.2.1 The Implementation of the GoldSim Model

In the GoldSim-based SDFAPR Model, the SDUs and overlaying closure caps are represented by sets of cell pathway elements (mixing cells) combined in series, using diffusive mass flux links to define the diffusive transport of radionuclides from the saltstone monolith upwards through the clean grout, the concrete roof, and the closure cap comprised of the lower lateral drainage layer, the lower backfill layer, the foundation, the upper lateral drainage layer, the middle backfill layer, and the erosion barrier. At the top of the erosion barrier, the radionuclides are released into the atmosphere.

As noted in Section 2.1.2, a number of closure cap layers are not included within the model to maintain conservatism (i.e., the following layers are not credited: topsoil, upper backfill, geotextile fabric, HDPE geomembrane, and GCL). In addition, because of the orders of magnitude difference between water diffusivities and air diffusivities, the air phase represents the only mobile zone in the model. The water and solid phases do provide a storage capacity for dissolved and/or sorbed species, but the storage capacity provided by the liquid and solid phases can be disregarded above the saltstone as an ultra-conservative assumption. Note that the model does allow for simulating the storage capacity provided by the liquid and solid phases above the saltstone if the user choses to consider it.

The basic mass balance equation for each Cell pathway *i*, can be written as follows:

$$m'_{is} = -m_{is}\lambda_s + \sum_{p=1}^{NP_s} m_{ip}\lambda_p f_p R_{sp}\left(\frac{A_s}{A_p}\right) + \sum_{c=1}^{NF_i} f_{cs} + S_{is} \qquad \text{(Eq. 2-1)}$$

where:

m'_{is} = rate of increase of mass of species s in Cell i [M/T];
m_{is} = mass of species s in Cell i [M];
λ_s = decay rate for species s [T^{-1}];
NP_s = number of direct parents for species s;
f_{ps} = fraction of parent p which decays into species s;
R_{sp} = stoichiometric ratio of moles of species s produced per mole of species p decayed;
A_s = molecular (or atomic) weight of species s [M/mol];
A_p = molecular (or atomic) weight of species p [M/mol];
NF_i = number of mass flux links from/to Cell i;
f_{cs} = influx rate of species s (into Cell i) through mass flux link c [M/T];
S_{is} = rate of direct input of species s to Cell i from "external" sources [M/T]; and
p = species index (s) for parent species.

The models initial condition (in this case S_{is}) is set by distributing the total inventory for each SDU using one of two options. The first option is to distribute the total inventory within each saltstone cell based on cell volume generating equal initial concentrations. The second option distributes the inventory among both the saltstone and clean grout cells allowing the user to evaluate the influence of the use of clean grout, which is expected to be considerable for air phase transport.

The initial distribution between solid, water (the reference fluid), and air in each cell is based on the assigned distribution coefficients (K_ds) for the solid/liquid phase partitioning and non-dimensional Henry's Law constants, c_{air}/c_{water} for the air/liquid phase partitioning, where c_{air} [M/L^3] is the air phase concentration and c_{water} [M/L^3] is the water phase concentration. The boundary condition at the bottom of the saltstone monolith is a no-flux boundary condition and the boundary condition at the top of the erosion barrier (representing the atmosphere) is a zero-concentration boundary condition. The use of a zero-concentration boundary condition is both conservative and will have little influence on results due to the rapid attenuation of gases in the atmosphere. The lateral boundary conditions are no-flux boundary conditions for each cell.

The transport of air phase (mobile zone) constituents in the model is controlled by the GoldSim Cell pathway diffusive mass flux links used to connect Cell pathway elements in series (GTG-2017b). An example of the linkage is depicted in Figure 2.2-1, showing the contents of the container where the calculation variables related to air-phase transport in the saltstone monolith of the 150-foot diameter SDUs are assembled. Blue arrows indicate diffusive-flux linkages between mixing cells.

Figure 2.2-1: Example of GoldSim Cell Pathway Elements Linked in Series to Simulate Air-Phase Transport Through Saltstone

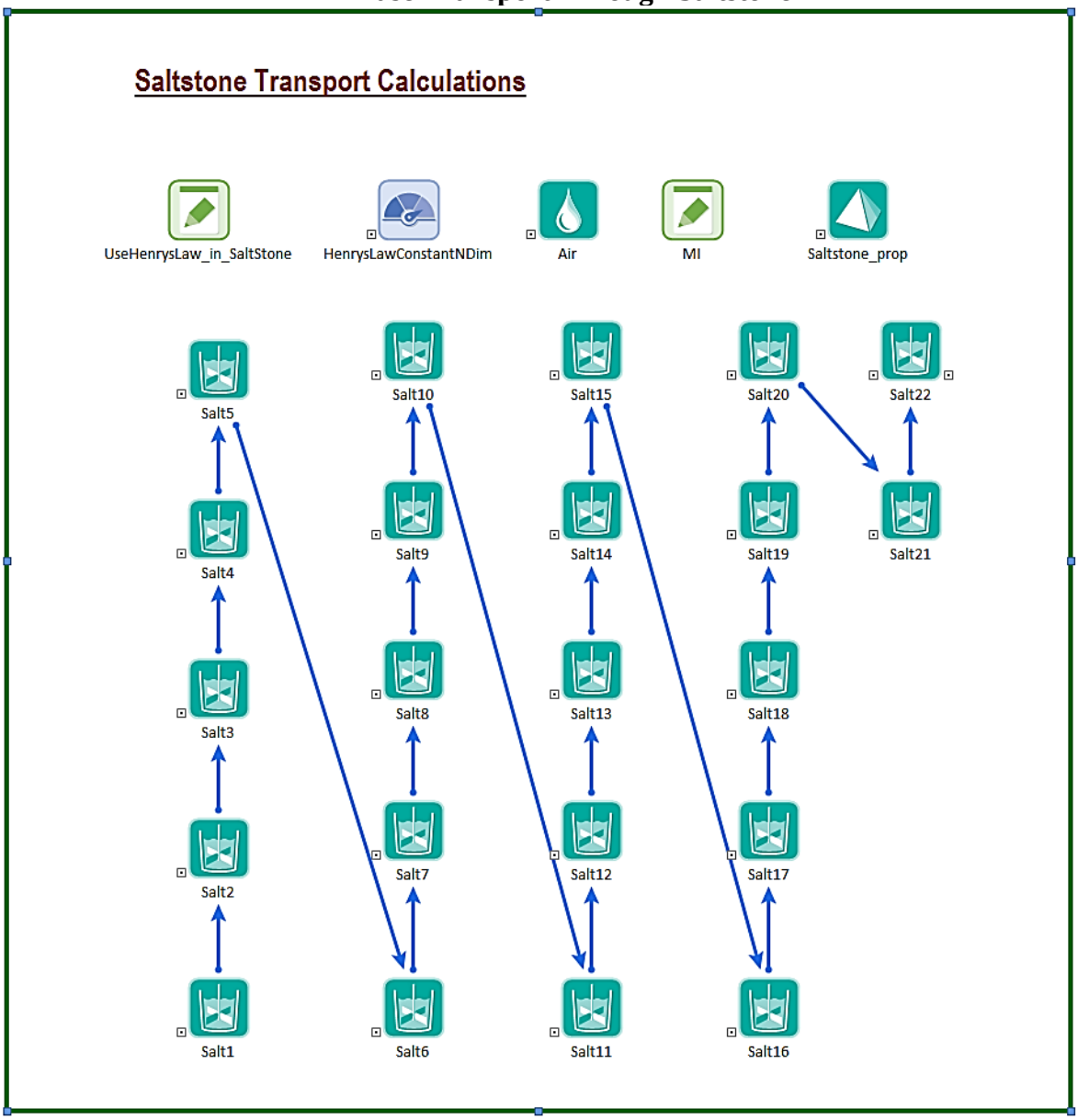

Figure 2.2-2 shows the containers for each zone with black arrows indicating links between containers including the diffusive-flux link between the top mixing cell in the lower zone and the bottom cell in the overlying zone. The numeric cell indexing, as depicted in Figure 2.2-1 and reflected in the cell names, is from the bottom of the Saltstone to the top of the Erosion Barrier. Global cell to cell indexing starts at the bottom of the Saltstone, increasing until reaching the top mixing cell in the Erosion Barrier which releases the diffusing radionuclide to a sink cell in the container *Sink* (see Figure 2.2-3). The geometry of the cells is fully described in Section 3.2.2.

Figure 2.2-2: Example of Zone-Specific GoldSim Containers for Cell Pathway Elements Linked in Series to Simulate Air-Phase Transport through SDUs and Closure Cap Layers

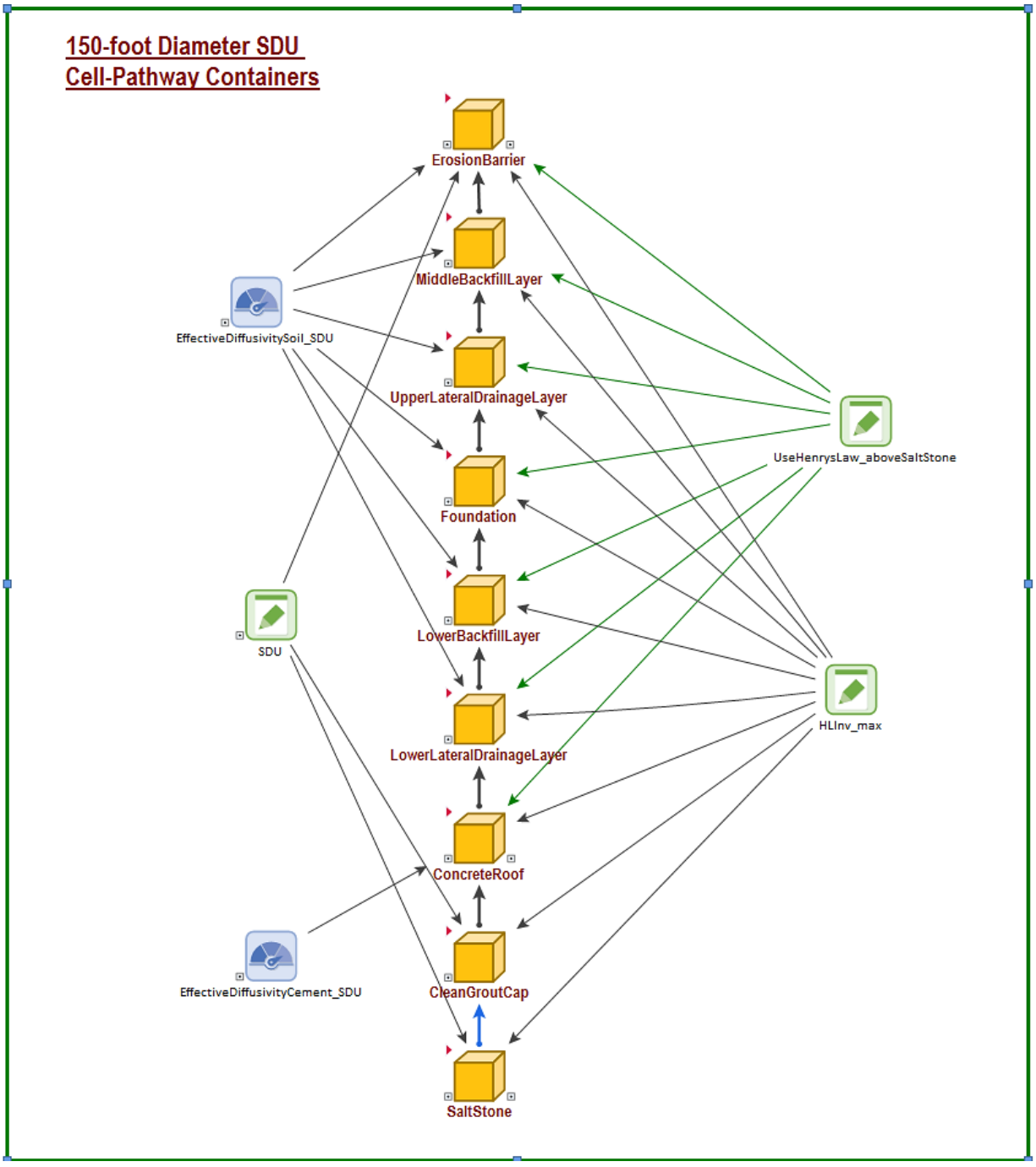

Figure 2.2-3: GoldSim Cell Pathway Elements Linked in Series to Simulate Air-Phase Transport through the Erosion Barrier for 150-foot Diameter SDUs

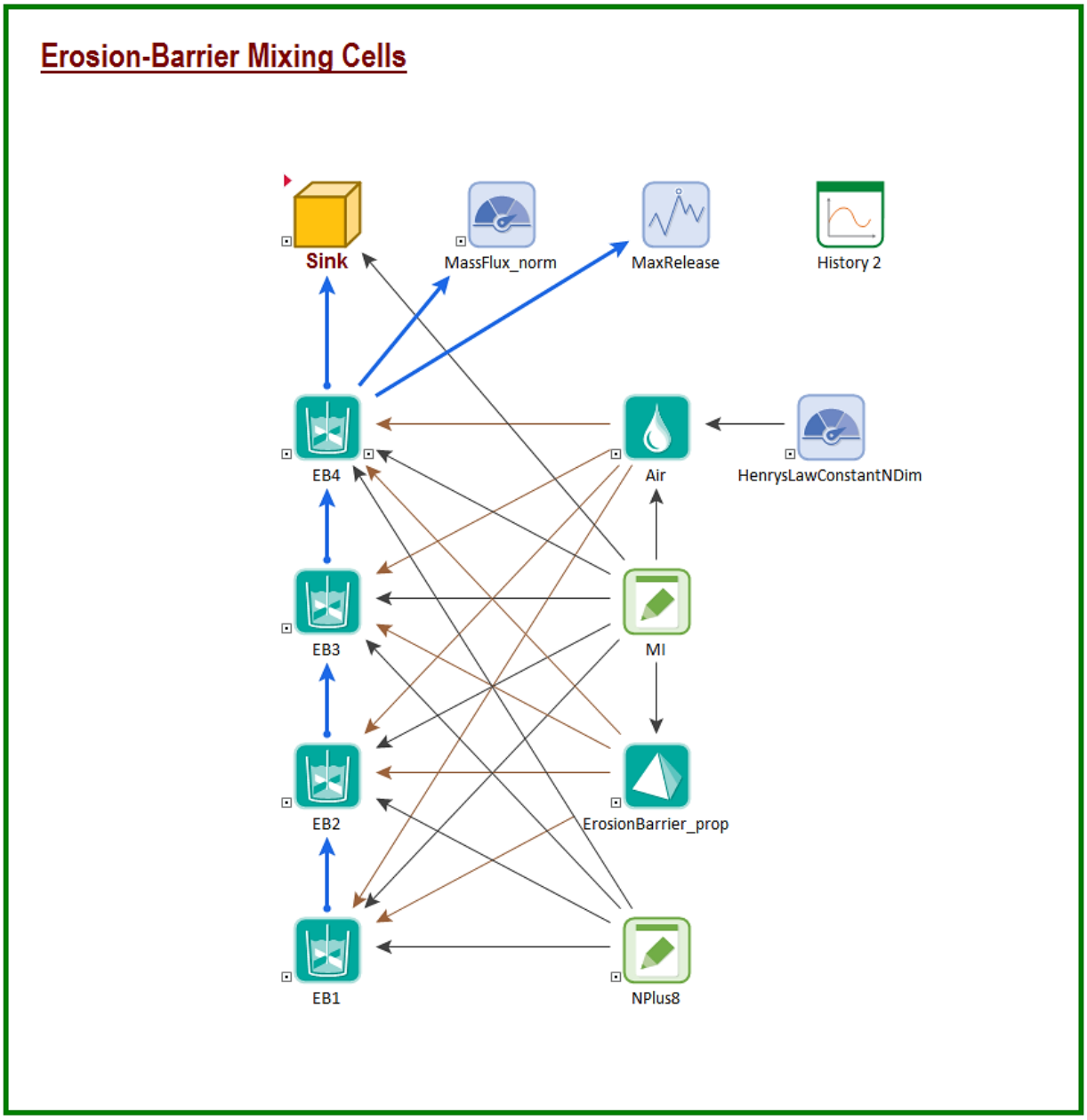

The governing equation for the diffusive mass flux link between Cell i and Cell j, can be written in the form:

$$f_{s,i\to j} = D_s\left(c_{ims} - \frac{c_{jns}}{K_{nms}}\right) \qquad \text{(Eq. 2-2)}$$

where:

D_s = diffusive conductance for species s in the mass flux link [L^3/T];

c_{ims} = the dissolved concentration of species s in medium m within Cell i [M/L^3];

c_{jns} = the dissolved concentration of species s in medium n within Cell j [M/L^3]; and

K_{nms} = partition coefficient between fluid medium n (in Cell j) and fluid medium m (in Cell i) for species s [L^3 medium m / L^3 medium n].

The diffusive conductance for species s in the mass flux link as defined in GTG-2017a can be written as:

$$D_s = \frac{A}{\frac{L_i}{f_{ms} d_{ms} \tau_{Pi} r_m(s_m) n_{Pi}} + \frac{L_j}{f_{ns} d_{ns} \tau_{Pj} r_n(s_n) n_{Pj} K_{nms}}} \quad \text{(Eq. 2-3)}$$

where:

A = the area of the diffusive mass flux link [L^2];

L_i = diffusive length for the diffusive mass flux link in Cell i [L];

L_j = diffusive length for the diffusive mass flux link in Cell j [L];

f_{ms} = available porosity for species s in medium m (≤ 1);

f_{ns} = available porosity for species s in medium n (≤ 1);

d_{ms} = diffusivity for species s for fluid m (in Cell i) [L^2/T];

d_{ns} = diffusivity for species s for fluid n (in Cell j) [L^2/T];

τ_{Pi} = tortuosity for the porous medium defined for the diffusive mass flux link in Cell i (≤ 1);

τ_{Pj} = tortuosity for the porous medium defined for the diffusive mass flux link in Cell j (≤ 1);

$r_m(s_m)$ = diffusive reduction formula for fluid m (in Cell i) to account for saturation level;

$r_n(s_n)$ = diffusive reduction formula for fluid m (in Cell j) to account for saturation level;

s_m = Saturation of fluid m (in Cell i);

s_n = Saturation of fluid m (in Cell j);

n_{Pi} = porosity for the porous medium defined for the diffusive mass flux link in Cell i; and

n_{Pj} = porosity for the porous medium defined for the diffusive mass flux link in Cell j.

The partition coefficient between fluid medium n (in Cell j) and fluid medium m (in Cell i) for species s, K_{nms}, is defined in GTG-2017a as:

$$K_{nms} = \frac{K_{nrs}}{K_{mrs}} \quad \text{(Eq. 2-4)}$$

where:

K_{mrs} = partition coefficient between fluid medium m and reference fluid r for species s [L^3 fluid r/L^3 fluid m]; and

K_{nrs} = partition coefficient between fluid medium n and reference fluid r for species s [L^3 fluid r/L^3 fluid n].

Combining Equations 2-2 and 2-4, the governing equation for the diffusive mass flux link between Cell i and Cell j as used in the SDFAPR Model, can be rewritten in the form:

$$f_{s,i \to j} = D_s \left(c_{ims} - \frac{c_{jns} K_{mrs}}{K_{nrs}} \right) \quad \text{(Eq. 2-5)}$$

As discussed in GTG-2017a, since the flux depends on the concentration on both sides of the link, the GoldSim transport module solves the equations for sets of Cell pathways connected by diffusive mass flux links simultaneously (i.e., treating them as a single coupled system of equations).

Note that spatially-averaged zone saturations are required input to the SDFAPR Model. The diffusive reduction formula term $r_m(s_m)$ is can be assigned these values to correctly assemble the diffusivity term, D_s. The model also allows the user to scale the Cell pathway length terms L_i and L_j instead to apply the saturation effects to Equation 2-3. Alternatively, if cell by cell saturation values were wanted, this could be used by adjusting the logic used to assemble the scaled Cell pathway lengths.

For Cell-pathway elements not subject to solubility limits, the equation for concentration of species s in Medium m of Cell i is written as:

$$c_{ims} = \left\{ \frac{K_{mrs}}{\sum_{g=1}^{NM_i} K_{grs} VM_{ig}} \right\} m_{is} \qquad \text{(Eq. 2-6)}$$

where:

c_{ims} = concentration of species s in medium m in Cell i [(M/L^3) for Fluids or (M/M) for Solids];

m_{is} = mass of species s in Cell i [M];

K_{mrs} = partition coefficient between medium m and Reference Fluid r for species s [(L^3/L^3) for Fluids or (L^3/M) for Solids];

K_{grs} = partition coefficient between medium g and Reference Fluid r for species s [(L^3/L^3) for Fluids or (L^3/M) for Solids];

VM_{ig} = quantity (volume or mass) of medium g in Cell i [L^3 for Fluids or M for Solids]; and

NM_i = the number of media in Cell i.

As noted in GTG-2017a, for all species, the partition coefficient between the Reference Fluid and itself is 1 (i.e., in the above equation, if *m* is the Reference Fluid, $K_{mrs} = 1$).

3.0 MODEL ORGANIZATION

This section is a roadmap to the SDFAPR Model and User's Guide to the data input required by the model.

3.1 Organization Overview

As discussed in GTG-2017a, the GoldSim software is designed to be amenable to model development using a "Top-down" approach, starting from the top (i.e., the ultimate objective of the modeling exercise) and concentrating on the integration and coupling of all system components. At its "top" level (Figure 3.1-1) the SDFAPR Model is comprised of four containers used to divide the model into four sections, one for selecting options and setting control parameters (*UserSettings*), a second section containing the input parameters (*GeneralInput*) used to define the system processes controlling the release of volatile radionuclides to the atmosphere, a third section where calculations needed to quantify the release of radionuclides to the atmosphere are performed (*Air_PathwayTransport*), and a fourth section used to capture and organize the results generated in the calculation section (*SDU_Output*).

Figure 3.1-1: "Top" level of the SDFAPR Model

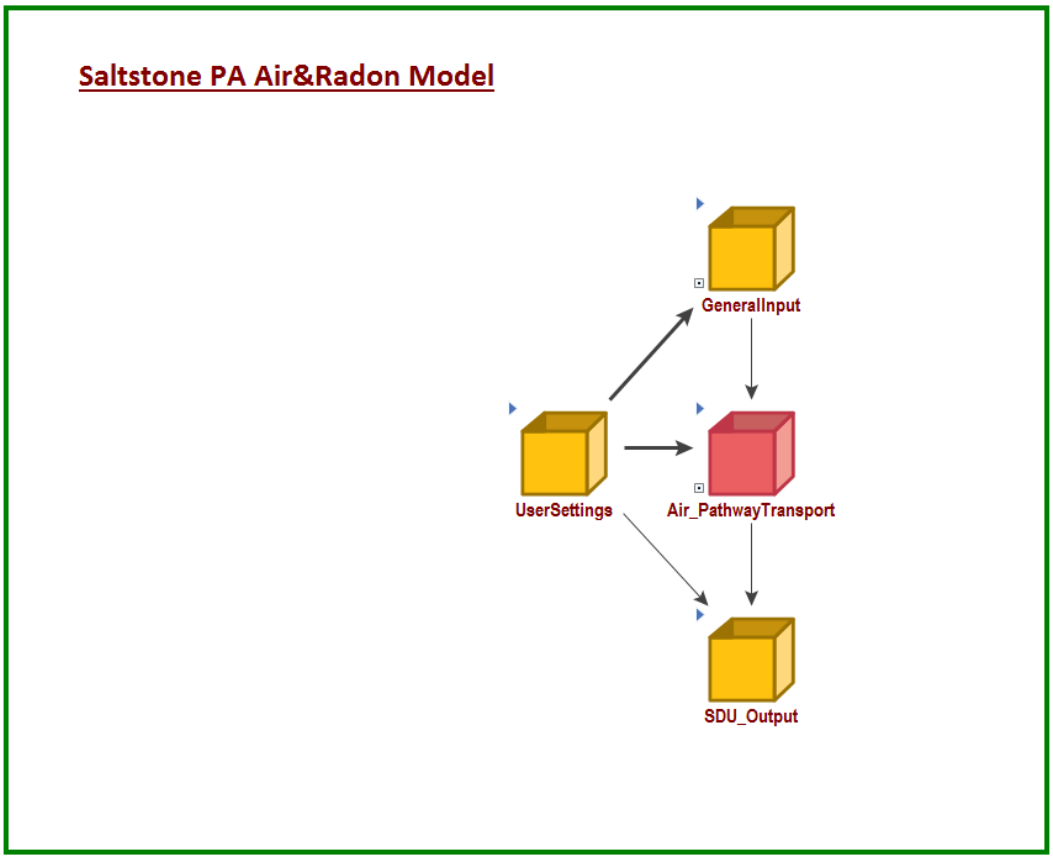

3.2 Input Organization

This section describes the organization and details for the two top-level containers wherein data input is required by the SDFAPR Model: *UserSettings* (Section 3.2.1) and *GeneralInput* (Section 3.2.2).

3.2.1 User Settings

The user-defined control parameters in the SDFAPR Model are presented in Figure 3.2-1 and described below. These user settings allow users to vary model inputs to modify the way the model runs; for example, users may elect to simulate a single SDU rather than running all 15 SDUs. Additionally, these settings provide options for alternative modeling assumptions regarding the "clean cap" grout (i.e., the use of a non-contaminated grout layer above the saltstone waste form as opposed to assuming the SDU is completely filled with radioactive saltstone).

Figure 3.2-1: Control Parameters Available in the SDFAPR Model

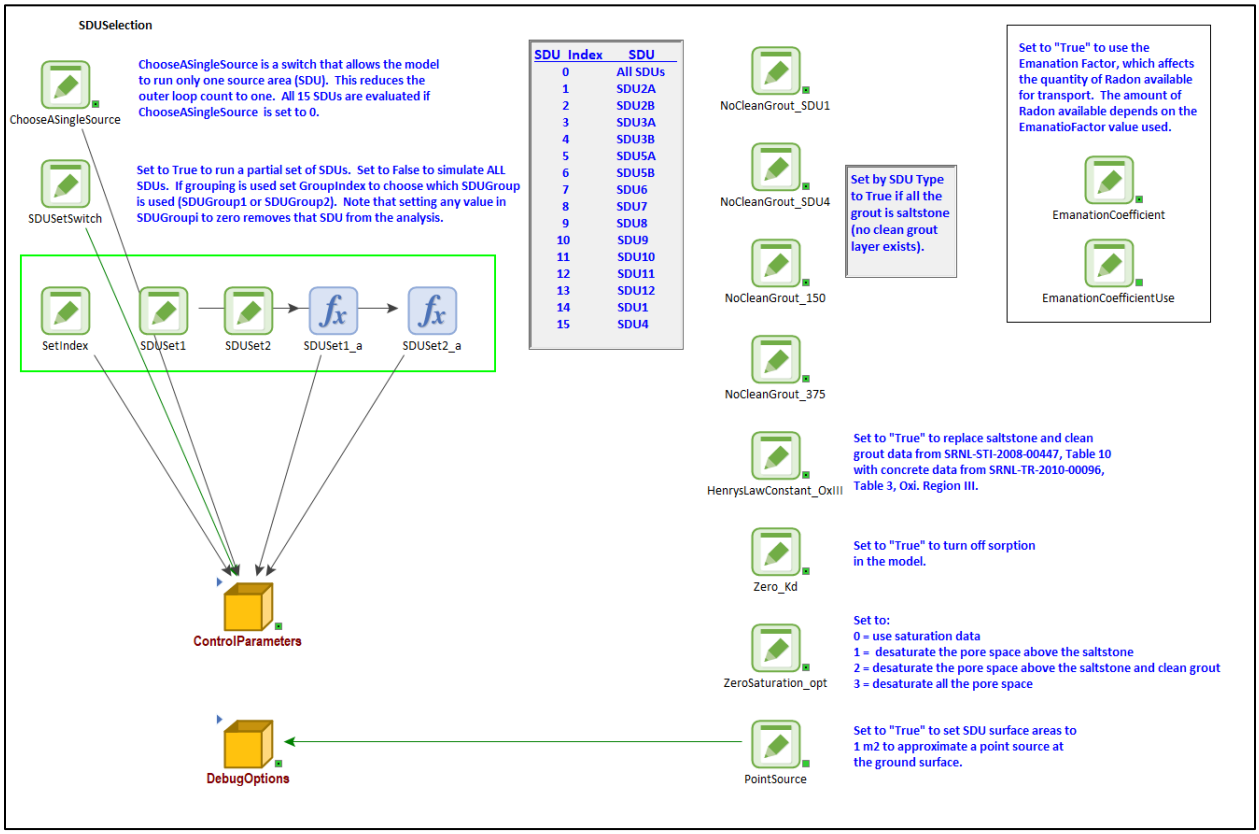

***ChooseASingleSource* –** The model user can choose to simulate the release of radionuclides, from a specified SDU, to the atmosphere, by setting the data element *ChooseASingleSource* to the SDU Index for the desired SDU before running the model (see Figure 3.2-1 and Table 3.2-1). Setting the data element to 0 will allow the user to simulate radionuclide releases from all SDUs or a subset of SDUs.

Table 3.2-1: SDU Index used in the *UserSettings* of the SDFAPR Model

Model Index Value	Simulated SDU
1	SDU 2A
2	SDU 2B
3	SDU 3A
4	SDU 3B
5	SDU 5A
6	SDU 5B
7	SDU 6
8	SDU 7
9	SDU 8
10	SDU 9
11	SDU 10
12	SDU 11
13	SDU 12
14	SDU 1
15	SDU 4
0	Every SDU

SDUSetSwitch – Setting the *SDUSetSwitch* input element to "True" allows the user to choose a subset of SDUs to simulate together.

SetIndex – If *SDUSetSwitch* is set to "True", *ChooseASingleSource* is set to 0, and *SetIndex* is set to 1, the subset of SDUs defined in the data element SDUSet1 will be simulated together.

If *SDUSetSwitch* is set to "True", *ChooseASingleSource* is set to 0, and *SetIndex* is greater than 1, the subset of SDUs defined in the data element SDUSet2 will be simulated together.

If *SDUSetSwitch* is set to "False", the full set of SDUs defined in the data element *NoGroups* will be simulated if *ChooseASingleSource* = 0.

SDUSet1 – A user specified group can be defined in the data element *SDUSet1* by setting specific rows to zero to deactivate SDUs with indices (see Figure 3.2-1) equivalent to the row number.

SDUSet2 – A second user specified group can be defined in the data element *SDUSet2* by setting specific rows to zero to deactivate SDUs with indices (see Figure 3.2-1) equivalent to the row number.

NoCleanGrout_SDU1 - If *NoCleanGrout_SDU1* is set to "True", saltstone replaces the clean grout in the clean grout layer of SDU 1.

NoCleanGrout_SDU4 - If *NoCleanGrout_SDU4* is set to "True", saltstone replaces the clean grout in the clean grout layer of SDU 4.

NoCleanGrout_SDU_150 **-** If *NoCleanGrout_SDU150* is set to "True", saltstone replaces the clean grout in the anticipated clean grout layers of the 150-foot diameter SDUs.

NoCleanGrout_SDU_375 **-** If *NoCleanGrout_SDU375* is set to "True", saltstone replaces the clean grout in the anticipated clean grout layers of the 375-foot diameter SDUs.

HenrysLawConstant_OxIII **-** Set to "True" to replace saltstone and clean cap grout data from SRNL-STI-2008-00447, Table 10 with concrete data from SRNL-TR-2010-00096, Table 3 (for Oxidized Region III).

Zero_Kd **-** Set to "True" to turn off sorption in the model.

ZeroSaturation_opt **-** Set to:

0 = use saturation data

1 = desaturate the pore space above the saltstone – this setting should not be used when a *NoCleanGrout_SDU#* selections(s) is made

2 = desaturate the pore space above the saltstone and clean cap grout, or

3 = desaturate all the pore space.

PointSource **-** Set to "True" to set SDU surface areas to 1 m^2 to approximate a point source at the ground surface.

EmanationCoefficientUse **-** Set to "True" to use the Emanation Coefficient. This coefficient affects the quantity of radon available for transport. The emanation coefficient is defined as the fraction of the total amount of Rn-222 produced by radium decay that escapes from soil particles and enters the pore spec of the medium. The default setting is false.

EmanationCoeffient – The current value is set to 0.25 which is consistent with previous uses. [SRNL-STI-2008-00447]

3.2.2 General Input

This section describes the organization and details of the input parameters used to define the system processes controlling the release of volatile radionuclides to the atmosphere. In the *GeneralInput* Container (Figure 3.2-2), the SDFAPR Model is comprised of six containers (noted in italics), organizing the data input into groups pertaining to:

1) model geometries (*Geometry*)
2) SDU-specific inventories (*Inventory*),
3) physical properties (*PhysicalProperties*),
4) chemical properties (*ChemicalProperties*),
5) transport properties (*TransportProperties*), and
6) GoldSim-specific material parameter assembly (*GoldSimMaterialProperties*).

Figure 3.2-2: Control Parameters Available in the SDFAPR Model

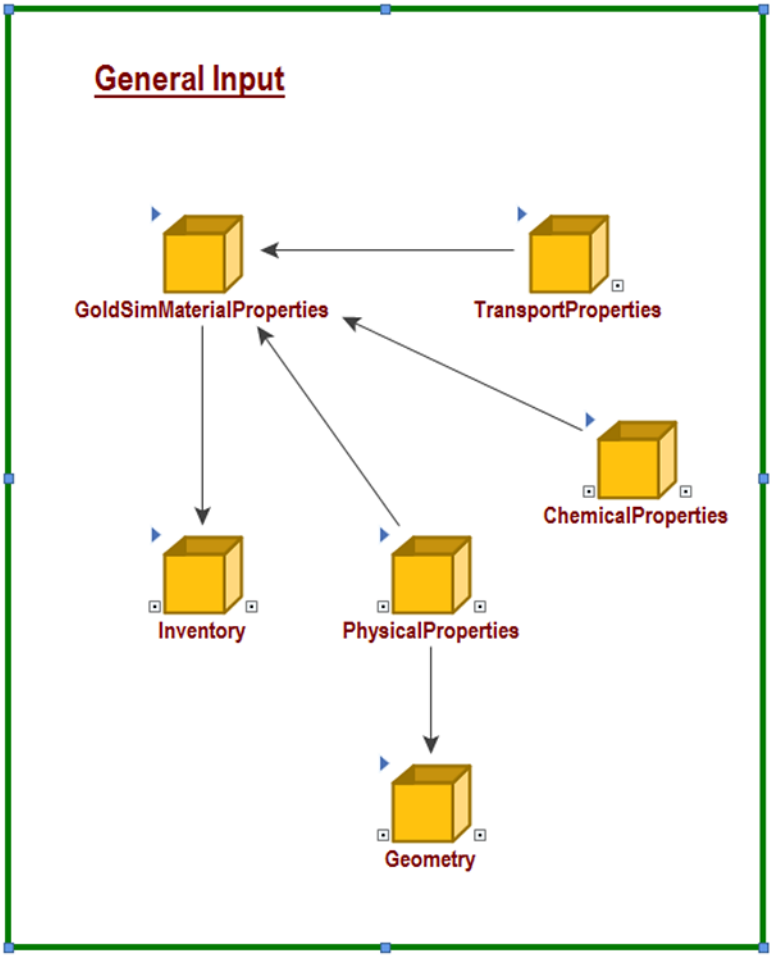

3.2.2.1 Model Geometries

The container *Geometry* holds four additional containers, each one comprised of the data needed to assemble the Cell-pathway elements for the four SDU types considered (see Figure 3.2-3).

The four SDU geometry types as reflected in Figure 3.2-3 include each of the rectangular SDUs (*SDU1* and *SDU4*), the 150-foot diameter cylindrical SDUs (*SDU*_150 for SDU 2A, SDU 2B, SDU 3A, SDU3B, SDU 5A, and SDU 5B), and the 375-foot diameter cylindrical SDUs (*SDU_375* for SDUs 6 through 12). Figure 2.1-1 shows the planned layout of the SDF with respect to each of these SDUs. The geometry input requirements for each SDU-type are described below.

Figure 3.2-3: Top Level of the *Geometry* Container

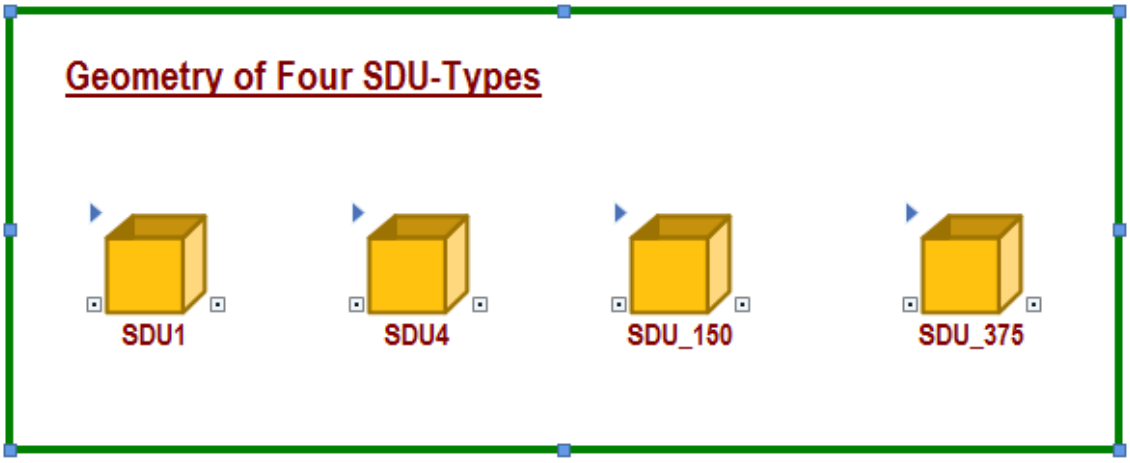

SDU1

The data elements used to assign the geometric attributes of SDU 1 to the SDFAPR Model are in the *SDU1* geometry container (Figure 3.2-4).

Figure 3.2-4: SDU 1 Geometry Container (SDU1)

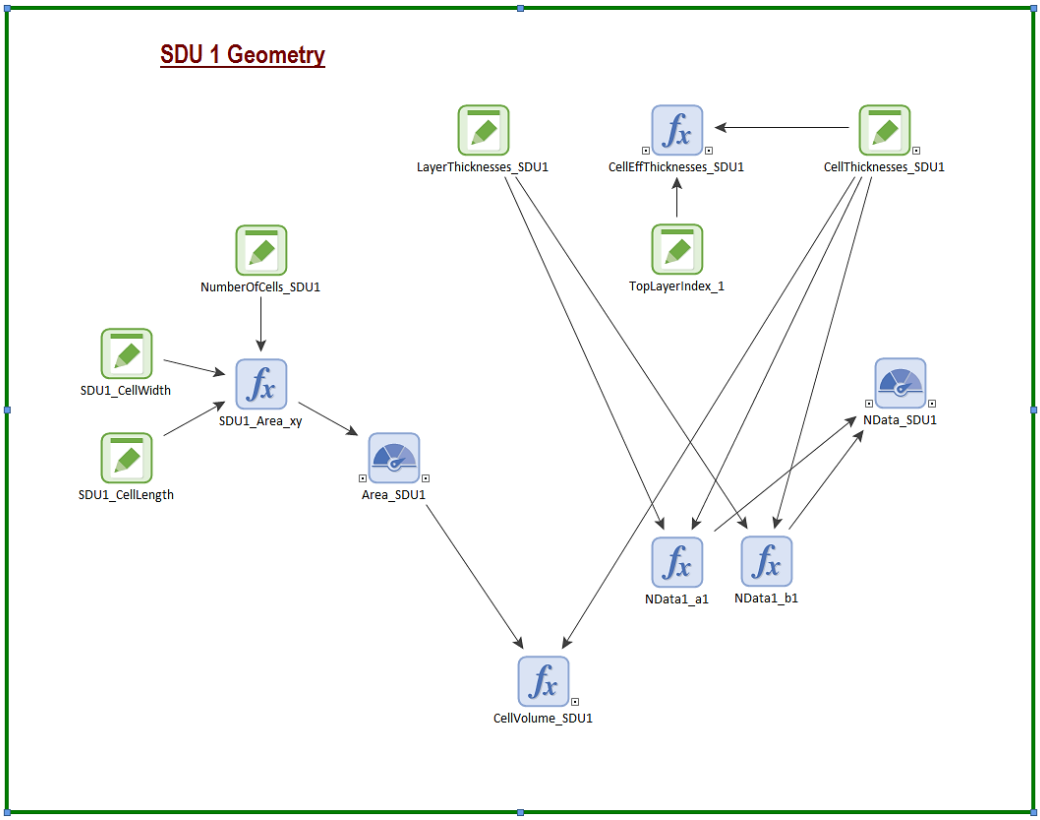

The contents and sources of the data elements describing the geometry of SDU 1 are as follows:

SDU1_CellWidth – The width of each cell in SDU 1, (98.5 ft or 30.0 m) is assigned to data element *SDU1_CellWidth*. [SRR-CWDA-2009-00017]

SDU1_CellLength – The length of each cell in SDU 1, (98.5 ft or 30.0 m) is assigned to data element *SDU1_CellLength*. [SRR-CWDA-2009-00017]

NumberOfCells_SDU1 – The number of disposal cells (6) contained in SDU 1 is assigned to data element *NumberOfCells_SDU1*. [SRR-CWDA-2009-00017]

LayerThicknesses_SDU1 – The material layer thicknesses for SDU 1 as presented in Table 3.2-2 are assigned to data element *LayerThicknesses_SDU1*. The layer thicknesses are the same as in the PORFLOW model used for air-phase transport in the 2009 SDF PA as documented in SRNL-STI-2008-00447 and depicted in Figure 3.2-5 for the SDU and Figure 3.2-6 for the closure cap.

CellThicknesses_SDU1 – Each simulated layer is represented by a series of modeled cells (see the left edge of Figure 3.2-5 for the SDU and Figure 3.2-6 for the closure cap). The thickness of each GoldSim cell-pathway element linked in series to simulate air-phase transport through SDU 1 is assigned by the data element: *CellThicknesses_SDU1*. The discretization defined by the vector in *CellThicknesses_SDU1* is slightly modified from the PORFLOW model used for air-phase transport in support of the 2009 SDF PA as documented in SRNL-STI-2008-00447 (Figure 3). The modifications consist of updating each of the 24-inch thick cells in the PORFLOW model to two 12-inch cells in the GoldSim model.

TopLayerIndex_1 – The indices for the top cell-pathway element in each layer of the SDU 1 model, presented in Table 3.2-3 are assigned to the data element: *TopLayerIndex_1*.

Table 3.2-2: Layer Thicknesses of SDU1

Layer	Layer Thicknesses (inches)
Saltstone	288
Clean Grout	6
SDU Roof	6
Lower Lateral Drainage	24
Lower Backfill	12
Foundation	12
Upper Lateral Drainage	12
Middle Backfill	12
Erosion Barrier	12

Table 3.2-3: Top Layer Index of SDU1

Layer	Top Layer Index
Saltstone	26
Clean Grout	29
SDU Roof	32
Lower Lateral Drainage	40
Lower Backfill	44
Foundation	48
Upper Lateral Drainage	52
Middle Backfill	56
Erosion Barrier	60

Figure 3.2-5: Schematic of Cementitious Layers of the SDFAPR Model Grid for SDU 1

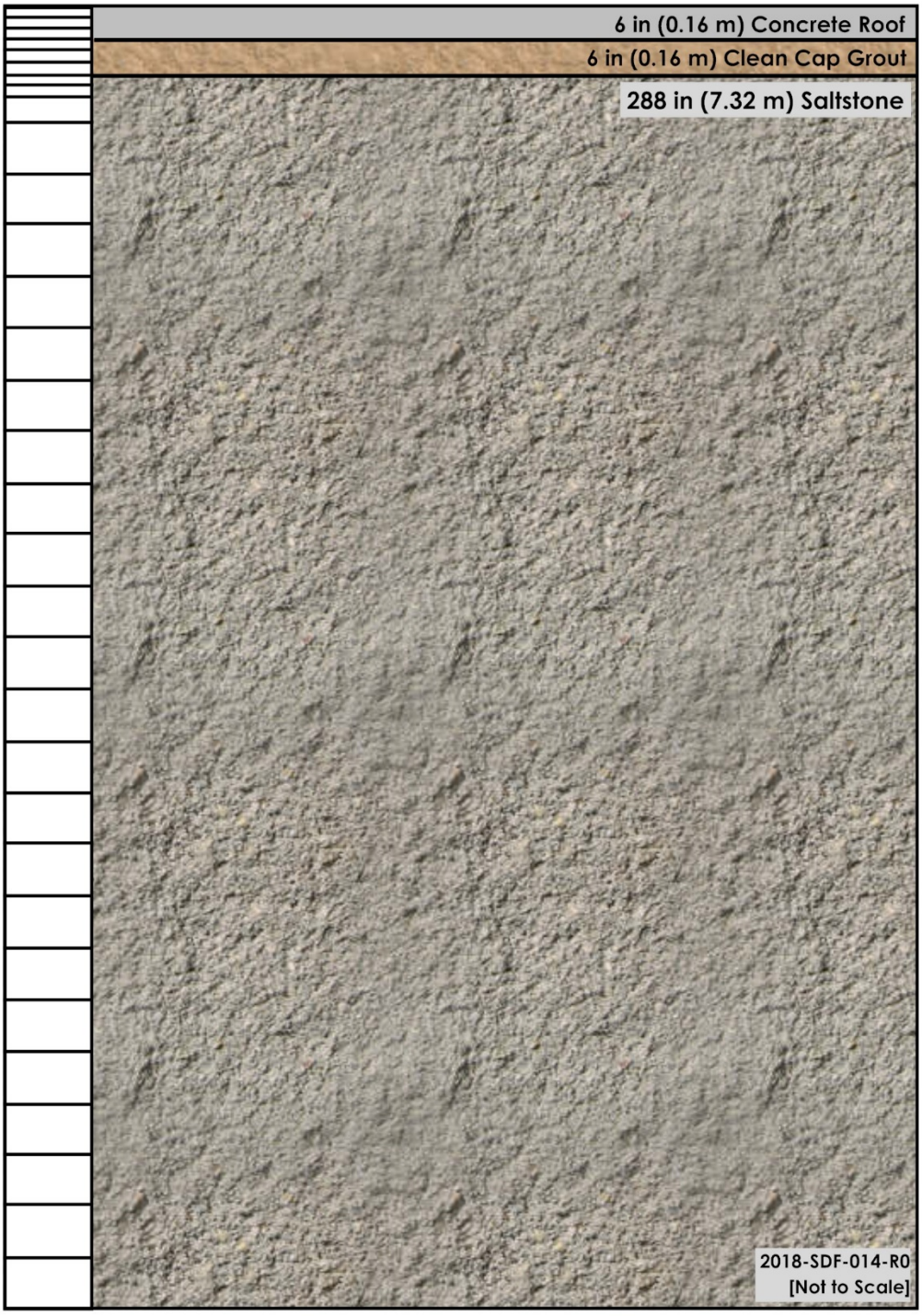

[Source: Modified from SRNL-STI-2008-00447, Figure 3]

.

Figure 3.2-6: Schematic of SDFAPR Model Grid for the Closure Cap for All SDUs

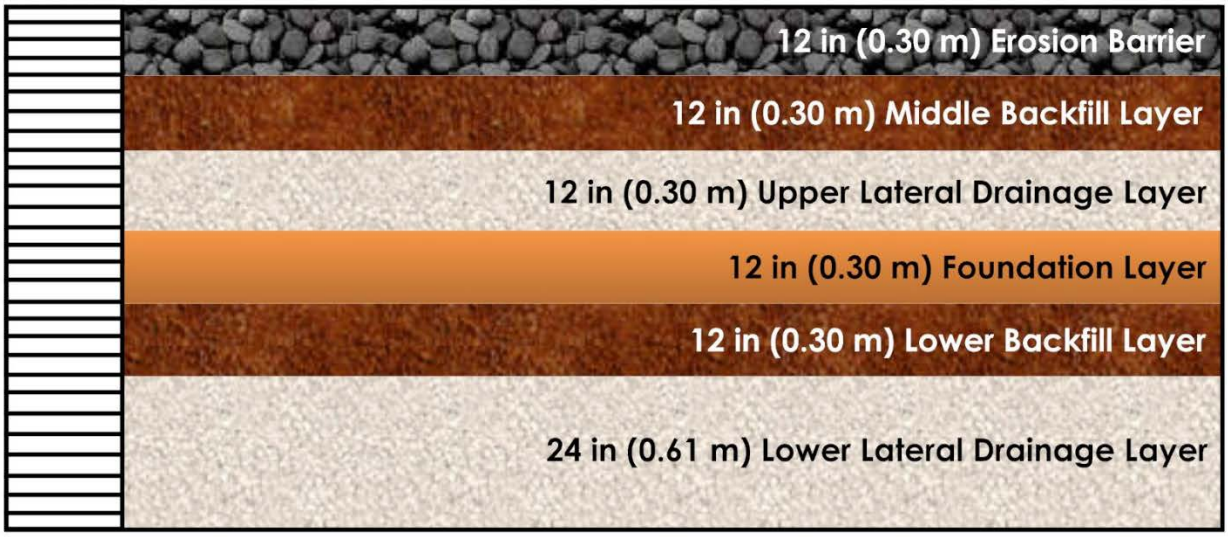

Note: For conservatism the model grid does not include the following layers: topsoil, upper backfill, geotextile fabric, HPDE, and GCL.

SDU 4

The data elements used to assign the geometric attributes of SDU 4 to the SDFAPR Model are in the *SDU4* geometry container (Figure 3.2-7).

Figure 3.2-7: SDU 4 Geometry Container (SDU4)

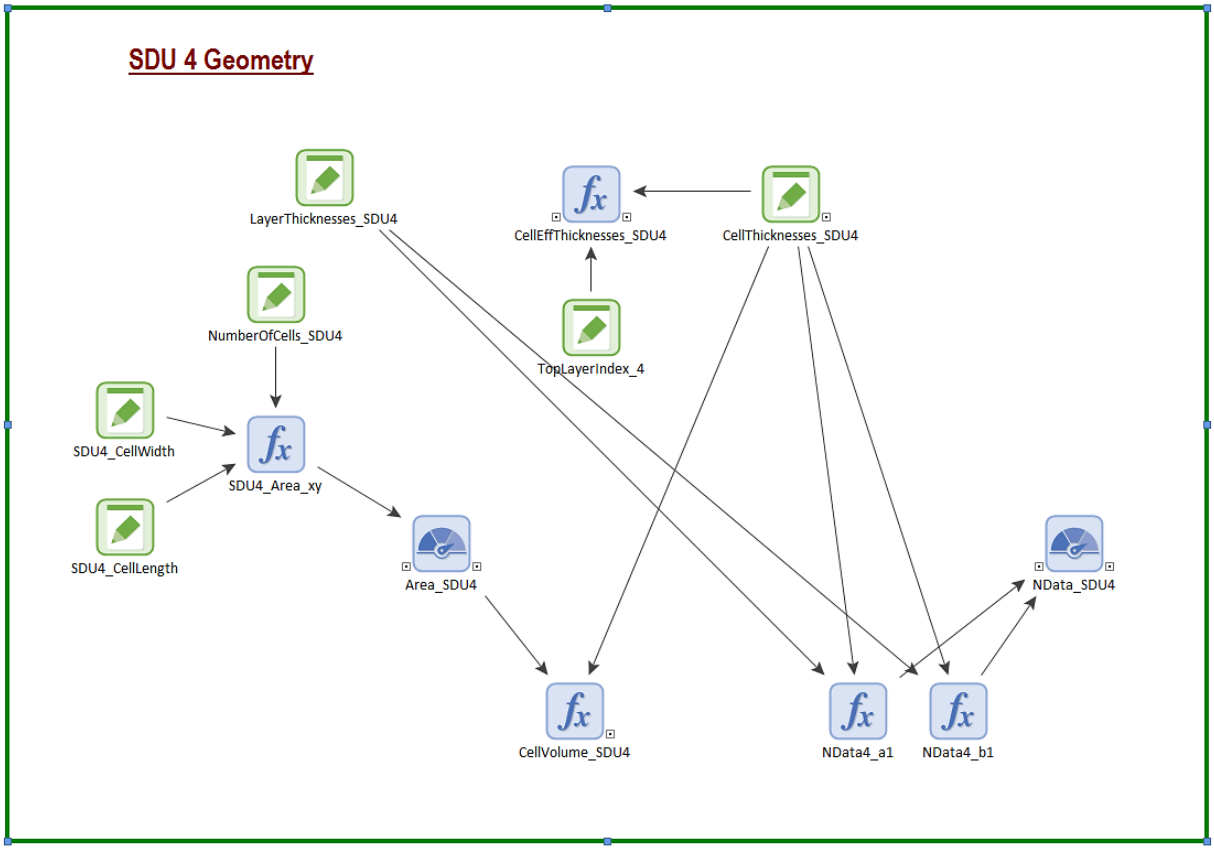

The contents and sources of the data elements describing the geometry of SDU 4 are as follows:

SDU4_CellWidth – The width of each cell in SDU 4 (98.5 ft or 30.0 m) is assigned to data element *SDU4_CellWidth*. [SRR-CWDA-2009-00017]

SDU4_CellLength – The length of each cell in SDU 4 (98.5 ft or 30.0 m) is assigned to data element *SDU4_CellLength*. [SRR-CWDA-2009-00017]

NumberOfCells_SDU4 – The number of disposal cells (12) contained in SDU 4 is assigned to data element *NumberOfCells_SDU4*. [SRR-CWDA-2009-00017]

LayerThicknesses_SDU4 – The material layer thicknesses for SDU 4 presented in Table 3.2-4 are assigned to data element *LayerThicknesses_SDU4*. The layer thicknesses are the same as in the PORFLOW model used for air-phase transport in the 2009 SDF PA as documented in SRNL-STI-2008-00447 and depicted in Figure 3.2-8 for the SDU and Figure 3.2-6 for the closure cap.

CellThicknesses_SDU4 – Each simulated layer is represented by a series of modeled cells (see the left edge of Figure 3.2-8 for the SDU and Figure 3.2-6 for the closure cap). The thickness of each GoldSim cell-pathway element linked in series to simulate air-phase transport through SDU 4 is assigned to data element *CellThicknesses_SDU4*. The discretization defined by the vector in *CellThicknesses_SDU4* is the same as in the PORFLOW model used for air-phase transport in the 2009 SDF PA as documented in SRNL-STI-2008-00447 (Figure 5).

TopLayerIndex_4 – The indices for the top cell-pathway element in each layer of the SDU 4 model as presented in Table 3.2-5 are assigned by the data element *TopLayerIndex_4*.

Table 3.2-4: Layer Thicknesses of SDU4

Layer	Layer Thicknesses (inches)
Saltstone	297
Clean Grout	15
SDU Roof	4
Lower Lateral Drainage	24
Lower Backfill	12
Foundation	12
Upper Lateral Drainage	12
Middle Backfill	12
Erosion Barrier	12

Table 3.2-5: Top Layer Index of SDU4

Layer	Top Layer Index
Saltstone	27
Clean Grout	33
SDU Roof	37
Lower Lateral Drainage	46
Lower Backfill	50
Foundation	54
Upper Lateral Drainage	58
Middle Backfill	62
Erosion Barrier	66

Figure 3.2-8: Schematic of Cementitious Layers of the SDFAPR Model Grid for the SDU 4

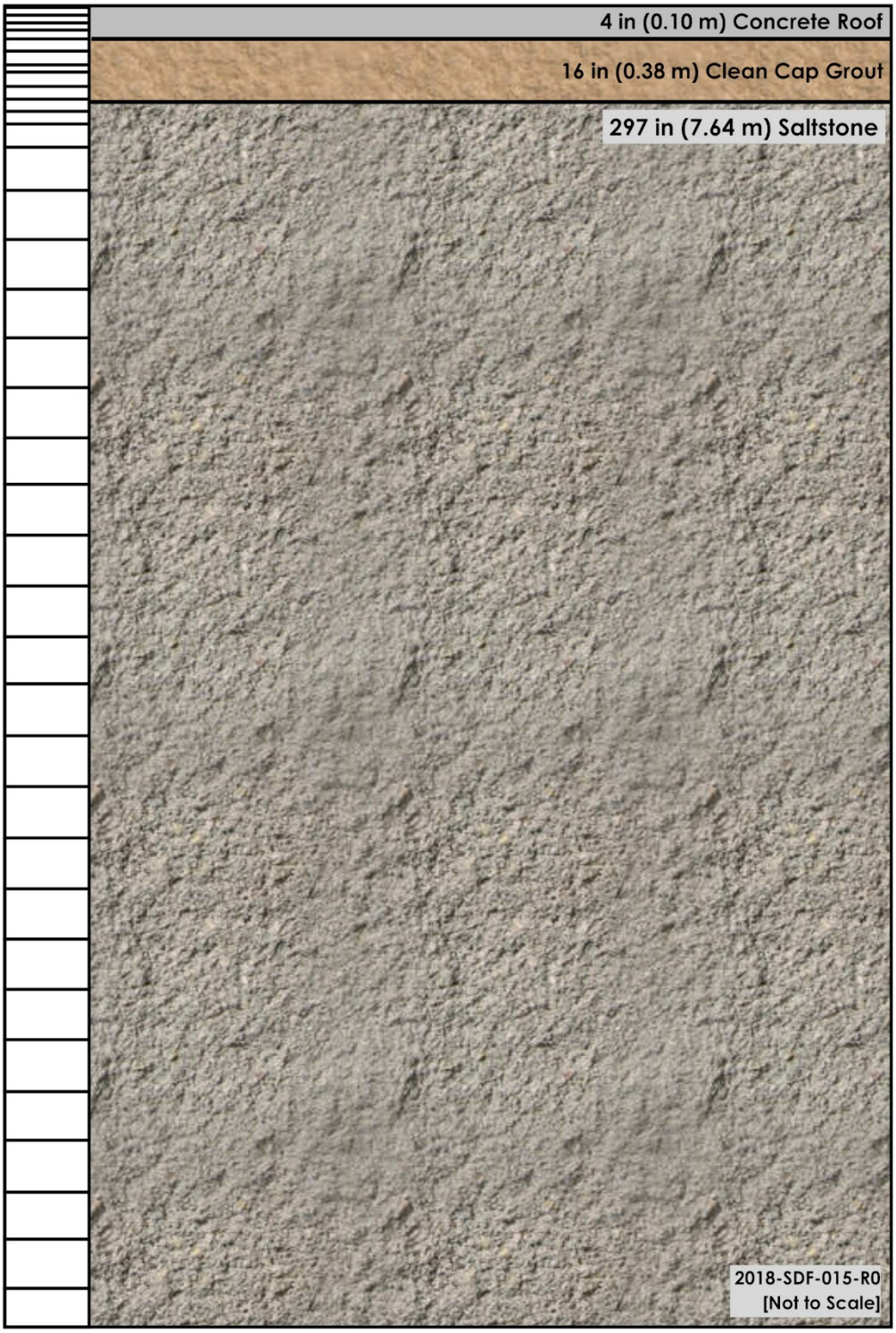

150-foot Diameter SDUs

The data elements used to assign the geometric attributes of the 150-foot diameter SDUs to the SDFAPR Model are in the *SDU_150* geometry container (Figure 3.2-9).

Figure 3.2-9: 150-foot Diameter SDU Geometry Container (SDU_150)

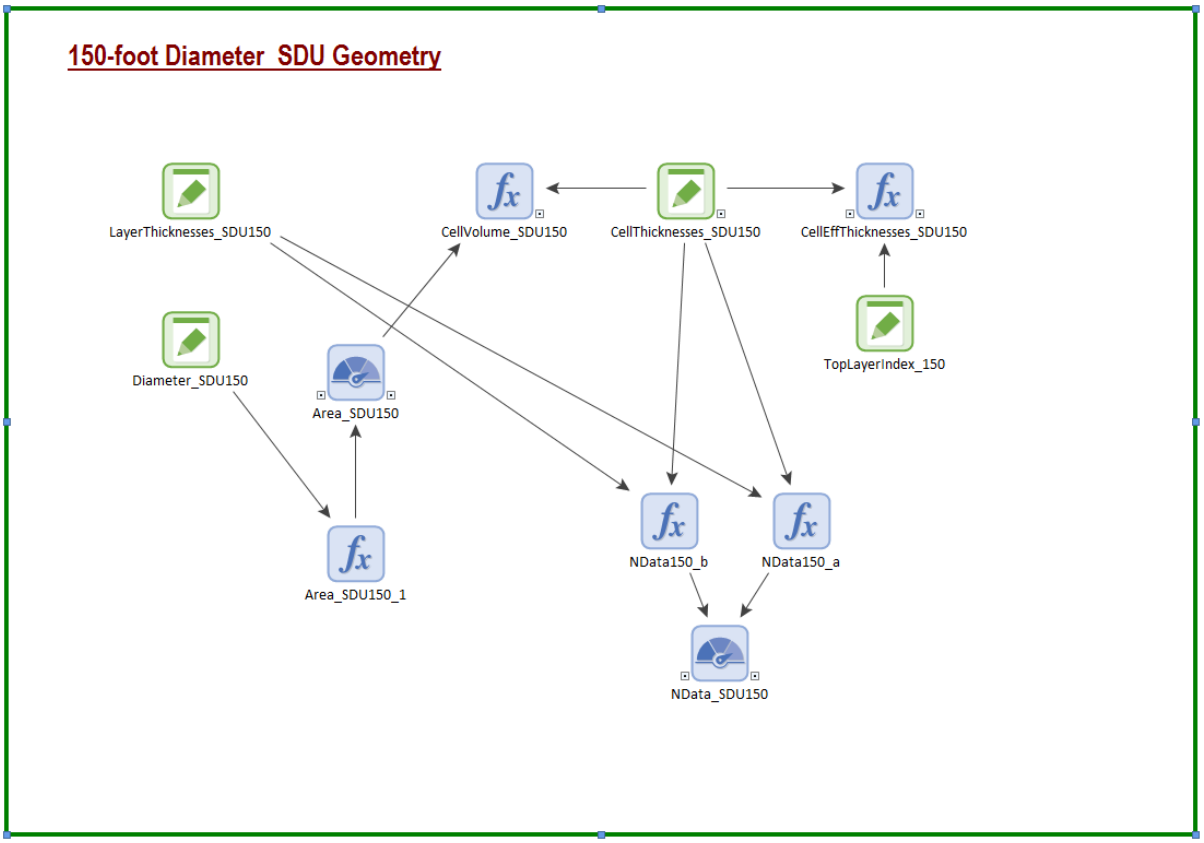

The contents and sources of the data elements describing the geometry of SDU 4 are as follows:

Diameter_SDU150 – The diameter of each 150-foot diameter SDU, (150 ft or 45.7 m) is assigned to data element *Diameter_SDU150*. [SRR-CWDA-2009-00017]

LayerThicknesses_SDU150 – The material layer thicknesses for the 150-foot diameter SDUs as presented in Table 3.2-6 are assigned to data element *LayerThicknesses_SDU150*. The layer thicknesses are the same as in the PORFLOW model used for air-phase transport in the 2009 SDF PA as documented in SRNL-STI-2008-00447 and depicted in Figure 3.2-10 for the SDU and Figure 3.2-6 for the closure cap. One exception to this arrangement deals with the clean grout (i.e., clean cap). No clean grout is assumed to be present and saltstone is assumed to completely fill the SDU. [SRR-CWDA-2018-00012] Note, while Table 3.2-6 lists and Figure 3.2-10 illustrates a thickness for Clean Grout, no clean grout is assumed and the selector *NoCleanGrout_150* is set at True.

CellThicknesses_SDU150 – Each simulated layer is represented by a series of modeled cells (see the left edge of Figure 3.2-10 for the SDU and Figure 3.2-6 for the closure cap). The thickness of each GoldSim cell-pathway element linked in series to simulate air-phase transport through the 150-foot diameter SDUs is assigned to data element *CellThicknesses_SDU150*. The discretization defined by the vector in *CellThicknesses_SDU150* is the same as in the PORFLOW model used for air-phase transport in the 2009 SDF PA as documented in SRNL-STI-2008-00447 (Figure 4).

TopLayerIndex_150 – The indices for the top cell-pathway element in each layer of the model for the 150-ft diameter SDUs as presented in Table 3.2-7 are assigned to data element *TopLayerIndex_150*.

Table 3.2-6: Layer Thicknesses of Each 150-foot Diameter SDU

Layer	Layer Thicknesses (inches)
Saltstone	240*
Clean Grout	24*
SDU Roof	8
Lower Lateral Drainage	24
Lower Backfill	12
Foundation	12
Upper Lateral Drainage	12
Middle Backfill	12
Erosion Barrier	12

*Setting the *NoCleanGrout_150* selector to true fills the Clean Grout Layer with Saltstone material

Table 3.2-7: Top Layer Index of Each 150-foot Diameter SDU

Layer	Top Layer Index
Saltstone	22
Clean Grout	30
SDU Roof	34
Lower Lateral Drainage	42
Lower Backfill	46
Foundation	50
Upper Lateral Drainage	54
Middle Backfill	58
Erosion Barrier	62

Figure 3.2-10: Schematic of Cementitious Layers of the SDFAPR Model Grid for the 150-ft Diameter SDUs

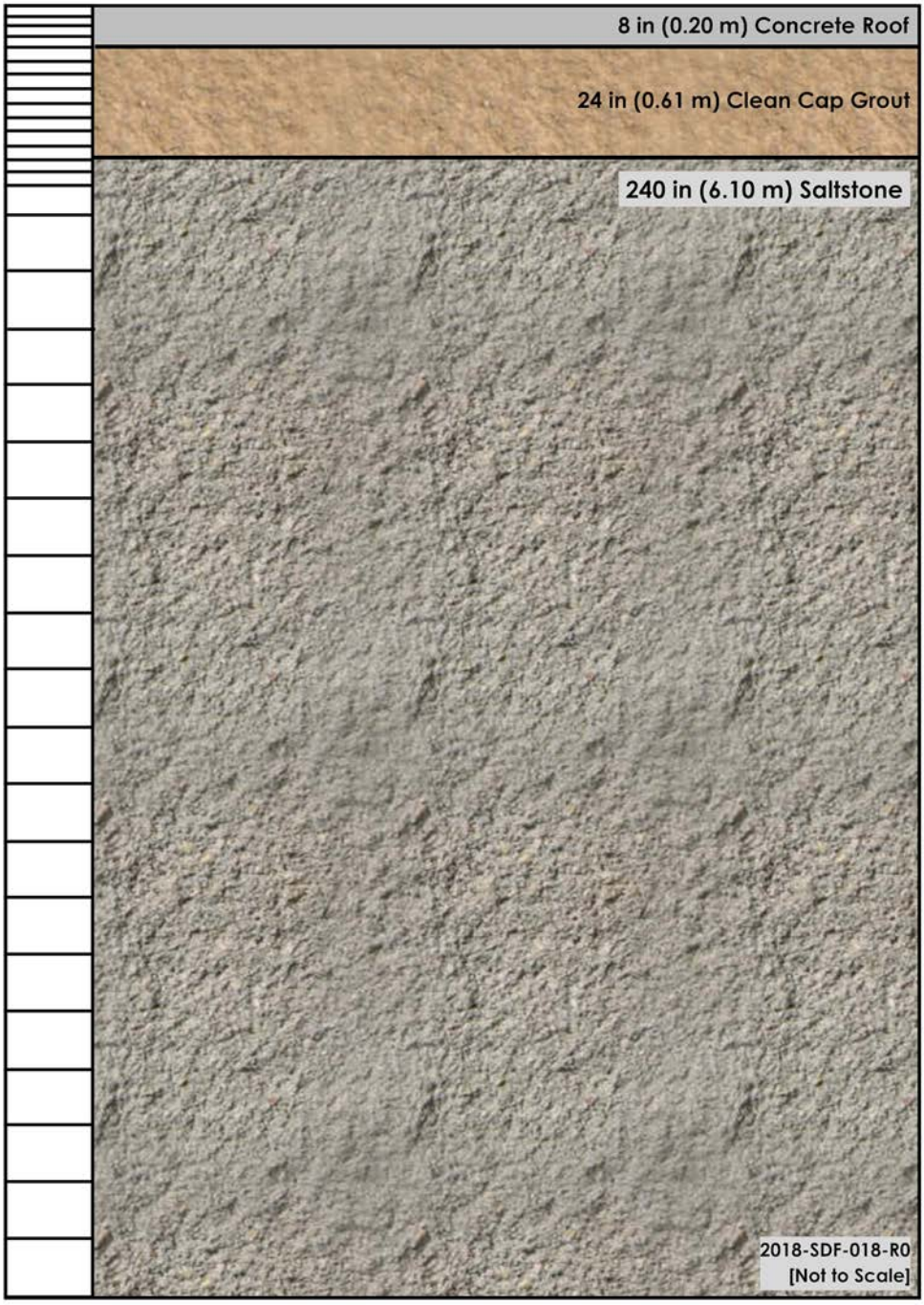

375-foot Diameter SDUs

The data elements used to assign the geometric attributes of the 375-foot diameter SDUs to the SDFAPR Model are in the *SDU_375* geometry container (Figure 3.2-11).

Figure 3.2-11: 375-foot Diameter SDU Geometry Container (SDU_375)

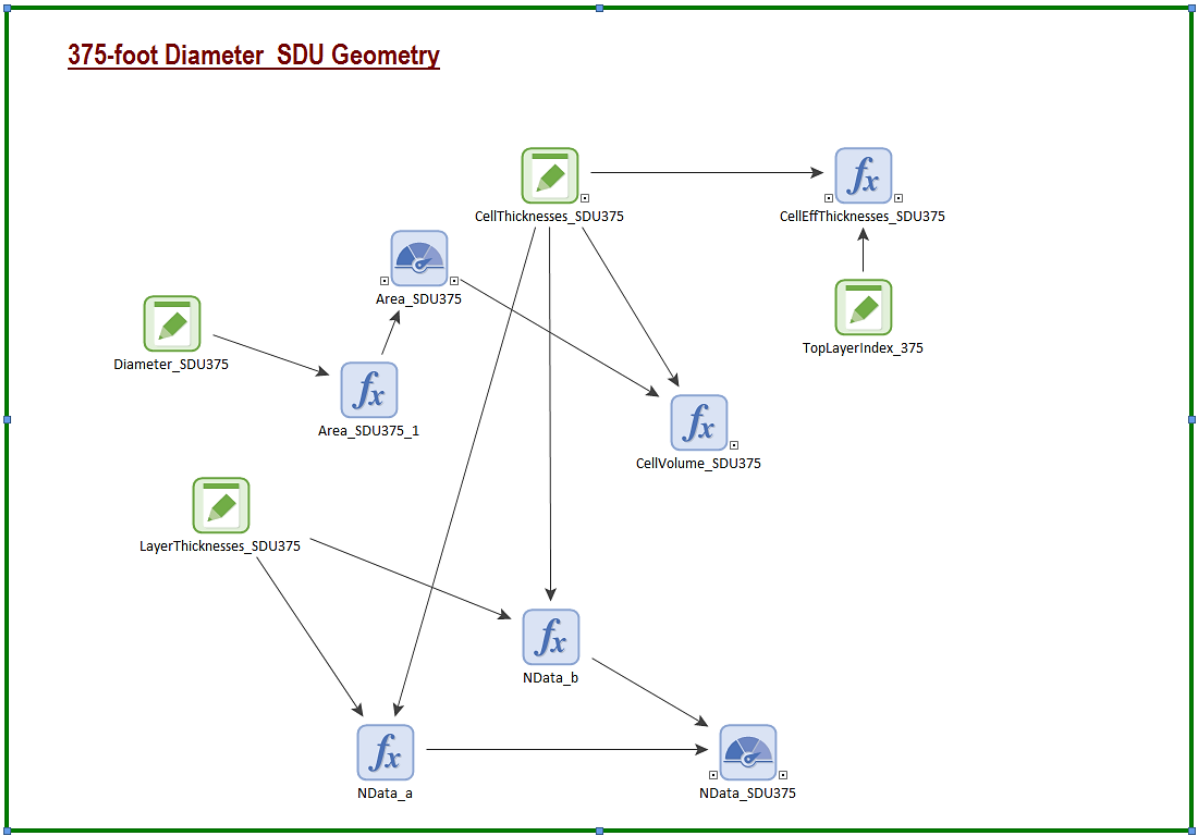

The contents and sources of the data elements describing the geometry of the 375-foot diameter SDUs are as follows:

Diameter_SDU375 – The diameter of each 375-foot diameter SDU (375 ft or 114.3 m) is assigned to data element *Diameter_SDU375*. [SRR-CWDA-2014-00006]

LayerThicknesses_SDU375 – The material layer thicknesses for the 375-foot diameter SDUs as presented in Table 3.2-8 are assigned to data element *LayerThicknesses_SDU375*. The layer thicknesses for the closure cap are the same as in the PORFLOW model used for air-phase transport in the 2009 SDF PA (SRNL-STI-2008-00447) except where superseded by *Additional Recommended Inputs to PORFLOW Modeling for SDU7*, SRR-CWDA-2018-00012 and depicted in Figure 3.2-12. The cementitious barrier thicknesses are based on information from the FY2014 SDF Special Analysis (SA), SRR-CWDA-2014-00006, and is depicted in Figure 3.2-12 for the SDU and Figure 3.2-6 for the closure cap. One exception to this arrangement deals with the clean grout (i.e., clean cap). No clean grout is assumed to be present and saltstone is assumed to completely fill the

SDU. [SRR-CWDA-2018-00012] Note, while Table 3.2-6 lists a thickness for Clean Grout, no clean grout is assumed and the selector *NoCleanGrout_375* is set at True.

CellThicknesses_SDU375 – Each simulated layer is represented by a series of modeled cells (see the left edge of Figure 3.2-12 for the SDU and Figure 3.2-6 for the closure cap). The thickness of each GoldSim cell-pathway element linked in series to simulate air-phase transport through the 375-foot diameter SDUs is assigned to data element *CellThicknesses_SDU375*. For the closure cap layers, the discretization defined by the vector in *CellThicknesses_SDU375* is the same as in the PORFLOW model used for air-phase transport in the 2009 SDF PA as documented in SRNL-STI-2008-00447 and depicted in Figure 3.2-6. For the cementitious (concrete and saltstone) layer (depicted in Figure 3.2-12), the discretization in was assigned to be consistent with those used for the other SDU types.

TopLayerIndex_375 – The indices for the top cell-pathway element in each layer of the 375-ft diameter SDUs as presented in Table 3.2-9 are assigned to data element *TopLayerIndex_375*.

Table 3.2-8: Layer Thicknesses of Each 375-foot Diameter SDU

Layer	Layer Thicknesses (inches)
Saltstone	489*
Clean Grout	27*
SDU Roof	12
Lower Lateral Drainage	24
Lower Backfill	12
Foundation	12
Upper Lateral Drainage	12
Middle Backfill	12
Erosion Barrier	12

*Setting the *NoCleanGrout_150* selector to true, fills the Clean Grout Layer with Saltstone material

Table 3.2-9: Top Layer Index of Each 375-foot Diameter SDU

Layer	Top Layer Index
Saltstone	42
Clean Grout	51
SDU Roof	55
Lower Lateral Drainage	63
Lower Backfill	67
Foundation	71
Upper Lateral Drainage	75
Middle Backfill	79
Erosion Barrier	83

Figure 3.2-12: Schematic of Cementitious Layers of the SDFAPR Model Grid for the 375-foot Diameter SDUs

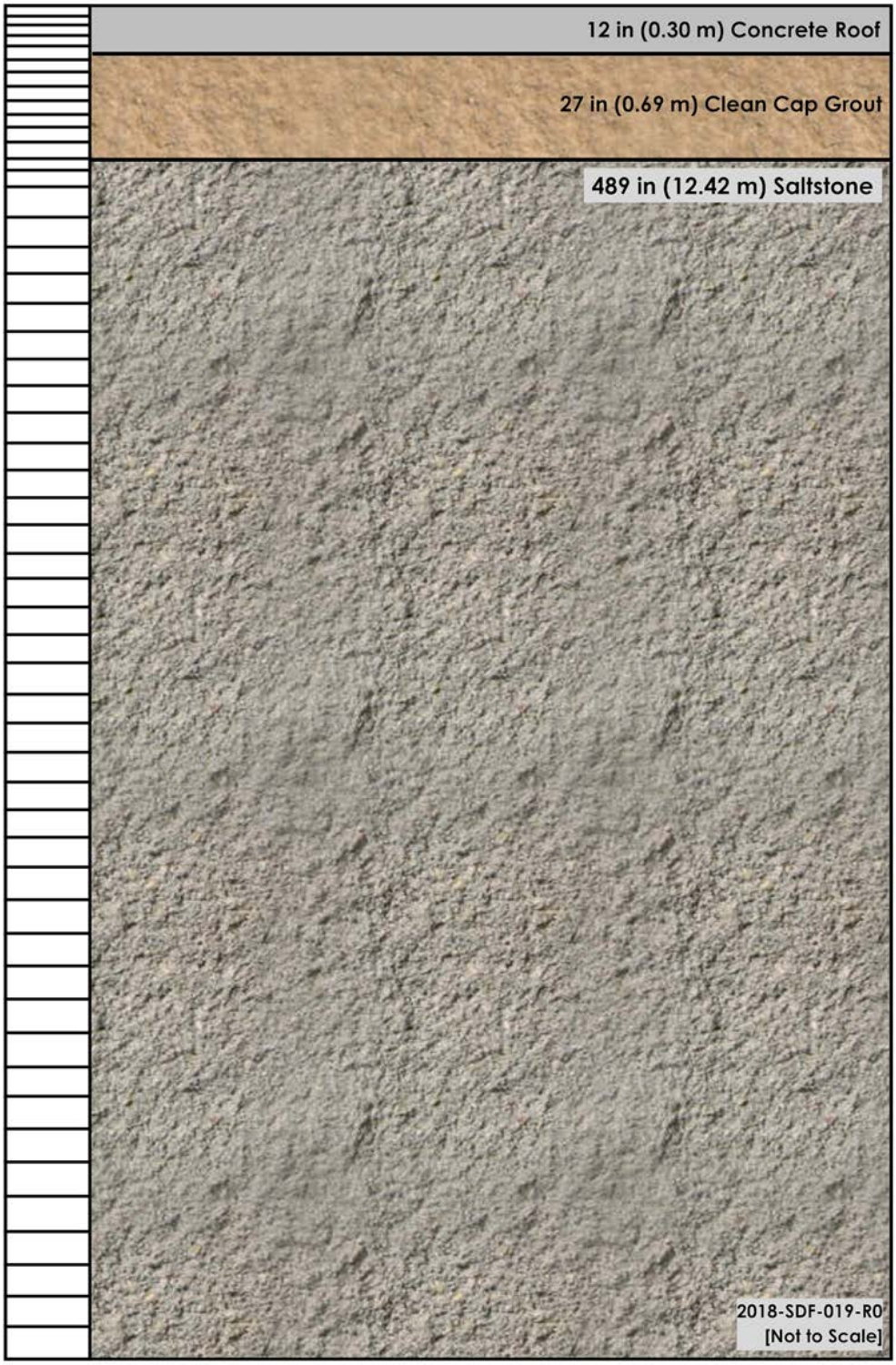

3.2.2.2 Physical Properties

The container *PhysicalProperties* is subdivided into four containers (see Figure 3.2-13), each one comprised of the data needed to assemble the Cell-pathway elements for each of the four SDU types.

Figure 3.2-13: Top Level of *PhysicalProperties* Container

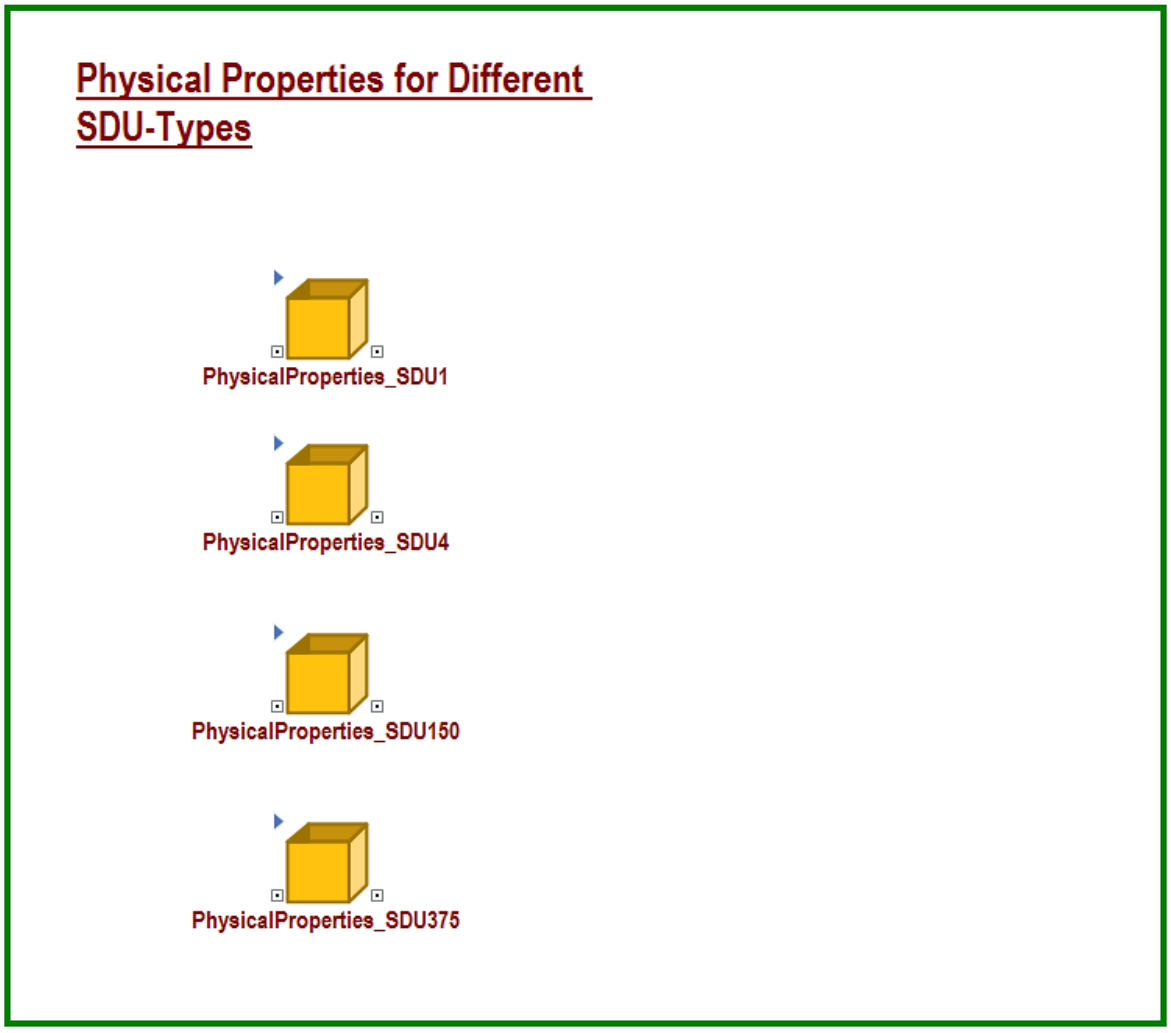

SDU 1

The data elements (and selector elements) used to assign the physical parameters used for the SDU 1 in the SAPR Model are found in the *PhysicalProperties_SDU1* container as depicted in Figure 3.2-14. The data input assigned to selector elements reflect saltstone parameters that may vary if the waste in SDU 1 is assumed to be DDA (Deliquification, Dissolution, and Adjustment) or ARP/MCU (Actinide Removal Process/Molecular Caustic Side Solvent Extraction Unit).

Figure 3.2-14: SDU 1 Physical Properties Container (*PhysicalProperties_SDU1*)

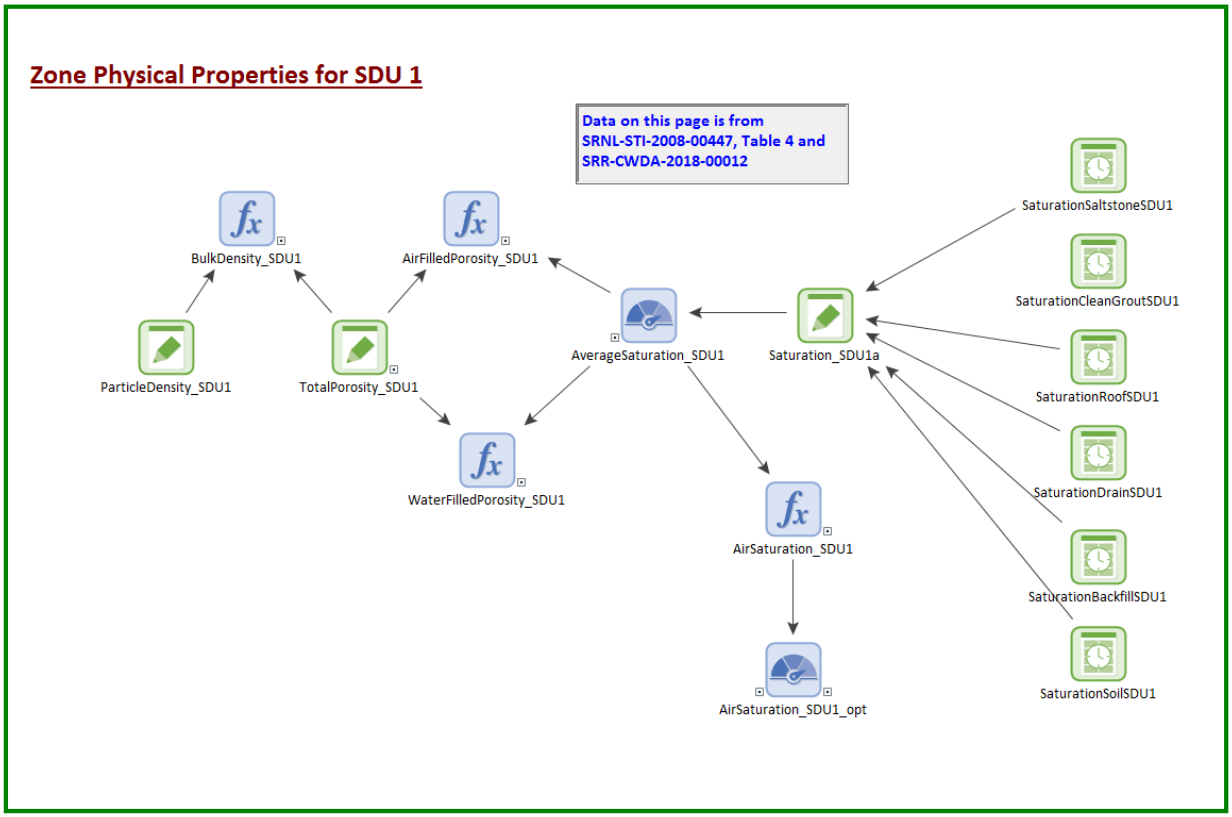

Table 3.2-10 (below) provides a summary of the values used to define the physical properties for SDU 1. The contents of the elements describing these physical properties for SDU 1 are as follows:

ParticleDensity_SDU1 – The particle density values used for SDU 1 as presented in Table 3.2-10 are assigned to data element *ParticleDensity_SDU1*. The particle density values are first taken from the recommended input values from SRR-CWDA-2018-00004.

TotalPorosity_SDU1 – The total porosity values used for SDU 1 as presented in Table 3.2-10 are assigned to data element *TotalPorosity_SDU1*. The total porosity values are first taken from the recommended input values from SRR-CWDA-2018-00004.

Table 3.2-10: Particle Density and Total Porosity for SDU 1

Layer	Particle Density (g/cm^3)	Total Porosity (fraction)
Erosion barrier	2.65	0.150
Middle backfill layer	2.63	0.350
Upper lateral drainage layer	2.65	0.417
Foundation layer	2.63	0.350
Lower backfill layer	2.63	0.350
Lower drainage layer	2.65	0.417
Concrete Roof	2.55	0.106
Saltstone (DDA & ARP/MCU), incl. Clean Grout	2.72	0.656

From SRNL-STI-2008-00447 Table 4 and SRR-CWDA-2018-00004 Table 1

Saturation_SDU1a – The saturation values used for SDU 1 as presented in Table 3.2-11 are assigned to data element *Saturation_SDU1a*. The time-based saturation values for saltstone, the roof, and the sand drainage layer were gathered from intermediate results generated by PORFLOW for the Vadose Zone Flow model of the SDF PA.

For the foundation layer, erosion barrier, and the backfill layers, the assumed saturation is assumed to be equal to the saturated volumetric water content for each layer, as presented in Table 1 of *Predicting Long-Term Percolation from the SDF Closure Cap* (SRRA107772-000009). However, it should be noted that saturated volumetric water content is not the same as saturation. For example, SRRA107772-000009 states that "the water content profile is relatively uniform with depth and near saturation in the erosion barrier and the middle backfill layer." Therefore, assuming that the saturated volumetric water content is equal to saturation is a conservative approach.

Table 3.2-11: Saturation by Layer for SDU 1

Time (yr)	Saltstone	Concrete Roof	Lower Sand Drainage Layer	Foundation and Erosion Barrier	Backfill Layers
0	0.9992	1.0000*	0.5141	0.15	0.40
23	0.9992	1.0000*	0.5141	0.15	0.40
100	0.9992	0.9516	0.5142	0.15	0.40
150	0.9992	0.8895	0.5144	0.15	0.40
200	0.9992	0.8515	0.5147	0.15	0.40
250	0.9992	0.8202	0.5149	0.15	0.40
300	0.9992	0.7939	0.5149	0.15	0.40
350	0.9992	0.7717	0.5153	0.15	0.40
400	0.9992	0.7527	0.5158	0.15	0.40
450	0.9992	0.7362	0.5165	0.15	0.40
500	0.9992	0.7218	0.5172	0.15	0.40
600	0.9997	0.7396	0.6230	0.15	0.40
700	0.9997	0.7217	0.6232	0.15	0.40
800	0.9997	0.7084	0.6232	0.15	0.40
853	0.9997	0.7048	0.6232	0.15	0.40
1000	0.9997	0.7127	0.6229	0.15	0.40
1200	0.9998	0.7328	0.6225	0.15	0.40
1400	0.9998	0.7466	0.6222	0.15	0.40
1600	0.9998	0.7508	0.6222	0.15	0.40
1800	0.9998	0.7519	0.6222	0.15	0.40
2000	0.9998	0.7521	0.6221	0.15	0.40
2300	0.9998	0.7638	0.6347	0.15	0.40
2600	0.9998	0.7638	0.6347	0.15	0.40
2900	0.9998	0.7638	0.6347	0.15	0.40
3200	0.9998	0.7638	0.6347	0.15	0.40
3600	0.9998	0.7638	0.6347	0.15	0.40
4000	0.9998	0.7638	0.6347	0.15	0.40
4579	0.9998	0.7638	0.6347	0.15	0.40
5000	0.9998	0.7638	0.6347	0.15	0.40
5500	0.9998	0.7638	0.6347	0.15	0.40
6000	0.9998	0.7638	0.6347	0.15	0.40
6500	0.9998	0.7638	0.6347	0.15	0.40
7000	0.9998	0.7638	0.6347	0.15	0.40
7500	0.9997	0.7638	0.6347	0.15	0.40
8000	0.9997	0.7638	0.6347	0.15	0.40
8500	0.9997	0.7638	0.6347	0.15	0.40
9000	0.9997	0.7638	0.6347	0.15	0.40
9500	0.9997	0.7638	0.6347	0.15	0.40
10000	0.9997	0.7638	0.6347	0.15	0.40
11000	0.9997	0.7638	0.6347	0.15	0.40
12000	0.9997	0.7638	0.6347	0.15	0.40
15000	0.9996	0.7638	0.6347	0.15	0.40
20000	0.9996	0.7638	0.6347	0.15	0.40
50000	0.9993	0.7638	0.6347	0.15	0.40
100000	0.9987	0.7639	0.6347	0.15	0.40

*To avoid mathematical errors, values of 0.9999 have been used in the model.

Other physical parameters used for SDU 1 that are based on the above input values, and the expression elements used to calculate their values (see Figure 3.2-14) include:

1) air saturation (*AirSaturation_SDU1*)
2) air-filled porosity (*AirFilledPorosity_SDU1*),
3) water-filled porosity (*WaterFilledPorosity_SDU1*), and
4) bulk density (*BulkDensity_SDU1*).

SDU 4

The data elements (and selector elements) used to assign the physical parameters used for the SDU 4 in the SDFAPR Model are found in the *PhysicalProperties_SDU4* container as depicted in Figure 3.2-15. The data input assigned to selector elements reflect saltstone parameters that may vary if the waste in SDU 4 is assumed to be DDA or ARP/MCU.

Figure 3.2-15: SDU 4 Physical Properties Container (PhysicalProperties_SDU4)

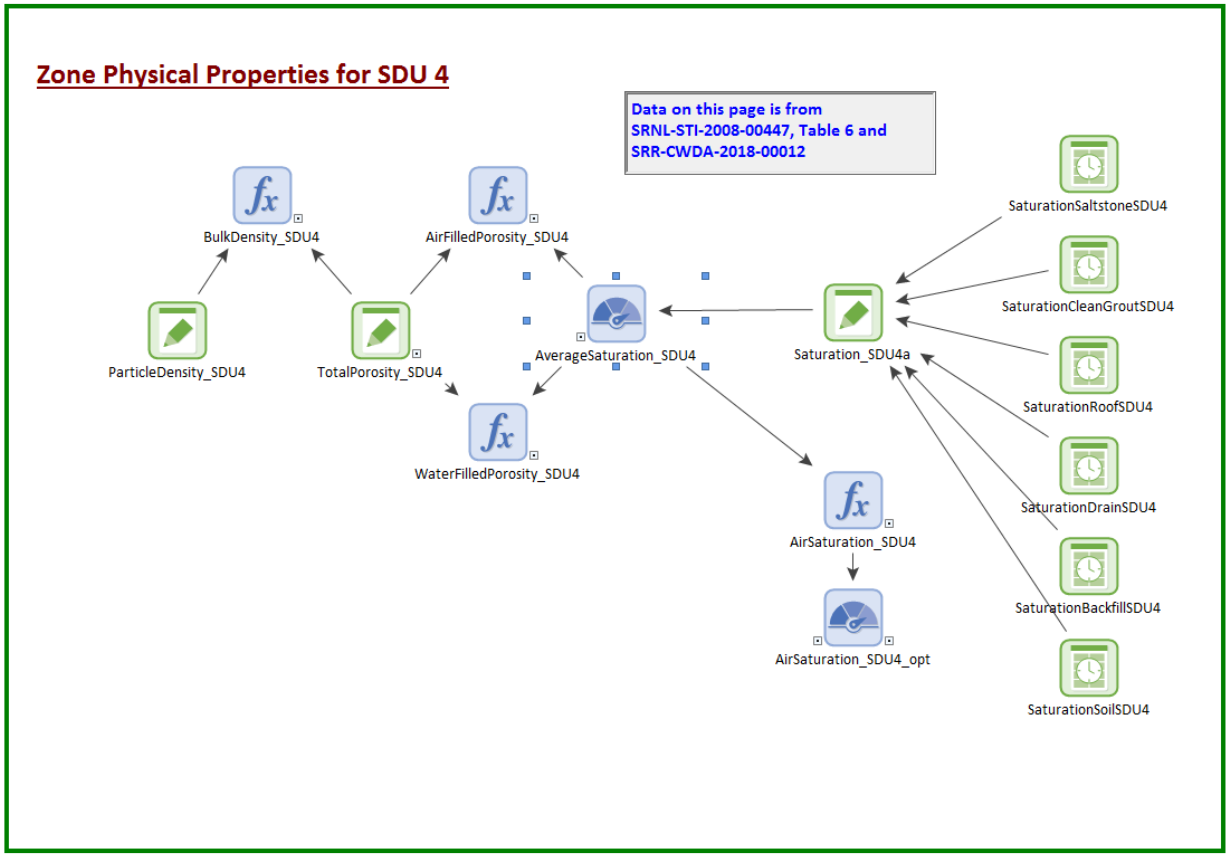

Table 3.2-12 (below) provides a summary of the values used to define the physical properties for SDU 4. The contents of the elements describing the physical properties of SDU 4 are as follows:

ParticleDensity_SDU4 – The particle density values used for SDU 4 as presented in Table 3.2-12 are assigned to data element *ParticleDensity_SDU4*. The particle density values are first taken from the recommended input values from SRR-CWDA-2018-00004.

TotalPorosity_SDU4 – The total porosity values used for SDU 4 as presented in Table 3.2-12 are assigned to data element *TotalPorosity_SDU4*. The total porosity values are first taken from the recommended input values from SRR-CWDA-2018-00004.

Table 3.2-12: Particle Density and Total Porosity for SDU 4

Layer	Particle Density (g/cm^3)	Total Porosity (fraction)
Erosion barrier	2.65	0.150
Middle backfill layer	2.63	0.350
Upper lateral drainage layer	2.65	0.417
Foundation layer	2.63	0.350
Lower backfill layer	2.63	0.350
Lower drainage layer	2.65	0.417
Concrete Roof	2.55	0.106
Saltstone (DDA & ARP/MCU), incl. Clean Grout	2.72	0.656

From SRNL-STI-2008-00447, Table 6 and SRR-CWDA-2018-00004 Table 1

Saturation_SDU4a – The saturation values used for SDU 4 as presented in Table 3.2-13 are assigned to data element *Saturation_SDU4a*. The time-based saturation values for saltstone, the roof, and the sand drainage layer were gathered from intermediate results generated by PORFLOW for the Vadose Zone Flow model of the SDF PA.

For the foundation layer, erosion barrier, and the backfill layers, the assumed saturation is conservatively assumed to be equal to the saturated volumetric water content for each layer, as presented in Table 1 of *Predicting Long-Term Percolation from the SDF Closure Cap* (SRRA107772-000009).

Table 3.2-13: Saturation by Layer for SDU 4

Time (yr)	Saltstone	Concrete Roof	Lower Sand Drainage Layer	Soil – Foundation and Erosion Barrier	Backfill Layers
0	0.9993	1.0000*	0.5081	0.15	0.40
50	0.9993	1.0000*	0.5081	0.15	0.40
100	0.9993	1.0000*	0.5081	0.15	0.40
144	0.9993	1.0000*	0.5081	0.15	0.40
200	0.9993	0.9478	0.5082	0.15	0.40
250	0.9993	0.8739	0.5084	0.15	0.40
300	0.9993	0.8235	0.5086	0.15	0.40
350	0.9993	0.7851	0.5089	0.15	0.40
400	0.9993	0.7552	0.5098	0.15	0.40
450	0.9993	0.7309	0.5105	0.15	0.40
500	0.9993	0.7111	0.5113	0.15	0.40
600	0.9997	0.7336	0.6495	0.15	0.40
698	0.9997	0.7125	0.6497	0.15	0.40
800	0.9997	0.7059	0.6497	0.15	0.40
900	0.9997	0.7184	0.6495	0.15	0.40
1000	0.9998	0.7331	0.6492	0.15	0.40
1200	0.9998	0.7548	0.649	0.15	0.40
1400	0.9998	0.7694	0.6489	0.15	0.40
1600	0.9998	0.7741	0.6488	0.15	0.40
1800	0.9998	0.7752	0.6488	0.15	0.40
2000	0.9998	0.7754	0.6488	0.15	0.40
2300	0.9998	0.7872	0.6635	0.15	0.40
2600	0.9998	0.7873	0.6636	0.15	0.40
2900	0.9998	0.7872	0.6635	0.15	0.40
3200	0.9998	0.7872	0.6635	0.15	0.40
3600	0.9998	0.7872	0.6635	0.15	0.40
4000	0.9998	0.7872	0.6635	0.15	0.40
4579	0.9998	0.7872	0.6635	0.15	0.40
5000	0.9998	0.7871	0.6635	0.15	0.40
5500	0.9998	0.7871	0.6635	0.15	0.40
6000	0.9998	0.7870	0.6634	0.15	0.40
6500	0.9998	0.7870	0.6634	0.15	0.40
7000	0.9999	0.7870	0.6634	0.15	0.40
7486	0.9999	0.7869	0.6634	0.15	0.40
8000	0.9999	0.7869	0.6634	0.15	0.40
8500	0.9999	0.7869	0.6633	0.15	0.40
9000	0.9999	0.7868	0.6633	0.15	0.40
9500	0.9999	0.7868	0.6633	0.15	0.40
10499	0.9999	0.7867	0.6632	0.15	0.40
11000	0.9999	0.7867	0.6632	0.15	0.40
12000	0.9999	0.7867	0.6632	0.15	0.40
15000	0.9998	0.7867	0.6632	0.15	0.40
20000	0.9998	0.7867	0.6632	0.15	0.40
50000	0.9995	0.7866	0.6632	0.15	0.40
100000	0.9989	0.7866	0.6632	0.15	0.40

*To avoid mathematical errors, values of 0.9999 have been used in the model.

Other physical parameters used for SDU 4, that are based on the above input values, and the expression elements used to calculate their values (see Figure 3.2-15) include:

1) air saturation (*AirSaturation_SDU4*),
2) air-filled porosity (*AirFilledPorosity_SDU4*),
3) water-filled porosity (*WaterFilledPorosity_SDU4*), and
4) bulk density (*BulkDensity_SDU4*).

150-foot Diameter SDUs

The data elements (and selector elements) used to assign the physical parameters used for the 150-foot diameter SDUs in the SDFAPR Model are found in the *PhysicalProperties_SDU150* container as depicted in Figure 3.2-16. The data input assigned to selector elements reflect saltstone parameters based on assuming that all waste in the 150-foot diameter SDUs reflect values appropriate for the SWPF saltstone.

Figure 3.2-16: 150-foot Diameter SDU Physical Properties Container (*PhysicalProperties_SDU150*)

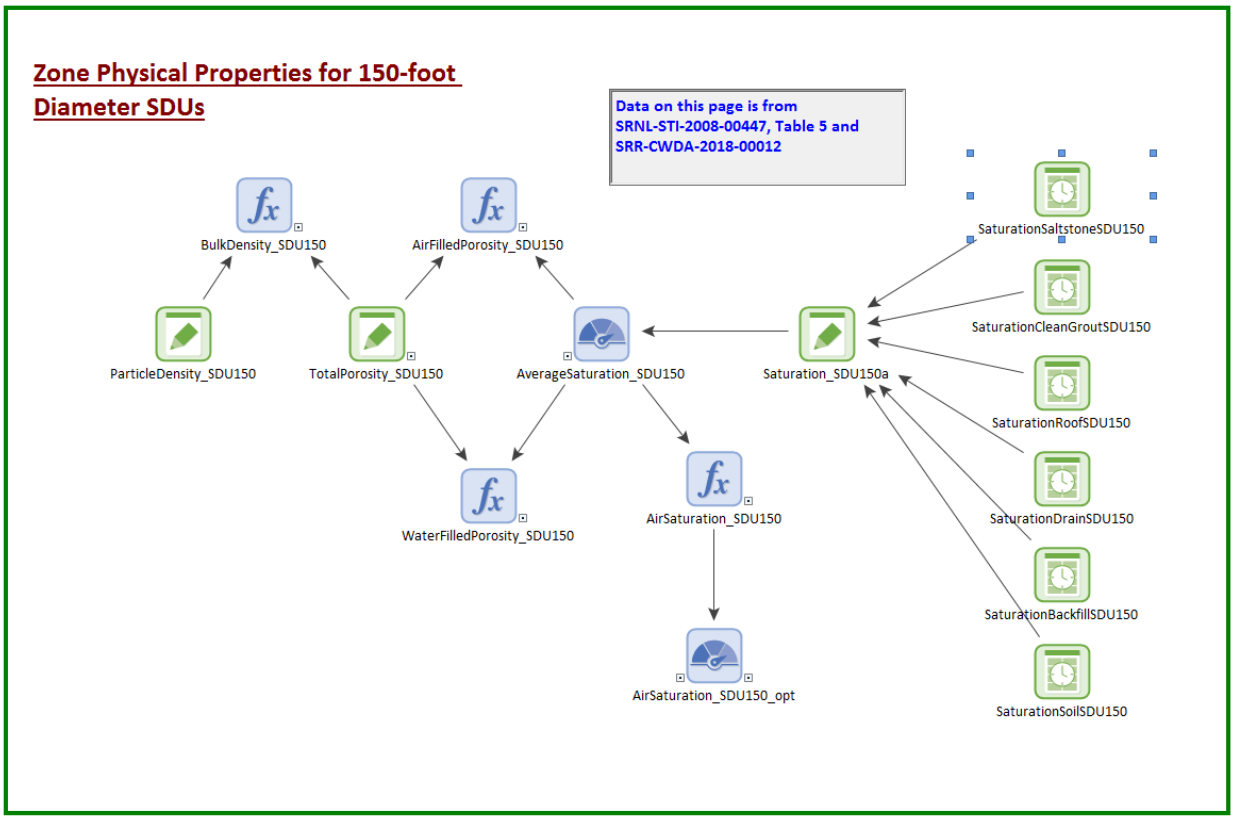

Table 3.2-14 (below) provides a summary of the values used to define the physical properties for the 150-foot diameter SDUs. The contents of the elements describing the physical properties of the 150-foot diameter SDUs are as follows:

ParticleDensity_SDU150 – The particle density values used for the 150-foot Diameter SDUs as presented in Table 3.2-14 are assigned to the data element *ParticleDensity_SDU150*. The particle density values are first taken from the recommended input values from SRR-CWDA-2018-00004.

TotalPorosity_SDU150 – The total porosity values used for the 150-foot Diameter SDUs as presented in Table 3.2-14 are assigned to data element *TotalPorosity_SDU150*. The total porosity values are first taken from the recommended input values from SRR-CWDA-2018-00004.

Table 3.2-14: Particle Density and Total Porosity for 150-Foot and 375-Foot Diameter SDUs

Layer	Particle Density (g/cm^3)	Total Porosity (fraction)
Erosion barrier	2.65	0.150
Middle backfill layer	2.63	0.350
Upper lateral drainage layer	2.65	0.417
Foundation layer	2.63	0.350
Lower backfill layer	2.63	0.350
Lower drainage layer	2.65	0.417
Concrete Roof	2.45	0.110
Saltstone, incl. Clean Grout	2.72	0.656

From SRNL-STI-2008-00447, Table 5 and SRR-CWDA-2018-00004 Table 1

Saturation_SDU150a – The saturation values used for the 150-foot Diameter SDUs as presented in Table 3.2-15 and are assigned to data element *Saturation_SDU150a*. The time-based saturation values for saltstone, the roof, and the sand drainage layer were gathered from intermediate results generated by PORFLOW for the Vadose Zone Flow model of the SDF PA.

For the foundation layer, erosion barrier, and the backfill layers, the assumed saturation is conservatively assumed to be equal to the saturated volumetric water content for each layer, as presented in Table 1 of *Predicting Long-Term Percolation from the SDF Closure Cap* (SRRA107772-000009).

Table 3.2-15: Saturation by Layer for 150-Foot Diameter SDUs

Time (yr)	Saltstone	Concrete Roof	Sand Drainage Layer	Soil – Foundation and Erosion Barrier	Backfill Layers
0	0.9996	0.9735	0.5212	0.15	0.40
54	0.9996	0.9735	0.5212	0.15	0.40
100	0.9996	0.9314	0.5213	0.15	0.40
150	0.9996	0.8976	0.5213	0.15	0.40
200	0.9996	0.8676	0.5214	0.15	0.40
250	0.9996	0.8419	0.5215	0.15	0.40
300	0.9996	0.8197	0.5215	0.15	0.40
350	0.9995	0.8002	0.5216	0.15	0.40
400	0.9995	0.7830	0.5218	0.15	0.40
450	0.9995	0.7677	0.5219	0.15	0.40
500	0.9995	0.7541	0.5220	0.15	0.40
600	0.9998	0.7727	0.6146	0.15	0.40
700	0.9998	0.7552	0.6148	0.15	0.40
800	0.9998	0.7414	0.6147	0.15	0.40
900	0.9998	0.7354	0.6146	0.15	0.40
1034	0.9999	0.7327	0.6144	0.15	0.40
1200	0.9999	0.7377	0.6142	0.15	0.40
1400	0.9999	0.7447	0.6141	0.15	0.40
1552	0.9999	0.7467	0.6141	0.15	0.40
1800	0.9999	0.7473	0.6141	0.15	0.40
2000	0.9998	0.7474	0.6141	0.15	0.40
2300	0.9999	0.7569	0.6253	0.15	0.40
2600	0.9999	0.7569	0.6253	0.15	0.40
2900	0.9998	0.7569	0.6253	0.15	0.40
3200	0.9998	0.7569	0.6252	0.15	0.40
3600	0.9998	0.7568	0.6252	0.15	0.40
4000	0.9998	0.7568	0.6252	0.15	0.40
4500	0.9998	0.7568	0.6252	0.15	0.40
5000	0.9998	0.7568	0.6252	0.15	0.40
5500	0.9998	0.7568	0.6252	0.15	0.40
6000	0.9998	0.7568	0.6252	0.15	0.40
6500	0.9998	0.7568	0.6252	0.15	0.40
7000	0.9998	0.7568	0.6252	0.15	0.40
7500	0.9998	0.7568	0.6252	0.15	0.40
8000	0.9998	0.7568	0.6252	0.15	0.40
8500	0.9998	0.7568	0.6252	0.15	0.40
9000	0.9997	0.7568	0.6252	0.15	0.40
9500	0.9997	0.7568	0.6252	0.15	0.40
10000	0.9997	0.7568	0.6252	0.15	0.40
11000	0.9997	0.7568	0.6252	0.15	0.40
12000	0.9997	0.7568	0.6252	0.15	0.40
15000	0.9997	0.7568	0.6252	0.15	0.40
20000	0.9996	0.7568	0.6252	0.15	0.40
50000	0.9993	0.7568	0.6252	0.15	0.40
100000	0.9986	0.7569	0.6252	0.15	0.40

Other physical parameters used for the 150-foot Diameter SDUs, that are based on the above input values, and the expression elements used to calculate their values (see Figure 3.2-16) include:

1) air saturation (*AirSaturation_SDU150*),
2) air-filled porosity (*AirFilledPorosity_SDU150*),
3) water-filled porosity (*WaterFilledPorosity_SDU150*), and
4) bulk density (*BulkDensity_SDU150*).

375-foot Diameter SDUs

The data elements (and selector elements) used to assign the physical parameters used for the 375-foot Diameter SDUs in the SDFAPR Model are found in the *PhysicalProperties_SDU375* container as depicted in Figure 3.2-17. The data input assigned to selector elements reflect saltstone parameters based on assuming that all waste in the 375-foot Diameter SDUs reflect values appropriate for the SWPF saltstone.

Figure 3.2-17: 375-foot Diameter SDU Physical Properties Container (*PhysicalProperties_SDU375*)

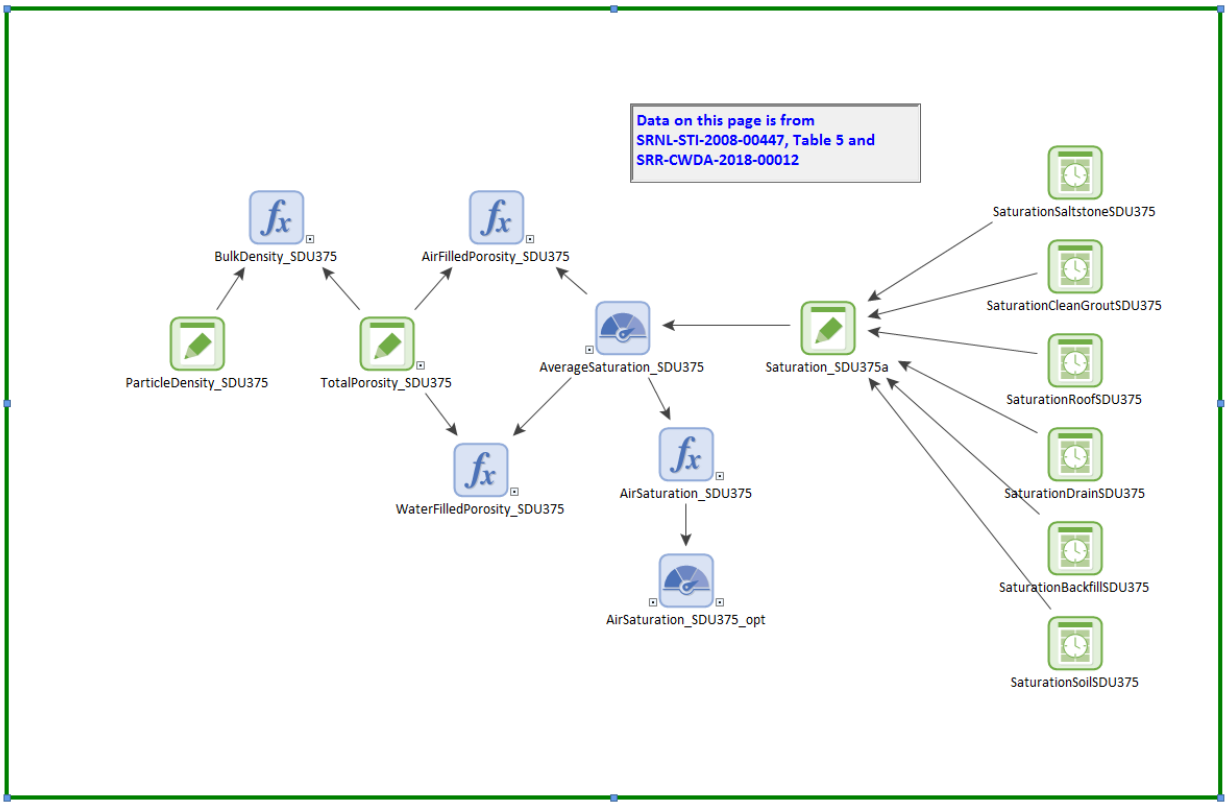

Table 3.2-14 (above) provides a summary of the values used to define the physical properties for the 375-foot diameter SDUs. The contents of the elements describing the physical properties of the 375-foot diameter SDUs are as follows:

ParticleDensity_SDU375 – The particle density values used for the 375-foot Diameter SDUs as presented in Table 3.2-14 are assigned to data element *ParticleDensity_SDU375*. The particle density values are first taken from the recommended input values from SRR-CWDA-2018-00004.

TotalPorosity_SDU375 – The total porosity values used for the 375-foot Diameter SDUs as presented in Table 3.2-14 are assigned to data element *TotalPorosity_SDU375*. The total porosity values are first taken from the recommended input values from SRR-CWDA-2018-00004.

Saturation_SDU375a – The saturation values used for the 375-foot Diameter SDUs as presented in Table 3.2-16 and are assigned to data element *Saturation_SDU375a*. The time-based saturation values for saltstone, the roof, and the sand drainage layer were gathered from intermediate results generated by PORFLOW for the Vadose Zone Flow model of the SDF PA.

For the foundation layer, erosion barrier, and the backfill layers, the assumed saturation is conservatively assumed to be equal to the saturated volumetric water content for each layer, as presented in Table 1 of *Predicting Long-Term Percolation from the SDF Closure Cap* (SRRA107772-000009).

Table 3.2-16: Saturation by Layer for 375-Foot Diameter SDUs

Time (yr)	Saltstone	Concrete Roof	Sand Drainage Layer	Soil – Foundation and Erosion Barrier	Backfill Layers
0	0.9995	0.9829	0.5167	0.15	0.40
50	0.9995	0.9829	0.5167	0.15	0.40
92	0.9995	0.9544	0.5171	0.15	0.40
150	0.9995	0.9270	0.5171	0.15	0.40
200	0.9995	0.9008	0.5171	0.15	0.40
250	0.9995	0.8793	0.5170	0.15	0.40
300	0.9995	0.8599	0.5170	0.15	0.40
350	0.9995	0.8424	0.5170	0.15	0.40
400	0.9995	0.8265	0.5170	0.15	0.40
450	0.9995	0.8120	0.5169	0.15	0.40
500	0.9995	0.7987	0.5169	0.15	0.40
600	0.9999	0.8249	0.6540	0.15	0.40
700	0.9998	0.8054	0.6541	0.15	0.40
800	0.9998	0.7895	0.6540	0.15	0.40
895	0.9999	0.7835	0.6537	0.15	0.40
1075	0.9999	0.7854	0.6534	0.15	0.40
1200	0.9999	0.7893	0.6532	0.15	0.40
1386	0.9999	0.7913	0.6531	0.15	0.40
1552	0.9999	0.7862	0.6531	0.15	0.40
1702	0.9999	0.7826	0.6531	0.15	0.40
2000	0.9999	0.7833	0.6531	0.15	0.40
2300	0.9999	0.7969	0.6677	0.15	0.40
2600	0.9999	0.7970	0.6677	0.15	0.40
2800	0.9999	0.7970	0.6677	0.15	0.40
3200	0.9999	0.7970	0.6677	0.15	0.40
3600	0.9999	0.7970	0.6677	0.15	0.40
4000	0.9999	0.7970	0.6677	0.15	0.40
4500	0.9999	0.7970	0.6677	0.15	0.40
5000	0.9999	0.7970	0.6677	0.15	0.40
5500	0.9998	0.7970	0.6677	0.15	0.40
6000	0.9998	0.7970	0.6677	0.15	0.40
6500	0.9998	0.7970	0.6677	0.15	0.40
7000	0.9998	0.7970	0.6677	0.15	0.40
7500	0.9998	0.7970	0.6677	0.15	0.40
8000	0.9998	0.7970	0.6677	0.15	0.40
8500	0.9998	0.7970	0.6677	0.15	0.40
9000	0.9998	0.7970	0.6677	0.15	0.40
9500	0.9998	0.7970	0.6677	0.15	0.40
10000	0.9998	0.7970	0.6677	0.15	0.40
11000	0.9998	0.7970	0.6677	0.15	0.40
12000	0.9998	0.7970	0.6677	0.15	0.40
15000	0.9998	0.7970	0.6677	0.15	0.40
20000	0.9998	0.7970	0.6677	0.15	0.40
50000	0.9996	0.7970	0.6677	0.15	0.40
100000	0.9993	0.7970	0.6677	0.15	0.40

Other physical parameters used for the 375-foot Diameter SDUs, that are based on the input values in Table 3.2-14, and the expression elements used to calculate their values (see Figure 3.2-17) include:

1) air saturation (*AirSaturation_SDU375*),
2) air-filled porosity (*AirFilledPorosity_SDU375*),
3) water-filled porosity (*WaterFilledPorosity_SDU375*), and
4) bulk density (*BulkDensity_SDU375*).

3.2.2.2 Chemical Properties

The chemical property data describing the partitioning of volatile radionuclides between the air and liquid phases and between the liquid and solid phases are found in the *ChemicalProperties* container. The container *ChemicalProperties* is subdivided into two containers (see Figure 3.2-18): one comprised of the data needed to describe partitioning between the air phase and the liquid phase (water) and the second comprised of the data needed to describe partitioning between the liquid phase (water) and the solid phase.

Figure 3.2-18: Top Level of *ChemicalProperties* Container

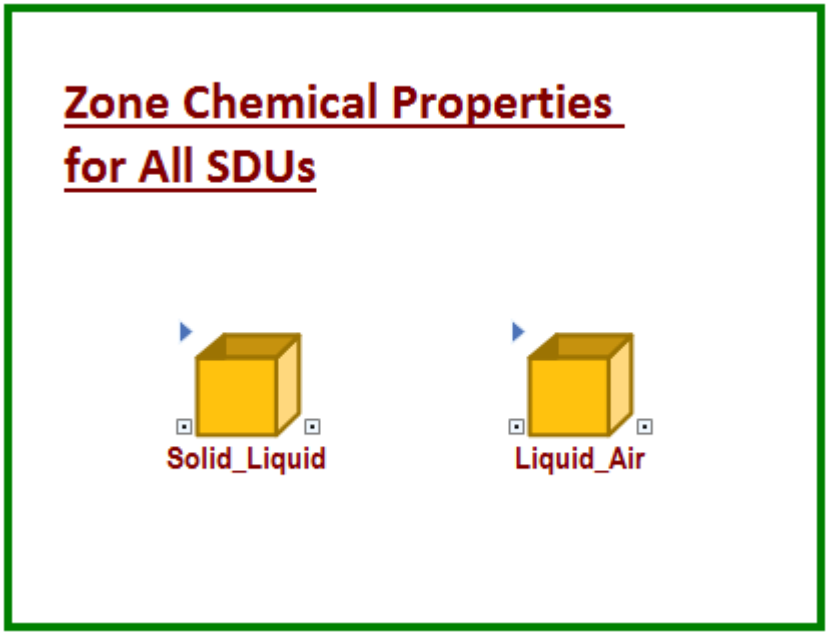

Liquid-Air Properties

The elements used to assign the chemical parameters describing partitioning between the water and air phases for SDU 1, SDU 4, the 150-foot diameter SDUs and the 375-foot diameter SDUs, in the SDFAPR Model are found in the *Liquid_Air* container depicted in the Figure 3.2-19. The inputted data include the apparent Henry's Law constants for saltstone, concrete, and soils, the Universal Gas Constant (0.082 atm-L/mol-K), and the temperature (in K) at which the apparent Henry's Law constants are evaluated.

Note that the model input in the form of apparent Henry's Law constants once set must be transformed to the required input for GoldSim Fluid media element, the air-water partitioning coefficient. The air-water partitioning coefficient is defined in terms of the inverse of the dimensionless Henry's Law solubility constant H^{cc} which is defined as follows in Sander, 2015:

$$H^{cc} = \frac{c_a}{c_g} \qquad \text{(Eq. 3-1)}$$

where:

c_a = the dissolved concentration of a species in the aqueous phase [M/L^3];

c_g = the dissolved concentration of a species in a gas phase [M/L^3].

Figure 3.2-19: Air-Water Partitioning Parameters (*Liquid_Air*)

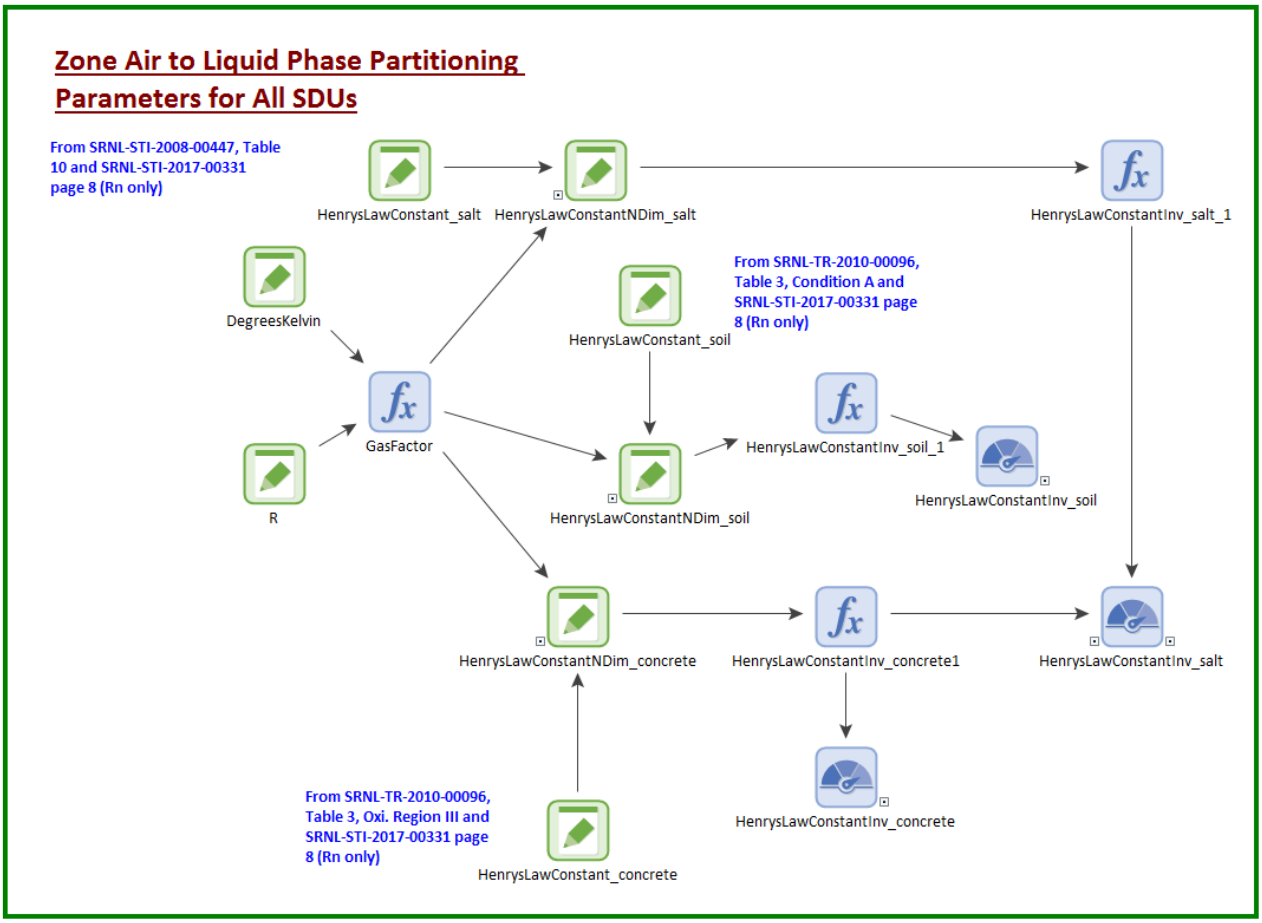

The conversion from the apparent Henry's Law constants to the air-water partitioning coefficient as calculated in the container *Liquid_Air* and used in the GoldSim model is based on the following equation:

$$K_{aw} = \frac{1}{H^a RT} \quad \text{(Eq. 3-2)}$$

where:

K_{aw} = the air-water partitioning coefficient;

H^a = the apparent Henry's Law constant [mol/atm-kg or mol/atm-liter assuming that $\rho_{water} \approx$ 1kg/liter];

R = the Universal Gas Constant (0.082 atm-L/mol-K).

T = the temperature [K].

All the apparent Henry's Law constants for the radionuclides of concern, except Rn-222, were estimated using The Geochemist's Workbench®, based on the potential gases considered for each radionuclide, their reactions with their aqueous components, and associated equilibrium constants for each reaction, as presented in Table 3.2-17. Where multiple gases were evaluated for one radionuclide, the gas with the highest fugacity was chosen. For Rn-222, the derivation of the apparent Henry's Law constants was based on data from SRNL-STI-2017-00331, wherein the apparent Henry's Law constants were developed to ensure the unitless inverse value was equal to 4.5 (i.e., the Rn value from SRNL-STI-2017-00331).

Table 3.2-17: Gases, Reactions with Aqueous Components, and Equilibrium Constants for Each Reaction used in The Geochemist's Workbench® for Each Radionuclide

Contaminant	Gas Species	Reaction	Log K (25°C)
C-14	CO_2	$CO_{2(g)} + H_2O = HCO_3^- + H^+$	-7.82
Cl-36	Cl_2	$Cl_{2(g)} + H_2O = 2Cl^- + 2H^+ + ½O_2$	3.03
Cl-36	$HClO_4$	$HClO_{4(g)} = Cl^- + 2O_2 + H^+$	33.38
Cl-36	HCl	$HCl_{(g)} = Cl^- + H^+$	6.31
H-3	H_2O	$H_2O_{(g)} = H_2O_{(l)}$	1.50
I-129	I_2	$I_{2(g)} + H_2O = 2I^- + ½O_2 + 2H^+$	-21.53
I-129	HI	$HI_{(g)} = I^- + H^+$	9.31
Sb-125, 126	$SbCl_3$	$SbCl_{3(g)} + 3H_2O = Sb(OH)_3^o + 3Cl^- + 3H^+$	4.83
Sb-125, 126	$SbCl_5$	$SbCl_{5(g)} + 4H_2O = Sb(OH)_3^o + 5Cl^- + ½O_2 + 5H^+$	2.74
Sb-125, 126	SbH_3	$SbH_{3(g)} + 3/2O_2 = Sb(OH)_3^o$	143.11
Se-79	H_2Se	$H_2Se_{(g)} + 3/2O_2 = SeO_3^{-2} + 2H^+$	71.83
Se-79	$SeCl_4$	$SeCl_{4(g)} + 3H_2O = SeO_3^{-2} + 4Cl^- + 6H^+$	13.78
Sn-121m, 126	$SnCl_4$	$SnCl_{4(g)} = Sn^{+4} + 4Cl^-$	15.85
Sn-121m, 126	SnH_4	$SnH_{4(g)} + 4H^+ = 4H_2 + Sn^{+4}$	20.10

From SRNL-STI-2008-00447, Table 8 (same as SRNL-TR-2010-00096, Table 1).

Table 3.2-18 provides additional parameters defining the pore-water chemistry used to estimate the apparent Henry's Law constants for saltstone.

Table 3.2-18: Parameters used in Estimating Apparent Henry's Law Constants for Saltstone

Parameter	Value Used
pH	11.0
Eh	-0.45 V
Na+	0.01 moles/kg
Cl-	0.01 moles/kg
T	25°C

From SRNL-STI-2008-00447, Table 9.

The different pore water compositions used in the calculations of apparent Henry's Law constants for the roof and closure cap were based on the chemical environments presented in Table 3.2-19. Conditions representing soil (Condition A) and aged concrete (Oxidized Region III) were used to represent the closure cap and roof, respectively.

Table 3.2-19: Pore Water Compositions Under Various Conditions

	pH	Eh (V)	Ca^{+2} (M)	Na^{+} (M)	Cl^{-} (M)	HCO_3^{-} (M)	SO_4^{-2} (M)
Reduced Region II	11.12	-0.48	3.3E-3	4.3E-4	4.3E-4	3.5E-8	1.0E-5
Oxidized Region II	11.13	0.58	3.2E-3	4.3E-4	4.3E-4	3.5E-8	1.0E-5
Oxidized Region III	8.23	0.73	4.6E-4	4.3E-4	4.3E-4	1.7E-6	1.0E-5
Condition A	5.4	0.37	6.2E-5	4.4E-5	8.5E-5	9.8E-5	6.3E-6
Condition B	9.3	0.27	2.0E-4	4.3E-5	1.5E-4	2.4E-4	6.2E-6
Condition C	9.8	-0.38	2.1E-4	4.0E-5	2.7E-4	4.2E-5	4.2E-5
Condition E	9.8	0.62	2.1E-4	4.1E-5	2.6E-4	4.2E-5	6.5E-6

From SRNL-TR-2010-00096, Table 2.

The contents and sources of the elements describing the partitioning of radionuclides between the air-to-liquid phases transport for saltstone, cementitious materials, and soils are as follows:

HenrysLawConstant_salt – In the SDFAPR Model, the species-dependent apparent Henry's Law constants for the radionuclides of concern within the saltstone monolith are assigned in the data element *HenrysLawConstant_salt*. The apparent Henry's Law constants values for saltstone, as assigned in *HenrysLawConstant_salt*, are listed in Table 3.2-20. Note that the Henry's Law constant values listed in Table 3.2-20 are listed in units of mole/atm-kg for consistency with the data source. The SDFAPR Model input is in terms of mole/atm-L which can be derived from the data in Table 3.2-20 by assuming that $\rho_{water} \approx 1$kg/liter.

Table 3.2-20: Radionuclides of Interest, the Dominant Gas Under Saltstone Conditions, and the Apparent Henry's Law Constant for Each Radionuclide

Radionuclide	Gas	H[a] (mole/atm-kg)
Tritium	Water Vapor	2.1×10^{3}
C-14	CO_2	1.4×10^{4}
Cl-36	HCl	2.3×10^{17}
I-129	HI	2.8×10^{20}
Rn-222	Rn	9.244×10^{-3}
Sn-126	SnH_4	2.2×10^{60}
Sb-125, 126	SbH_3	3.3×10^{34}
Se-79	H_2Se	1.1×10^{6}
Tc-99	Tc2O7	1.5×10^{67}

From SRNL-STI-2008-00447, Table 10, except for Rn-222. For Rn-222 the value was derived such that the inverse of the Henry's Law constant would be equal to 4.5 to reflect data from SRNL-STI-2017-00331.

HenrysLawConstant_concrete – In the SDFAPR Model, the species-dependent apparent Henry's Law constants for the radionuclides of concern within the concrete roof are assigned in the data element *HenrysLawConstant_concrete*. The apparent Henry's Law constants values for the roof, as assigned in *HenrysLawConstant_concrete*, are listed in Table 3.2-21. For the roof, the chemical environment is assumed to be Oxidized Region III. Note that the Henry's Law constant values listed in Table 3.2-21 are listed in units of mole/atm-kg for consistency with the data source. The SDFAPR Model input is in terms of mole/atm-L which can be derived from the data in Table 3.2-21 by assuming that $\rho_{water} \approx 1$kg/liter.

Table 3.2-21: Estimated Apparent Inverse of Henry's Law Constants (*moles/atm-kg*) for Each Radionuclide in Different Pore Water Compositions

	C-14	Cl-36	H-3	I-129	Rn-222	Sb-125	Se-79	Sn-126	Tc-99
Reduced Region II	8E+04 (CO_2)	3E+17 (HCl)	2.1E+03 (H_2O)	3.6E+20 (HI)		1.8E+35 (SbH_3)	1.8E+06 (H_2Se)	1.3E+61 (Sn)	4.8E+67 (Tc_2O_7)
Oxidized Region II	8.1E+04 (CO_2)	3.2E+17 (HCl)	2.1E+03 (H_2O)	1.1E+33 (HI)		8.7E+70 ($SbCl_3$)	2.5E+101 (H_2Se)	1.8E+71 ($SnCl_4$)	5.7E+51 (Tc_2O_7)
Oxidized Region III	2.8E+00 (CO_2)	3.6E+14 (HCl)	2.1E+03 (H_2O)	1.3E+29 (HI)	9.2E-03 (Rn)	4.9E+38 ($SbCl_3$)	3.8E+87 ($SeCl_4$)	6.1E+61 ($SnCl_4$)	7.2E+45 (Tc_2O_7)
Condition A	3.8E-02 (CO_2)	5.2E+11 (HCl)	2.1E+03 (H_2O)	6.3E+14 (HI)	9.2E-03 (Rn)	6.9E+32 ($SbCl_3$)	2.8E+25 (H_2Se)	9.6E+53 ($SnCl_4$)	1.5E+40 (Tc_2O_7)
Condition B	3.6E+01 (CO_2)	4.1E+15 (HCl)	2.1E+03 (H_2O)	5.1E+18 (HI)		4.3E+44 ($SbCl_3$)	2.4E+44 (H_2Se)	5.1E+69 ($SnCl_4$)	9.6E+47 (Tc_2O_7)
Condition C	1.6E+02 (CO_2)	1.4E+16 (HCl)	2.1E+03 (H_2O)	1.7E+19 (HI)		3.5E+34 ($SbCl_3$)	8.5E+04 (H_2Se)	4.7E+60 (Sn)	2.1E+68 (Tc_2O_7)
Condition D	1.6E+02 (CO_2)	1.4E+16 (HCl)	2.1E+03 (H_2O)	7.0E+29 (HI)		9.9E+44 ($SbCl_3$)	1.6E+96 (H_2Se)	4.8E+98 ($SbCl_4$)	!.2E+49? (Tc_2O_7)

Note: Adapted from SRNL-TR-2010-00096, Table 3, except for Rn-222, which was derived based on SRNL-STI-2017-00331. The pore water compositions are provided in Table 3.2-19. The dominant gas for each radionuclide is shown in parentheses.

HenrysLawConstant_soil – In the SDFAPR Model, the species-dependent apparent Henry's Law constants for the radionuclides of concern within the closure cap are assigned in the data element *HenrysLawConstant_soil*. The apparent Henry's Law constants for the closure cap, assigned in *HenrysLawConstant_soil*, are listed in Table 3.2-21. For the closure cap, comprised of backfill and sand, the chemical environment is assumed to be Condition A.

R – The Universal Gas Constant (0.082 atm-L/mol-K) is assigned to the data element *R*, in the SDFAPR Model.

DegreesKelvin – The temperature, of 293 K, at which the Henry's Law constants used in the SDFAPR Model were evaluated (assumes a temperature of 20 °C) is assigned to the data element *DegreesKelvin*.

Solid-Liquid Properties

The elements used to assign the chemical parameters describing partitioning between the solid and water phases for SDU 1, SDU 4, the 150-foot diameter SDUs, and the 375-foot diameter SDUs, in the SDFAPR Model are found in the *Solid_Liquid* container, as depicted in Figure 3.2-20. The inputted data include linear solid-liquid phase partition coefficients (K_ds) for the cementitious materials (saltstone, clean grout, and the roof), clayey material (backfill), and sandy material (drainage layers).

Figure 3.2-20: Solid-Water Partitioning Parameters (*Solid_Liquid*)

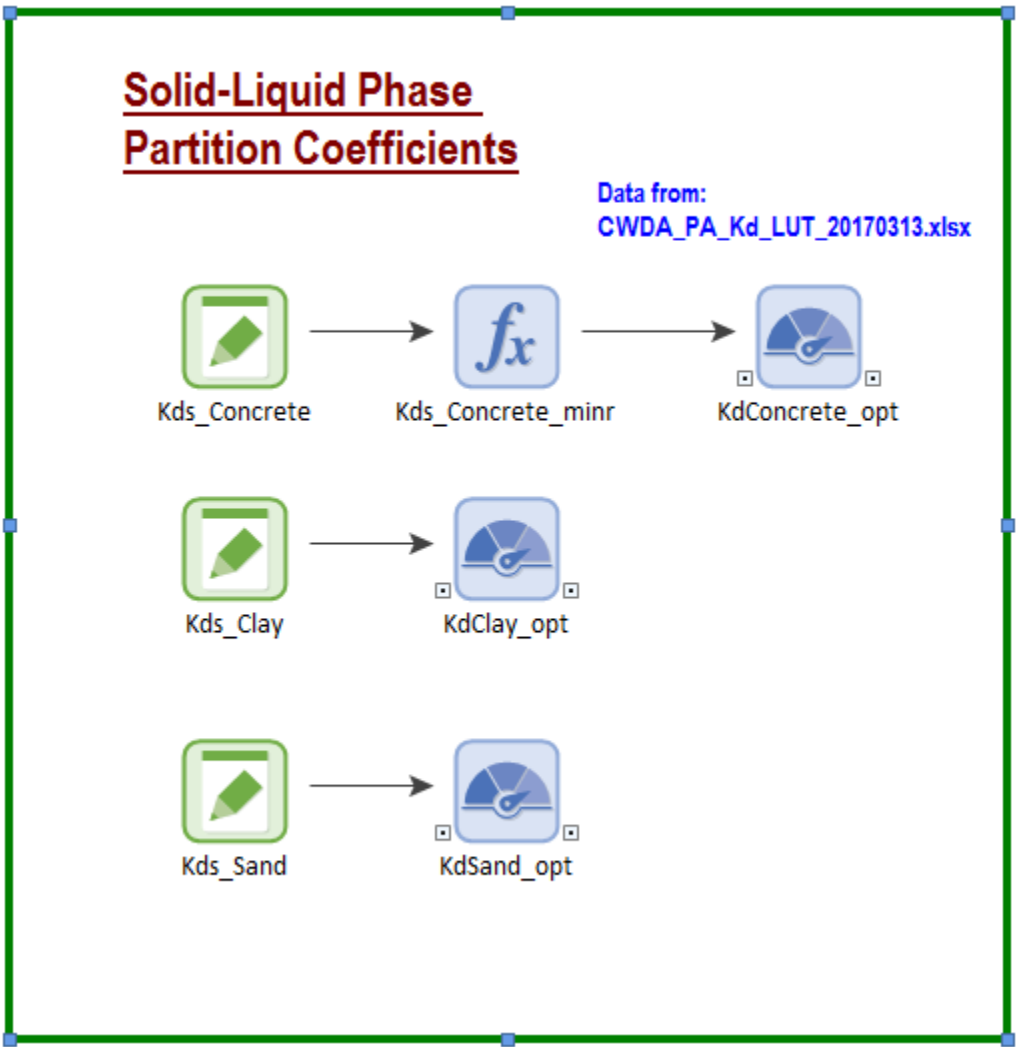

Kds_Concrete – The linear solid-liquid phase partition coefficients, K_ds, for cementitious materials are assigned in the element *Kds_Concrete*. The K_d matrix shown in Table 3.2-22 contains species-specific values for the Reduced Region I, Reduced Region II, Reduced Region III, Oxidized Region I, Oxidized Region II, and Oxidized Region III chemical environments. As a conservative assumption, the minimum K_d in each row (for each species) of Table 3.2-22 is used in the model.

Kds_Clay – The linear solid-liquid phase partition coefficients, K_ds, for clayey backfill type materials, listed in Table 3.2-23, are assigned in the element: *Kds_Clay*.

Kds_Sand – The linear solid-liquid phase partition coefficients, K_ds, for sandy-type materials used in the drainage layers are assigned in the element: *Kds_Sand*. The values assigned to *Kds_Sand* are listed in Table 3.2-23.

Table 3.2-22: Solid-Liquid Phase Partition Coefficients (K_ds) for Cementitious Materials

	Reduced Region I (ml/g)	Reduced Region II (ml/g)	Reduced Region III (ml/g)	Oxidized Region I (ml/g)	Oxidized Region II (ml/g)	Oxidized Region III (ml/g)
C-14	2000	5000	50	2000	5000	50
Cl-36	0	10	1	0	10	1
Cm-246	7000	7000	1000	6000	6000	600
H-3	0	0	0	0	0	0
***I-129**	0	2	0	8	10	4
***I-129**	0.07	0.71	0.71	0.71	0.71	0.71
Pu-238	10000	10000	2000	10000	10000	2000
Pu-242	10000	10000	2000	10000	10000	2000
***Ra-226**	6000	6000	600	200	100	200
***Ra-226**	6000	6000	600	6000	6000	600
Rn-222	0	0	0	0	0	0
Sb-125	200	200	100	200	200	100
Sb-126	200	200	100	200	200	100
Se-79	300	300	200	3	3	3
Sn-126	4000	4000	2000	4000	4000	2000
Tc-99	1000	1000	1000	0.8	0.8	0.5
Th-230	10000	10000	2000	10000	10000	2000
U-234	5000	5000	5000	1000	5000	5000
U-238	5000	5000	5000	1000	5000	5000

Note: * I-129 and Ra-226 each have two sets of K_d values for cementitious materials. The first values listed are specific to the SDU concrete only, while the second values listed (shaded) are specific to the saltstone waste form. Note that the recommended I-129 K_ds for saltstone are based on SRR-CWDA-2018-00045; however, this reference recommends a K_d change after only a single pore volume has infiltrated through the material. While the transition from Reduced Region I to Reduced Region II is expected to take more than a single pore volume, this chemical transition is conservatively assumed as the trigger for the I-129 K_d change. [Source: SRNL-STI-2009-00473, SRR-CWDA-2017-00019, and SRR-CWDA-2018-00045]

Table 3.2-23: Solid-Liquid Phase Partition Coefficients (K_ds) for Soils

	Clayey/ Backfill (ml/g)	Sand (ml/g)
C-14	400	10
Cl-36	8	1
Cm-246	9000	1000
H-3	0	0
I-129	3	1
Pu-238	6000	650
Pu-242	6000	650
Ra-226	200	30
Rn-222	0	0
Sb-125	3000	3000
Sb-126	3000	3000
Se-79	1000	1000
Sn-126	5000	2000
Tc-99	1.8	0.6
Th-230	2000	900
U-234	400	300
U-238	400	300

[Source: SRNL-STI-2009-00473 and SRR-CWDA-2017-00019]

3.2.2.3 Transport Properties

The SDFAPR Model assumes that diffusion in the air phase is the dominant radionuclide transport process. In the SDFAPR Model, the reference (Rn-222) diffusion coefficient value from SRNL-STI-2008-00447 is used as an input. Then, an effective reference (Rn-222) air phase diffusion coefficient is calculated based on material-specific conditions using the equation below. [Rogers, 1991]

$$D_{eff(Rn-222)} = D_{air(Rn-222)} \varphi e^{-(6S\varphi + 6S^{14\varphi})} \quad \text{(Eq. 3-3)}$$

where:

$D_{eff(Rn\text{-}222)}$ = effective air diffusion coefficient for Rn-222 [L^2/T];

$D_{air(Rn\text{-}222)}$ = reference diffusion coefficient for Rn-222 in air [L^2/T];

φ = total porosity

S = saturation

The species-specific diffusivity values are generated internally from the reference values using Graham's Law which can be defined as follows:

$$D_{Rad} = D_{Ref} \sqrt{\frac{MWT_{Ref}}{MWT_{Rad}}} \quad \text{(Eq. 3-4)}$$

where:

D_{Rad} = effective air diffusion coefficient for species *Rad* [L^2/T];

D_{Ref} = effective air diffusion coefficient for the reference species (Rn-222) [L^2/T];

MWT_{Rad} = molecular weight for species *Rad*;

MWT_{Ref} = molecular weight for the reference species (Rn-222).

The transport properties container, *TransportProperties*, is subdivided into three containers (see Figure 3.2-21). One container is comprised of the effective diffusion coefficient inputs for the grout materials (saltstone and clean cap grout) and used to generate the species-specific effective diffusivities for grout (*EffectiveDiffusivity_salt*). Another container holds the species-specific effective diffusion coefficient inputs for the concrete roof (*EffectiveDiffusivity_cement*). The last container holds the species-specific effective diffusion coefficient inputs for the closure-cap materials (*EffectiveDiffusivity_soil*). Note that because grout and other cementitious materials may differ between SDU types, diffusivity data is generated for each SDU type.

Figure 3.2-21: Top Level of *TransportProperties* Container

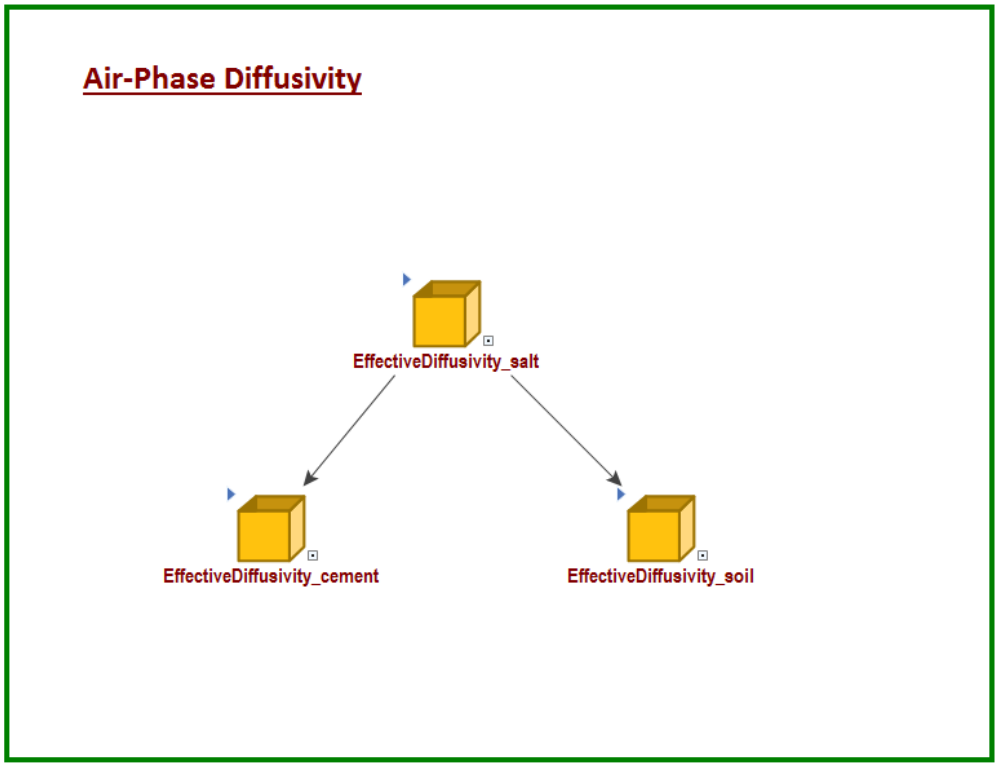

Saltstone/Grout Diffusivity Data

The contents of *EffectiveDiffusivity_salt*, are depicted in Figure 3.2-22. The reference (Rn-222) diffusion coefficient value from SRNL-STI-2008-00447 is input in the container *EffectiveDiffusivity_salt*. The effectivity diffusivity of Rn-222 is calculated for each of the materials using Equation 3-3. Note that molecular weights used here for saltstone and clean

cap grout represent the molecular weights of the expected gases containing the radionuclide or as a conservatism the radionuclide alone.

Figure 3.2-22: Contents of the *EffectiveDiffusivity_salt* Container

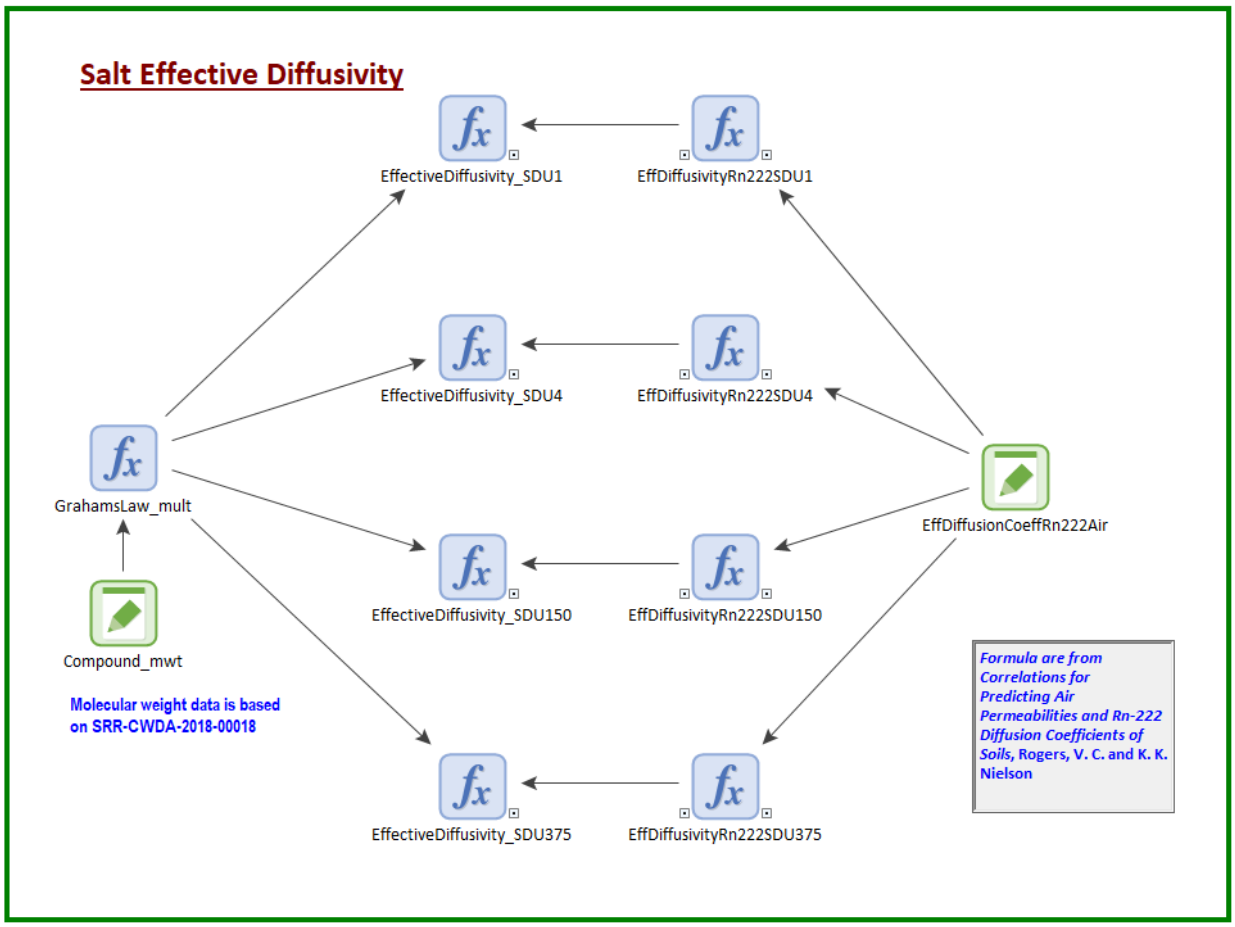

Compound_mwt – The molecular weights for the expected saltstone (and clean cap grout) volatile gases, containing the radionuclide or as a conservatism assumed to be the radionuclide alone, are listed in Table 3.2-24 and assigned in the GoldSim element *Compound_mwt*. These molecular weights were developed from the *Database Compilation of Radionuclides Standardized with Half-Lives in Seconds and Specific Activity in Ci/g* (SRR-CWDA-2018-00018), and represent molecular weights for volatile gases expected in a saltstone/clean cap grout or as a conservatism the atomic weights of specific radionuclides are used (for Sb-125, Sb-126, Se-79, Sn-126, and Tc-99). Note that for consistency with the assumption that pore spaces in materials above the saltstone are fully unsaturated with respect to water (ZeroSaturation>0), all molecular weights used here for saltstone and clean cap grout will also be used for all materials above the saltstone monolith.

Table 3.2-24: Molecular Weights for Expected Gases in Saltstone and Clean Cap Grout Material

Radionuclide	Molecular Form in Gaseous State	Molecular Weight
C-14	CO_2	46.00
Cl-36	Cl_2	71.94
H-3	H_2	6.032
I-129	I_2	257.8
Rn-222	Rn	222.0
Sb-125	Sb	124.9
Sb-126	Sb	124.9[a]
Se-79	Se	78.92
Sn-126	Sn	125.9
Tc-99	Tc	98.91

[Source: Developed from SRR-CWDA-2018-00018]
Notes: (a) The molecular weight for Sb-126 is set equal to Sb-125 to avoid warning messages associated with GoldSim's requirement that all diffusion coefficients for isotopes be the same. GoldSim would use the Sb-125 diffusion coefficient value (the smaller) for Sb-126 even if an atomic weight of 126 was used, but it would also generate a number of warning messages.

The remaining elements within the *EffectiveDiffusivity_salt* container use these inputs to perform Equation 3-3 to determine the remaining radionuclide-specific effective diffusion coefficients.

SDU Roof Diffusivity Data

The contents of *EffectiveDiffusivity_cement* are depicted in Figure 3.2-23. Note that the reference effective diffusion coefficients are the same as assigned in the *EffectiveDiffusivity_salt* container. The molecular weights used here are mostly consistent

with the radionuclide bearing molecules found in Table 3.2-21 for the Oxidized Region III chemical environment (for all except for technetium).

Figure 3.2-23: Contents of the *EffectiveDiffusivity_cement* Container

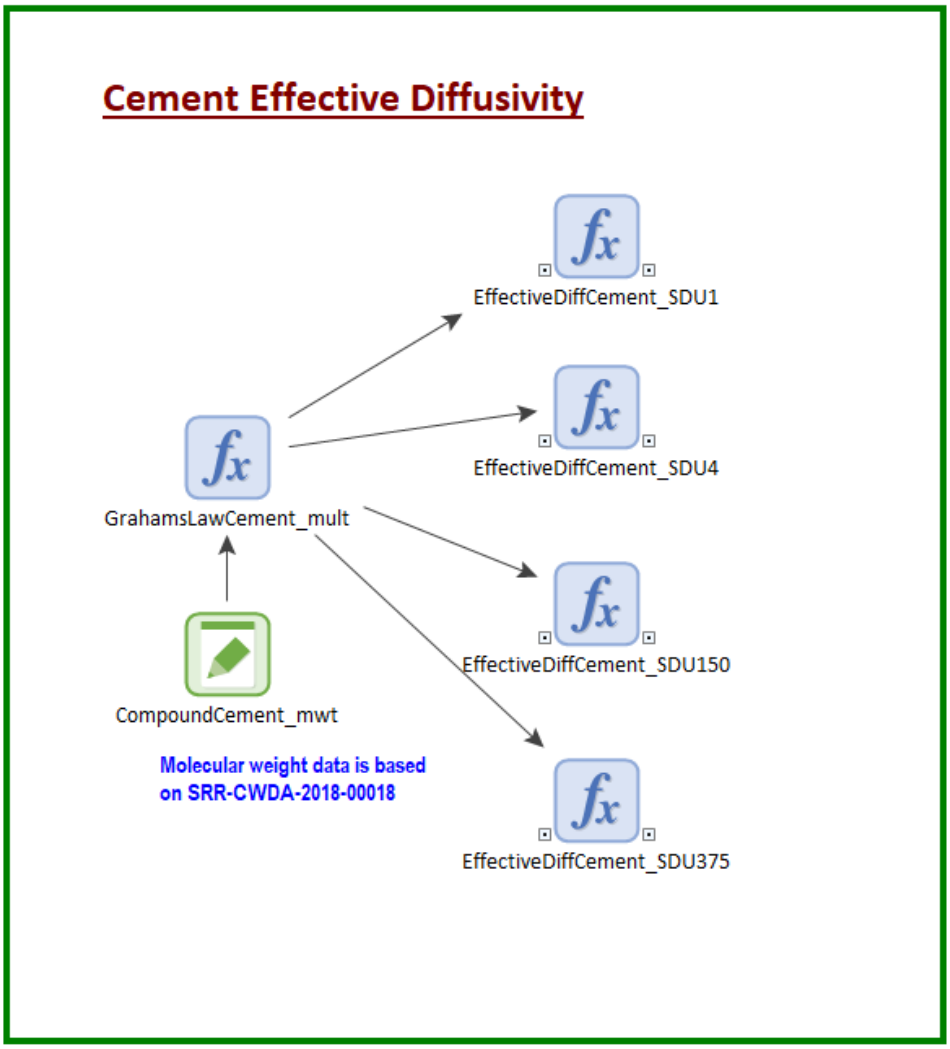

CompoundCement_mwt – The molecular weights for radionuclide gases that would be expected to form in the Oxidized Region III cementitious chemical environment assumed for the SDU roof (see Table 3.2-21) are listed in Table 3.2-25 and assigned in the GoldSim data element *CompoundCement_mwt*. These molecular weights represent molecular weights for volatile gases expected in the roof or as a conservatism based on a molecule of lower molecular weight (as is assumed for Tc-99).

Table 3.2-25: Molecular Weights for Expected Gases Generated in the Roof

Radionuclide	Molecular Form in Gaseous State	Molecular Weight
C-14	CO_2	46.00
Cl-36	HCl	36.98
H-3	H_2O (^3HOH)	20.02
I-129	HI	129.9
Rn-222	Rn	222.0
Sb-125	$SbCl_3$	231.3
Sb-126[a]	$SbCl_3$	231.3
Se-79	H_2Se	80.93
Sn-126	$SnCl_4$	267.7
Tc-99	TcO_3	146.9

[Source: Developed from SRR-CWDA-2018-00018]
Notes: (a) The molecular weight for Sb-126 is set equal to Sb-125 to avoid warning messages associated with GoldSim's requirement that all diffusion coefficients for isotopes be the same. GoldSim would use the Sb-125 diffusion coefficient value (the smaller) for Sb-126 even if an atomic weight of 126 was used, but it would also generate a number of warning messages.

Closure-Cap Diffusivity Data

The contents of *EffectiveDiffusivity_soil* are depicted in Figure 3.2-24. Note that the reference effective diffusion coefficients are the same as assigned in the *EffectiveDiffusivity_salt* container. The molecular weights used here are mostly consistent with the radionuclide bearing molecules found in Table 3.2-21 for the Condition A chemical environment (for all except for technetium).

CompoundSoil_mwt – The molecular weights for radionuclide gases that would be expected to form in the Condition A cementitious environment assumed for the closure cap (see Table 3.2-21) are listed in Table 3.2-26 and assigned in the GoldSim data element *CompoundSoil_mwt*. These molecular weights represent volatile gases expected to form in the closure cap, or as a conservatism based on a molecule of lower molecular weight (for Tc-99).

Figure 3.2-24: Contents of the *EffectiveDiffusivity_soil* Container

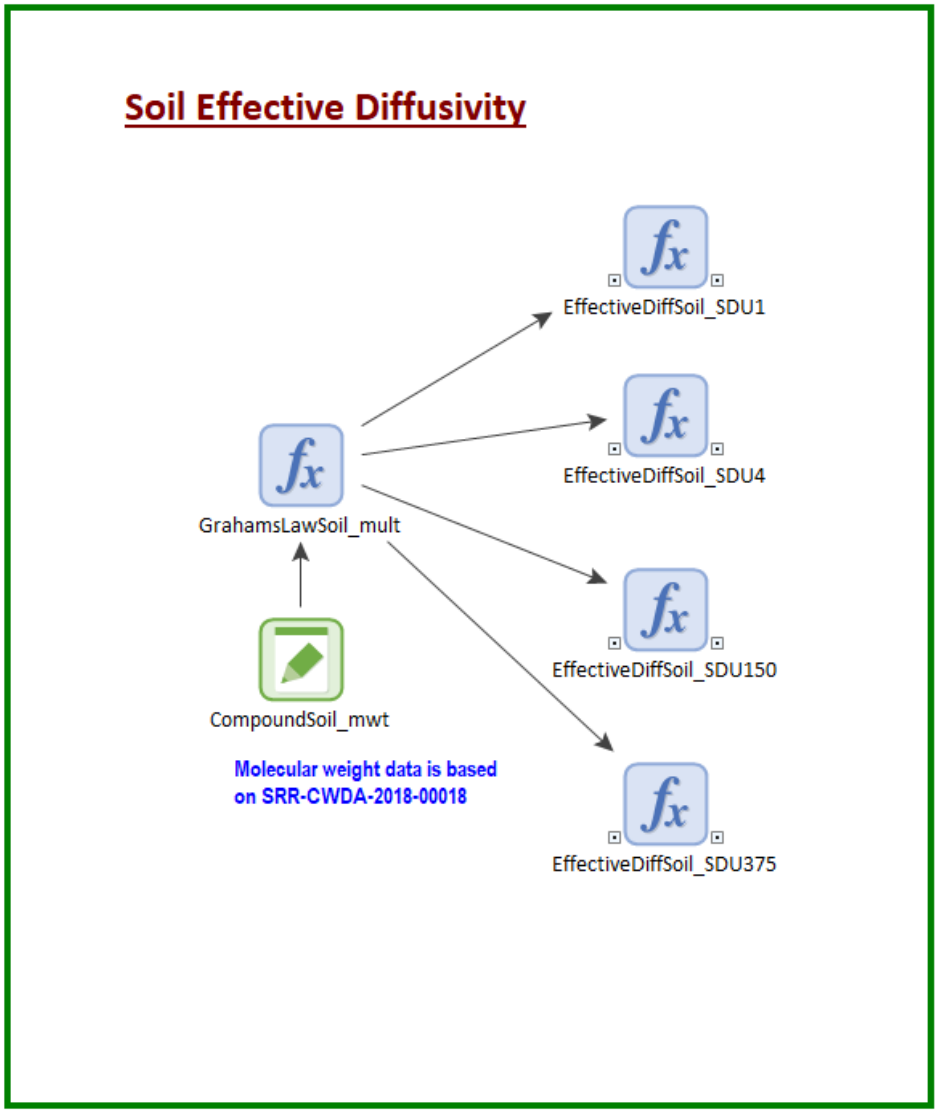

Table 3.2-26: Molecular Weights for Expected Gases in the Closure Cap

Radionuclide	Molecular Form in Gaseous State	Molecular Weight
C-14	CO_2	46.00
Cl-36	HCl	36.98
H-3	H_2O	20.02
I-129	HI	129.9
Rn-222	Rn	222.0
Sb-125	$SbCl_3$	231.3
Sb-126[a]	$SbCl_3$	231.3
Se-79	$SeCl_4$	220.7
Sn-126	$SnCl_4$	267.7
Tc-99	TcO_3	146.9

[Source: Developed from SRR-CWDA-2018-00018]
Notes: (a) The molecular weight for Sb-126 is set to 125 for consistency with Sb-125 to avoid warning messages associated with GoldSim's requirement that all diffusion coefficients for isotopes be the same. GoldSim would use the Sb-125 diffusion coefficient value (the smaller) for Sb-126 even if an atomic weight of 126 was used, but it would also generate a number of warning messages.

3.2.2.4 SDU Inventories

The data element *NominalInventory* used to assign the SDU inventories for SDU 1, SDU 4, the 150-foot diameter SDUs and the 375-foot diameter SDUs, in the SDFAPR Model, is found in the *Inventory* container depicted in Figure 3.2-25. The specific inventory values are provided in the following tables.

The *Inventory* container also contains GoldSim Stochastic Elements to allow the user to evaluate the influence of uncertainty with respect to the inventory values relative to the release of radionuclides to the atmosphere. The data elements used to control the inventories released in the SDFAPR Model are discussed below.

NominalInventory – The radionuclide mass inventories (in Curies) used to set the initial conditions within the cell pathway elements defining saltstone monoliths within the SDU 1, SDU 4, the 150-foot diameter SDUs and the 375-foot diameter SDUs are assigned in the GoldSim data element *NominalInventory*. The inventory values were taken from *Inventory Screening Methodology and Application to the FY2019 Saltstone Disposal Facility (SDF) Performance Assessment (PA) Inventory* using the MPAD case and are presented below in the following tables. [SRR-CWDA-2018-00044]

Figure 3.2-25: SDU Inventory Containers (*Inventory*)

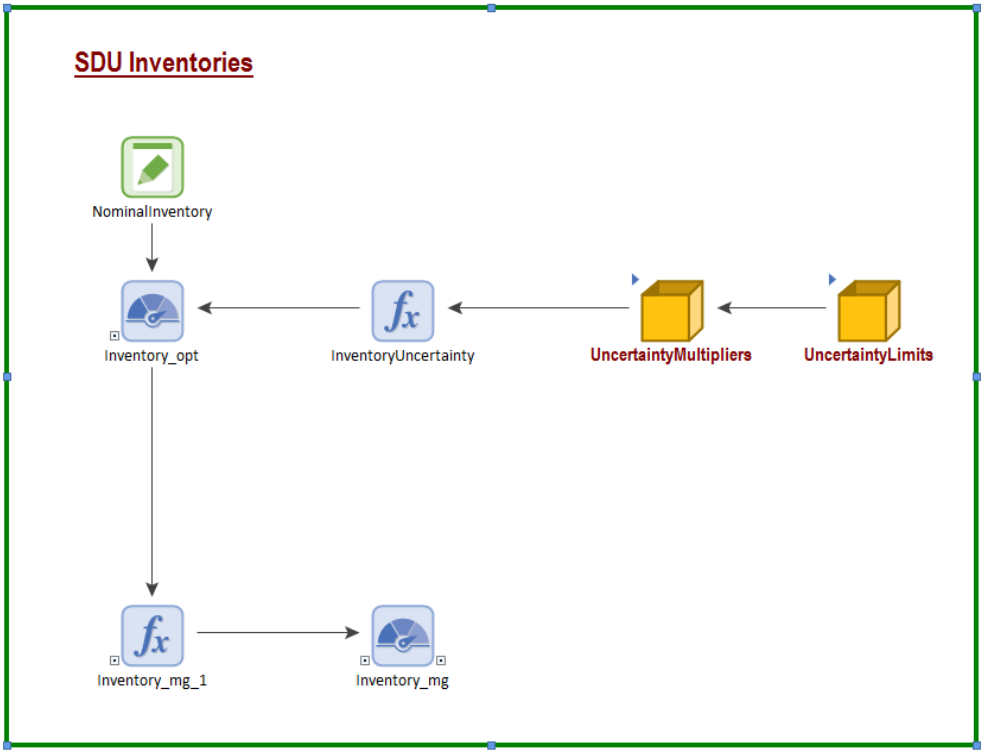

Table 3.2-27: Inventories (Ci) for SDUs 1 and 4

Radionuclides	SDU 1	SDU 4
C-14	1.31E+00	6.50E+00
Cl-36	7.02E-08	1.49E-02
Cm-246	0.00E+00	0.00E+00
H-3	4.61E+00	1.22E+01
I-129	2.01E-01	2.77E-01
Pu-238	6.18E-03	2.69E+02
Pu-242	1.57E-03	4.12E+00
Ra-226	9.53E-07	8.19E-05
Rn-222	0.00E+00	0.00E+00
Sb-125	0.00E+00	0.00E+00
Sb-126	0.00E+00	0.00E+00
Se-79	3.44E-01	9.75E+00
Sn-126	1.22E+00	2.22E+00
Tc-99	4.93E+01	6.34E+02
Th-230	6.48E-05	6.27E-03
U-234	9.93E-02	8.90E+00
U-238	1.07E-02	7.93E-02

Table 3.2-28: Inventories (Ci) for 150-foot Diameter SDUs

Radionuclides	SDU 2A	SDU 2B	SDU 3A	SDU 3B	SDU 5A	SDU 5B
C-14	2.40E+00	2.44E+00	8.21E+00	9.14E+00	3.17E+00	3.77E+00
Cl-36	1.06E-04	1.30E-04	1.33E-02	1.55E-02	3.10E-03	7.71E-04
Cm-246	0.00E+00	0.00E+00	0.00E+00	0.00E+00	0.00E+00	0.00E+00
H-3	7.97E-01	6.76E-01	4.54E+01	5.36E+01	1.94E+00	1.19E+00
I-129	7.31E-02	6.83E-02	1.92E-01	1.88E-01	1.39E-01	8.68E-02
Pu-238	4.92E+00	4.67E+00	2.12E+03	2.51E+03	6.52E+01	2.25E+01
Pu-242	3.76E-01	5.21E-01	1.05E-01	5.23E-02	4.61E-01	4.21E-01
Ra-226	8.56E-06	4.93E-06	1.18E-06	1.12E-06	2.30E-06	2.18E-06
Rn-222	0.00E+00	0.00E+00	0.00E+00	0.00E+00	0.00E+00	0.00E+00
Sb-125	0.00E+00	0.00E+00	0.00E+00	0.00E+00	0.00E+00	0.00E+00
Sb-126	0.00E+00	0.00E+00	0.00E+00	0.00E+00	0.00E+00	0.00E+00
Se-79	1.34E-01	1.23E-01	1.35E+00	1.58E+00	2.72E-01	1.68E-01
Sn-126	7.62E-01	6.83E-01	5.58E+00	6.13E+00	1.65E+00	9.47E-01
Tc-99	1.14E+02	1.37E+02	3.63E+02	3.80E+02	1.75E+02	1.20E+02
Th-230	9.00E-04	5.55E-04	1.01E-04	7.86E-05	3.13E-04	2.87E-04
U-234	6.16E-01	8.54E-01	3.83E-01	3.36E-01	7.60E-01	6.88E-01
U-238	2.24E-02	2.65E-02	2.27E-01	2.66E-01	3.28E-02	2.85E-02

Table 3.2-29: Inventories (Ci) for 375-foot Diameter SDUs

Radionuclides	SDU 6	SDU 7	SDU 8	SDU 9	SDU 10	SDU 11	SDU 12
C-14	1.07E+02	1.07E+02	1.07E+02	1.07E+02	1.07E+02	1.07E+02	1.07E+02
Cl-36	1.81E-01	1.81E-01	1.81E-01	1.81E-01	1.81E-01	1.81E-01	1.81E-01
Cm-246	0.00E+00	0.00E+00	0.00E+00	0.00E+00	0.00E+00	0.00E+00	0.00E+00
H-3	6.26E+02	6.26E+02	6.26E+02	6.26E+02	6.26E+02	6.26E+02	6.26E+02
I-129	2.20E+00	2.20E+00	2.20E+00	2.20E+00	2.20E+00	2.20E+00	2.20E+00
Pu-238	2.93E+04	2.93E+04	2.93E+04	2.93E+04	2.93E+04	2.93E+04	2.93E+04
Pu-242	6.11E-01	6.11E-01	6.11E-01	6.11E-01	6.11E-01	6.11E-01	6.11E-01
Ra-226	1.30E-05	1.30E-05	1.30E-05	1.30E-05	1.30E-05	1.30E-05	1.30E-05
Rn-222	0.00E+00	0.00E+00	0.00E+00	0.00E+00	0.00E+00	0.00E+00	0.00E+00
Sb-125	0.00E+00	0.00E+00	0.00E+00	0.00E+00	0.00E+00	0.00E+00	0.00E+00
Sb-126	0.00E+00	0.00E+00	0.00E+00	0.00E+00	0.00E+00	0.00E+00	0.00E+00
Se-79	1.84E+01	1.84E+01	1.84E+01	1.84E+01	1.84E+01	1.84E+01	1.84E+01
Sn-126	7.15E+01	7.15E+01	7.15E+01	7.15E+01	7.15E+01	7.15E+01	7.15E+01
Tc-99	4.43E+03	4.43E+03	4.43E+03	4.43E+03	4.43E+03	4.43E+03	4.43E+03
Th-230	9.18E-04	9.18E-04	9.18E-04	9.18E-04	9.18E-04	9.18E-04	9.18E-04
U-234	3.92E+00	3.92E+00	3.92E+00	3.92E+00	3.92E+00	3.92E+00	3.92E+00
U-238	3.10E+00	3.10E+00	3.10E+00	3.10E+00	3.10E+00	3.10E+00	3.10E+00

3.3 Air-Phase Transport Submodel

This section describes the organization and details of the air-phase transport submodel.

3.3.1 Looping Containers

The upper-level contents of the Air_PathwayTransport container controlling the repeated processing of the GoldSim SubModel containing the radionuclide air-phase release calculation elements for SDU 1, SDU4, the 150-foot diameter SDUs and the 375-foot diameter SDUs are shown in Figure 3.3-1. A GoldSim SubModel is a specialized container-like element that has the full functionality of GoldSim Model including time settings and Monte Carlo (and LHS) sampling that behaves as a separate "inner" model within an "outer" model. The air-pathway model's transport calculation submodel, hereafter referred to as the "SDU Transport Submodel," is imbedded within two nested GoldSim looping containers (*OuterLoop_SDUs* and *InnerLoop_SDUs*). These looping containers behave like "Do Loops" in other computer languages such as FORTRAN or C^{++}. The SDU Transport Submodel is controlled by the outer loop that loops over the individual SDUs of interest in a simulation (see Figure 3.3-1). *NSDU* is the data element that identifies maximum number of SDUs that can be modeled.

Figure 3.3-1: Contents of the *Air_PathwayTransport* Container

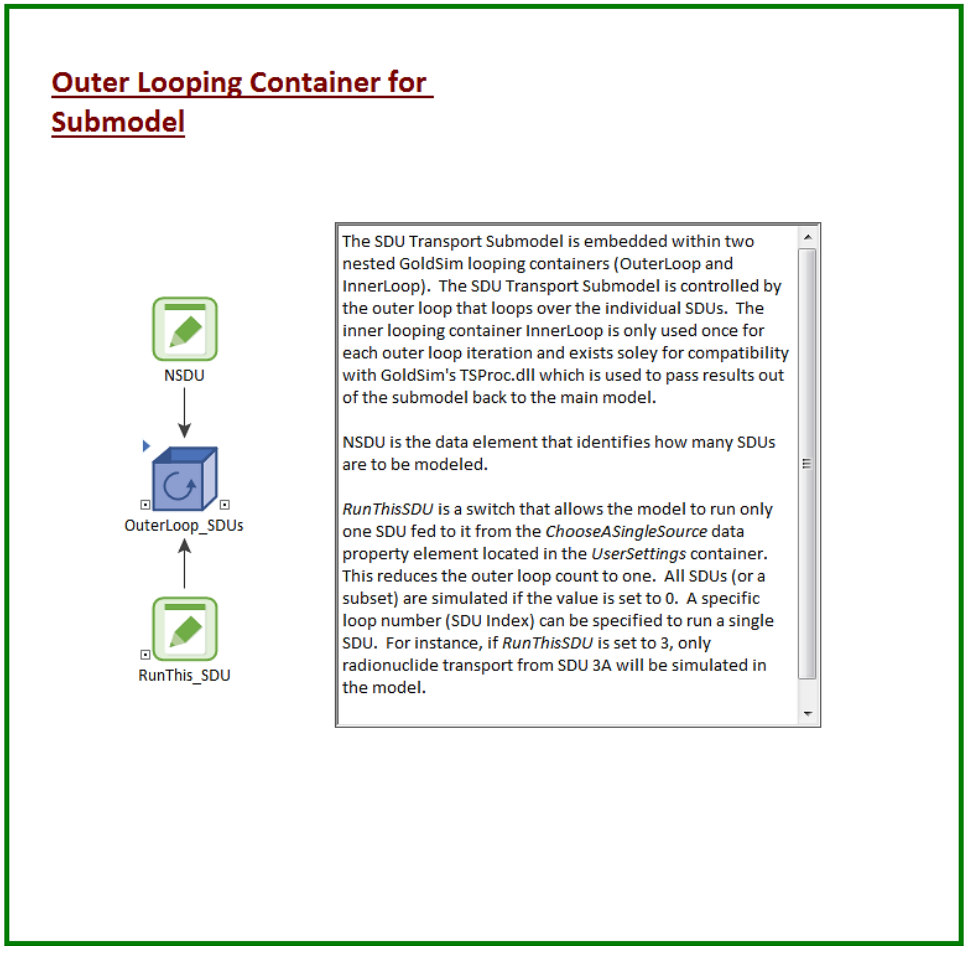

RunThisSDU is a switch that allows the model to run a single SDU based on the SDU Index (Table 3.2-1) selection fed from the *ChooseASingleSource* data element located in the *UserSettings* container. When users opt to run the model for only a specific SDU, this reduces the outer loop count to one. All SDUs (or a subset of) are simulated if the value is set to 0. A specific loop number (based on the SDU Index in Table 3.2-1) can be specified to run a single SDU. For instance, if *RunThisSDU* is set to 3, only radionuclide transport from SDU 3A will be simulated in the model.

The inner looping container *InnerLoop_SDUs* (see Figure 3.3-2) is only used once for each outer loop iteration and exists solely for compatibility with GoldSim's vendor-provided dynamic link library (DLL): *TSProc.dll*. This DLL is used to pass time series results out of the submodel back to the main model. The GoldSim External element *TSProc*, found in the container *TS_Proc_SDUs*, controls the external DLL *TSProc.dll* by calling it as a subroutine.

Figure 3.3-2: Contents of Container *OuterLoop_SDUs*

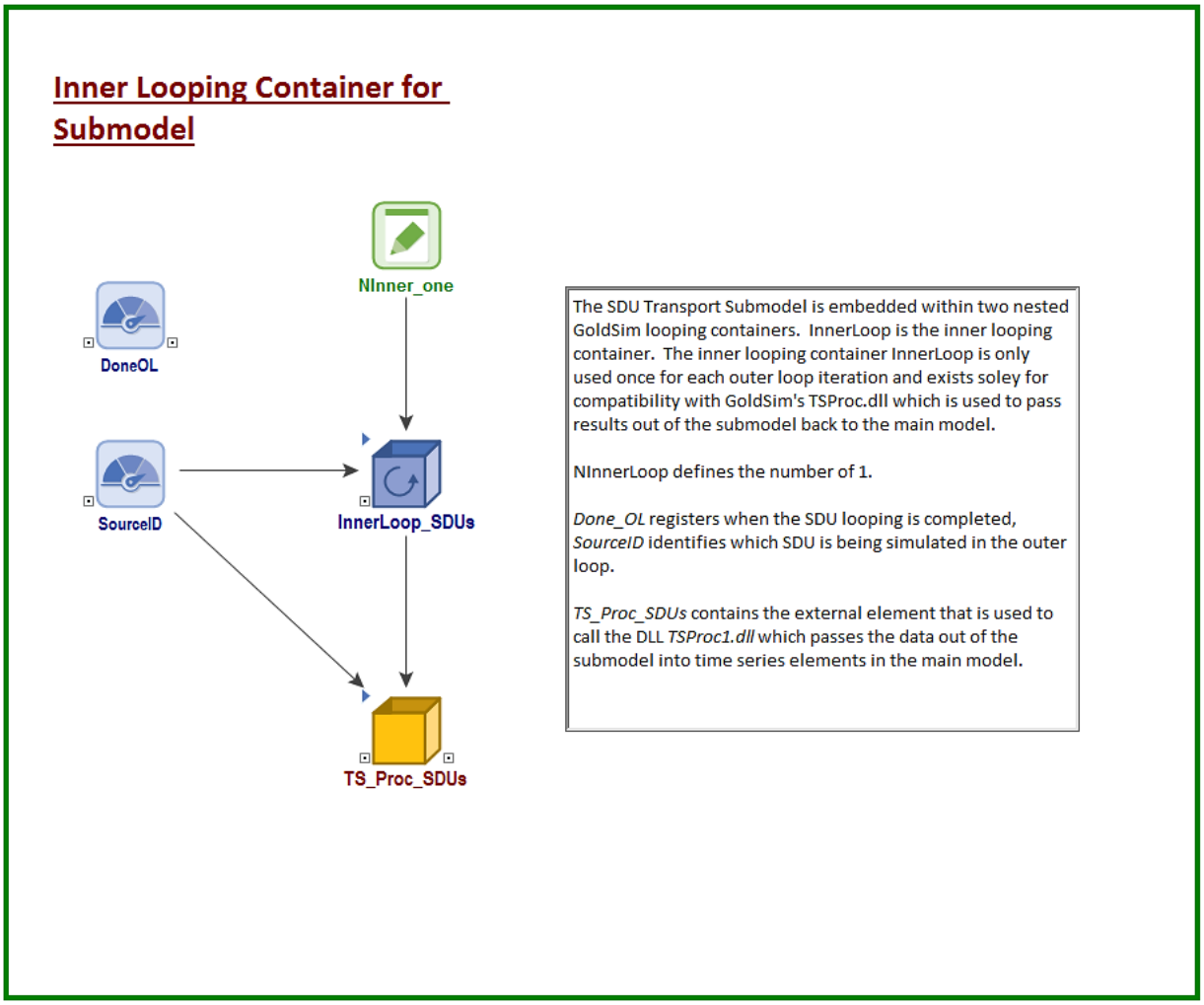

3.3.2 The Air-Phase Transport Submodel

Within the looping container InnerLoop_SDUs, resides *SDUTransportSubmodel* (see Figure 3.3-3). This is an independent GoldSim Submodel that is initialized prior to the occurrence of time-stepping in the main model, calculates the radionuclide releases from the user-selected SDUs, and subsequently passes the release values back to the main model in the form of a time series. The time series can then be used as data for calculations in the main model such as evaluating transport in the atmosphere and/or calculating doses over time.

Figure 3.3-3: Contents of Container *InnerLoop_SDUs*

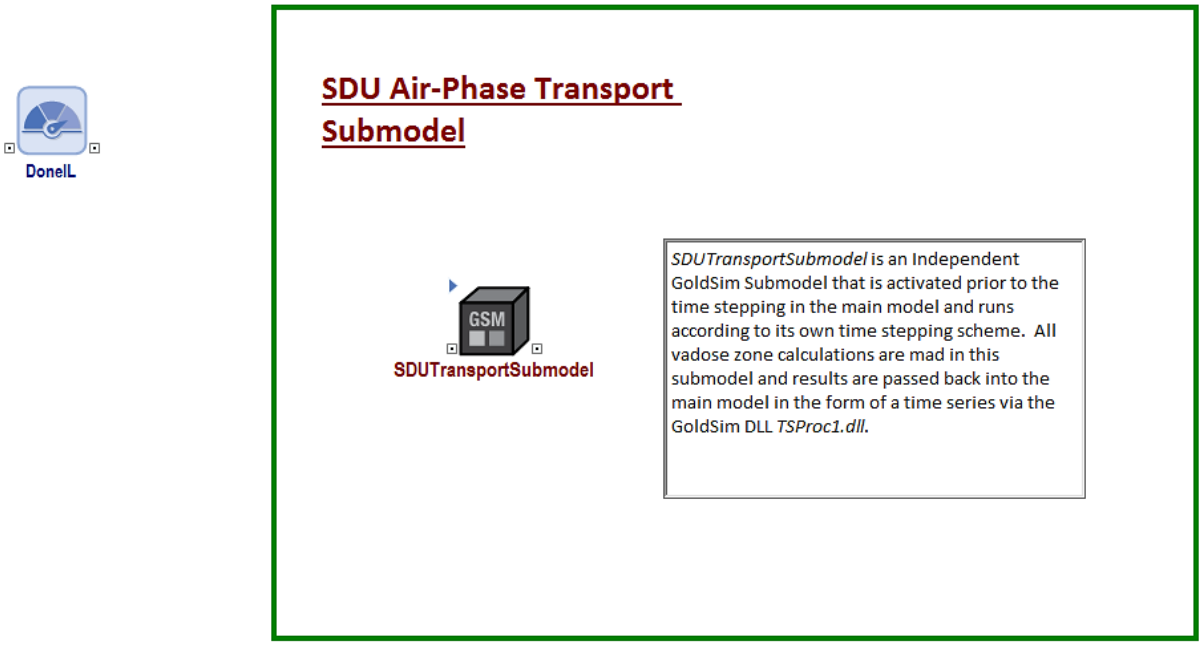

The SDU Transport Submodel is comprised of an *InputData* container, a *SDU_Transport_Results* container, and four SDU-type containers. The *InputData* container contains a set of selector elements used to capture input parameters fed from the main model through the submodel interface into the submodel. The *SDU_Transport_Results* container contains time series elements used to feed the main model through the submodel interface. The air-phase diffusive transport calculation section of the submodel is comprised of four containers, representing the four SDU-types found at the SDF (see Figure 3.3-4):

- SDU 1, a 100-foot by 600-foot rectangular vault [Container SDU_V1],
- SDU 4, a 200-foot by 600-foot rectangular vault [Container SDU_V4],
- 150-foot diameter cylindrical vaults (i.e., SDUs 2A, 2B, 3A, 3B, 5A, and 5B) [Container SDU_150], and
- 375-foot diameter cylindrical vaults (i.e., SDUs 6, 7, 8, 9, 10, 11, and 12) [Container SDU_375].

Figure 3.3-4: Submodel Upper Level

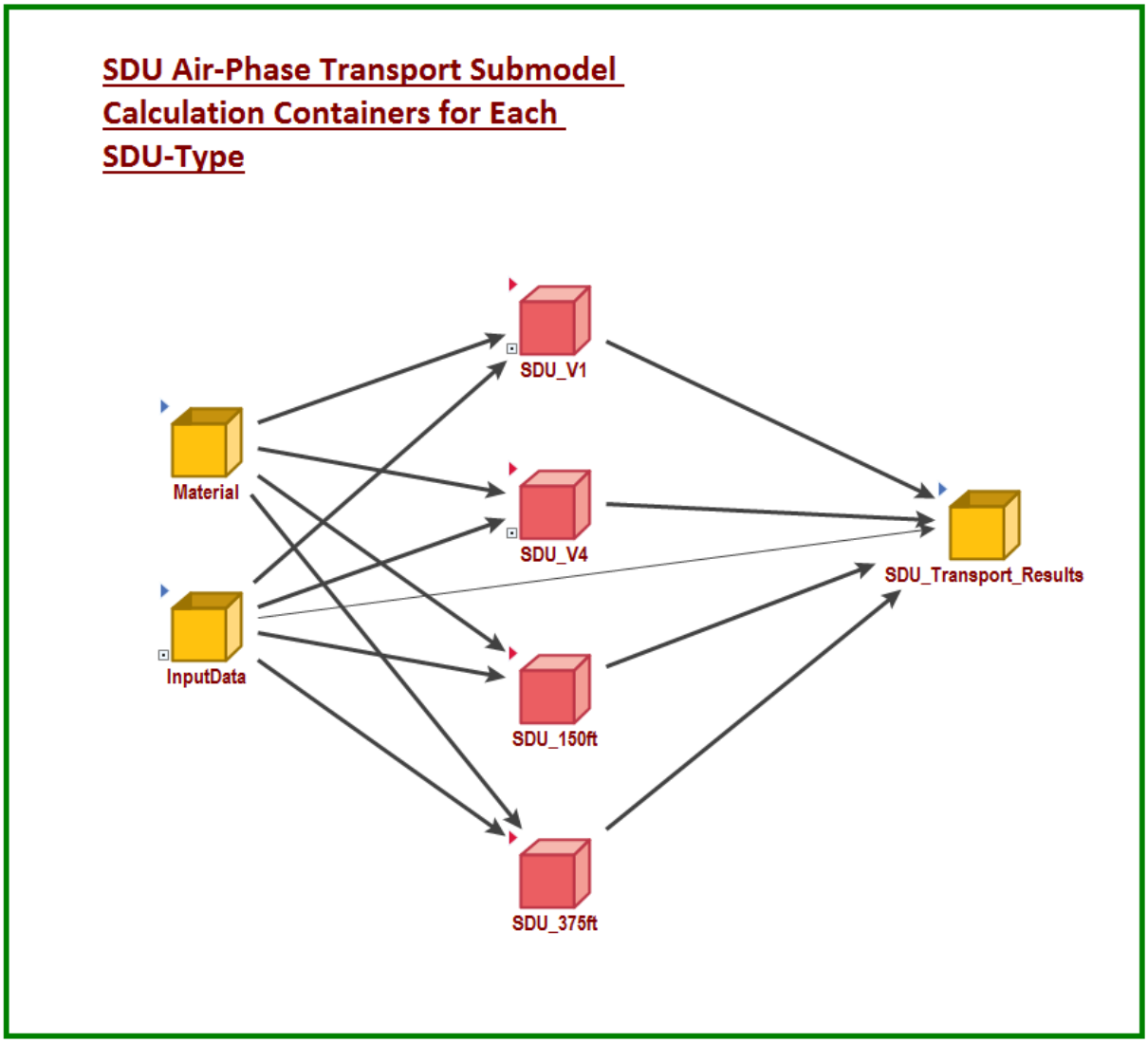

Within each of the four containers there are SDU-type specific GoldSim cell-pathway networks used to calculate air-phase diffusive transport from the bottom of the saltstone monolith to the top of the closure cap (conservatively assumed to be the erosion barrier).

SDU_150ft is used here for an example. The top-level of *SDU_150ft* container is comprised of an inner container (*SDU_150*) and a set of expression elements used to feed layer-specific parameter vectors to all the layer-specific containers within *SDU_150*. Figure 2.2-2 depicts the layer-specific containers for the 150-foot diameter cylindrical SDUs. Each layer-specific container houses a string of mixing cells linked in series via diffusive-flux links.

Figure 2.2-1 illustrates the segment of the linked cell-pathway (mixing-cell) network representing the saltstone monolith. The blue arrows represent the diffusive-flux linkages between the cells.

The lack of a linkage at the bottom of the *Salt1* cell pathway (Figure 2.2-1) indicates that the bottom boundary condition has a zero-flux condition, which together with the inventory placement (equally distributed in the saltstone monolith) will force the system to simulate upwards diffusion only.

Figure 2.2-3 illustrates the segment of the linked cell-pathway (mixing-cell) network representing the erosion barrier. The diffusive-flux link between the top erosion-barrier cell *EB4* and the container *Sink*, which contains a cell pathway element, *ZeroBC*, controls the release of radionuclide gases. A cell pathway element option in *ZeroBC*, is set to approximate a Dirichlet boundary condition of zero-concentration.

Figure 3.3-5 through Figure 3.3-12 depict the remaining segments of the linked cell-pathway (mixing-cell) network connecting the top of the saltstone monolith to the bottom of the erosion barrier (see also Figure 2.2-2). Note that the blue arrows between the layer specific containers in the 150-foot diameter SDU model in Figure 2.2-2, reflect the diffusive-flux links between the top of the underlying layer and the bottom of the layer indicated by the arrow head.

Figure 3.3-5: Layer-Based Vector Feeds to 150-Foot Diameter SDU Mixing Cells

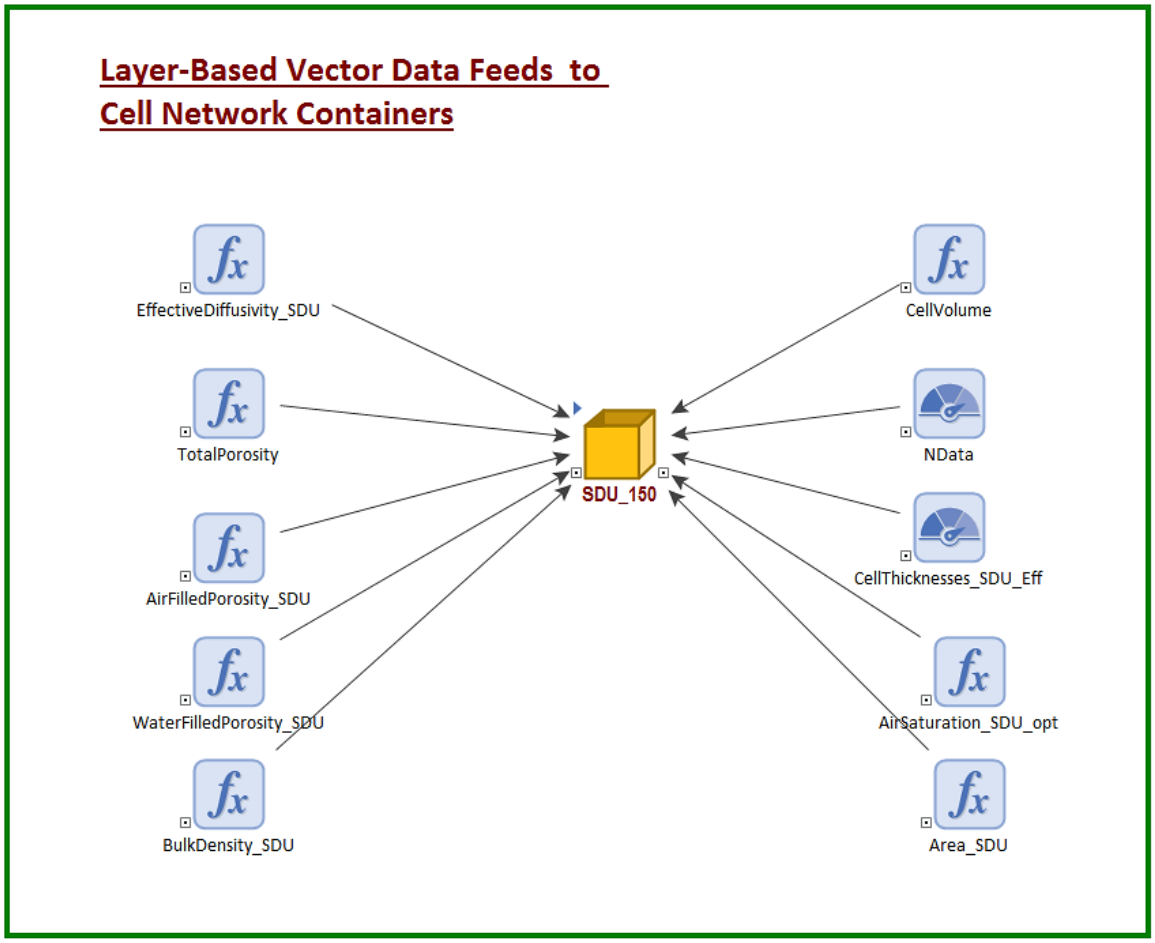

Figure 3.3-6: Clean Grout Cap Mixing Cells for 150-Foot Diameter SDUs

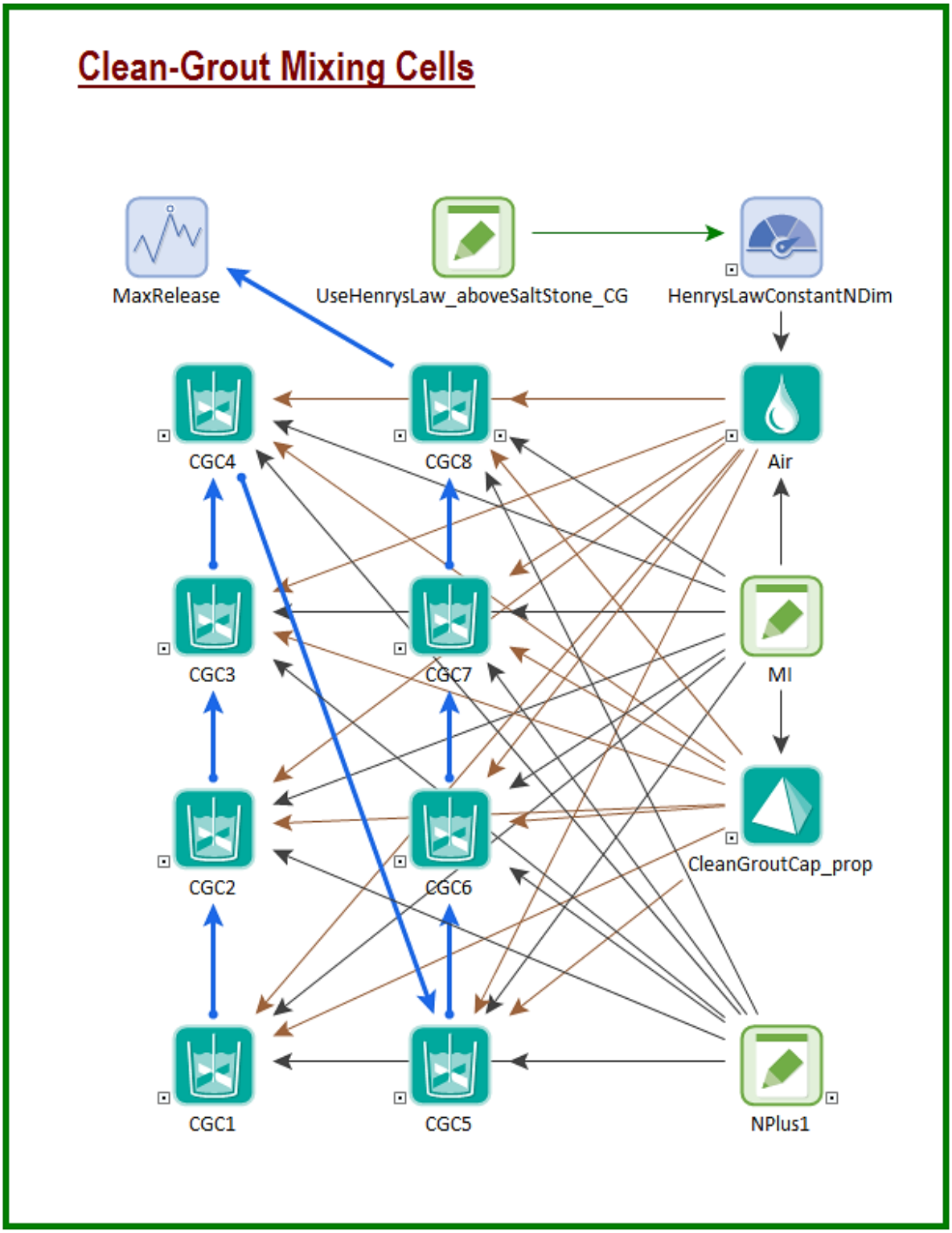

Figure 3.3-7: Concrete Roof Mixing Cells for 150-Foot Diameter SDUs

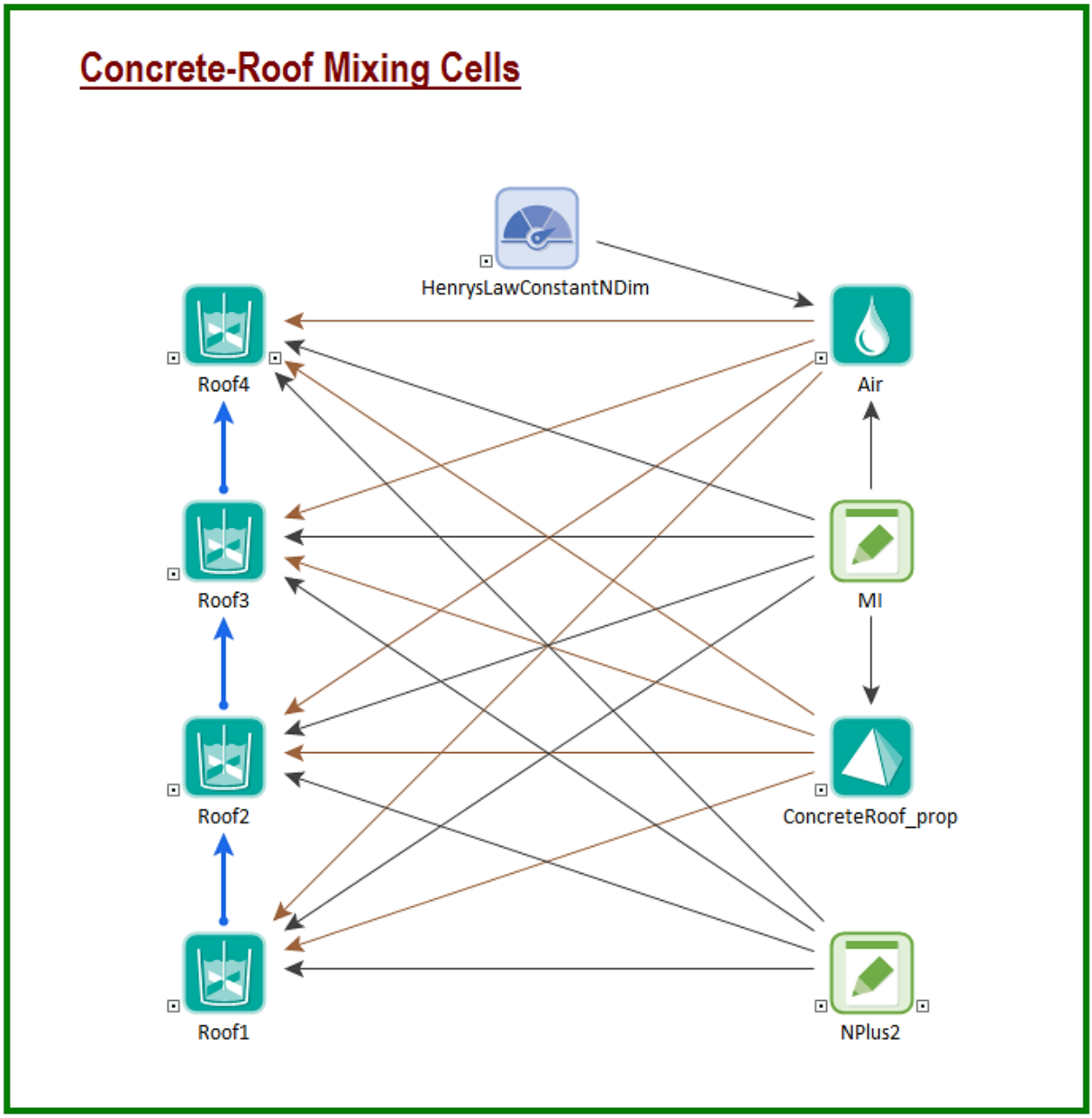

Figure 3.3-8: Lower Drainage Layer Mixing Cells for 150-Foot Diameter SDUs

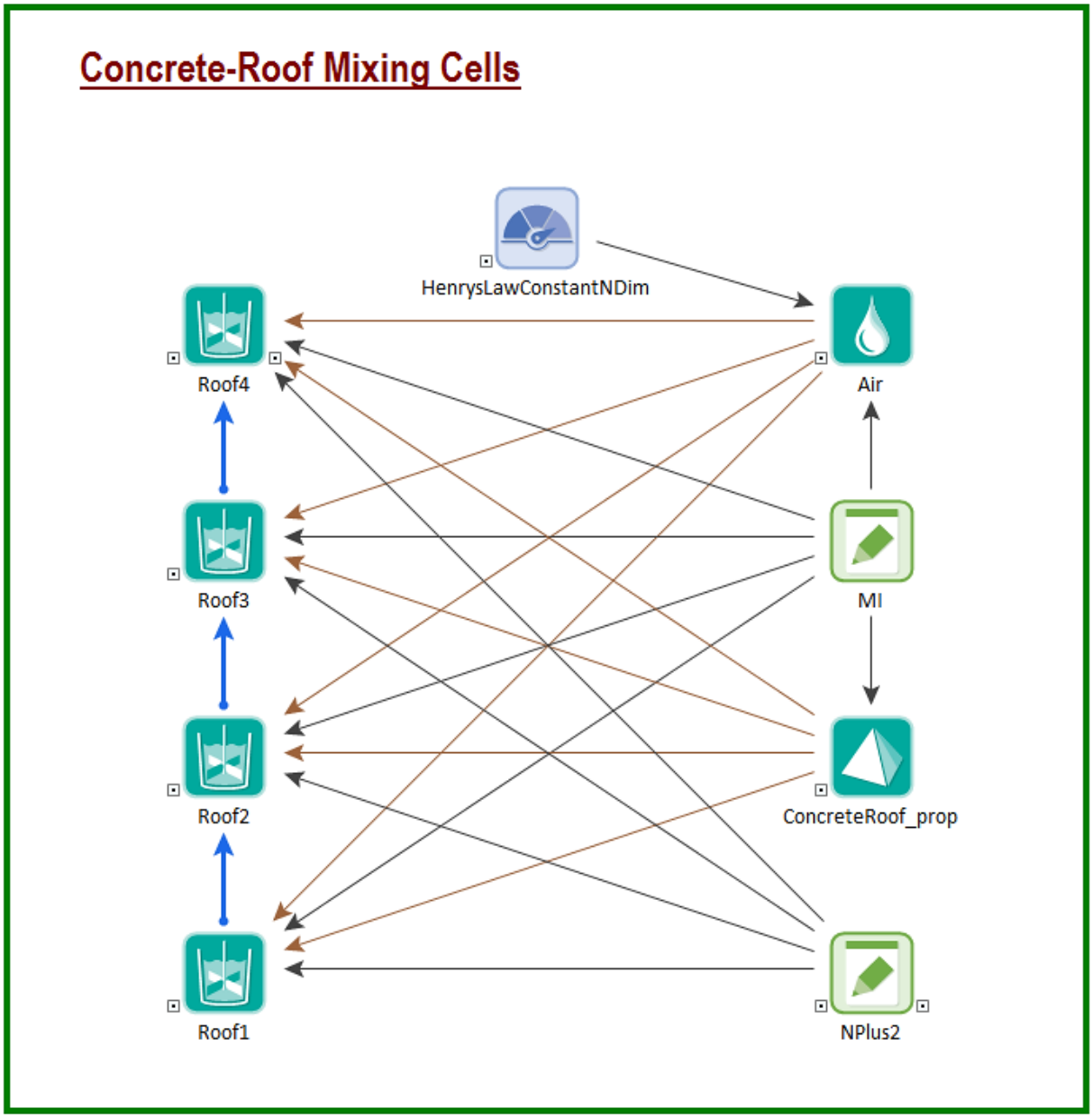

Figure 3.3-9: Lower Backfill Layer Mixing Cells for 150-Foot Diameter SDUs

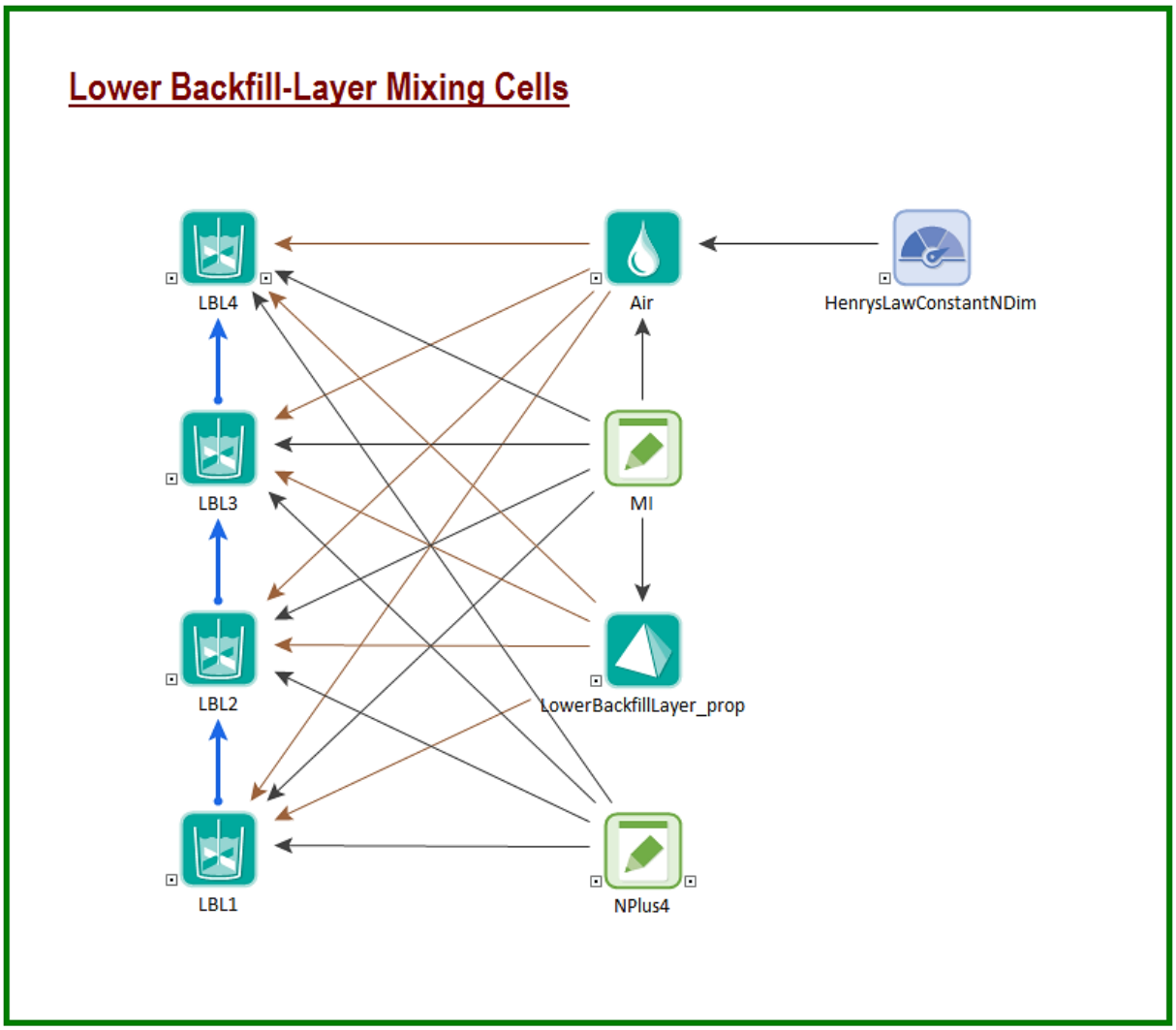

Figure 3.3-10: Foundation Mixing Cells for 150-Foot Diameter SDUs

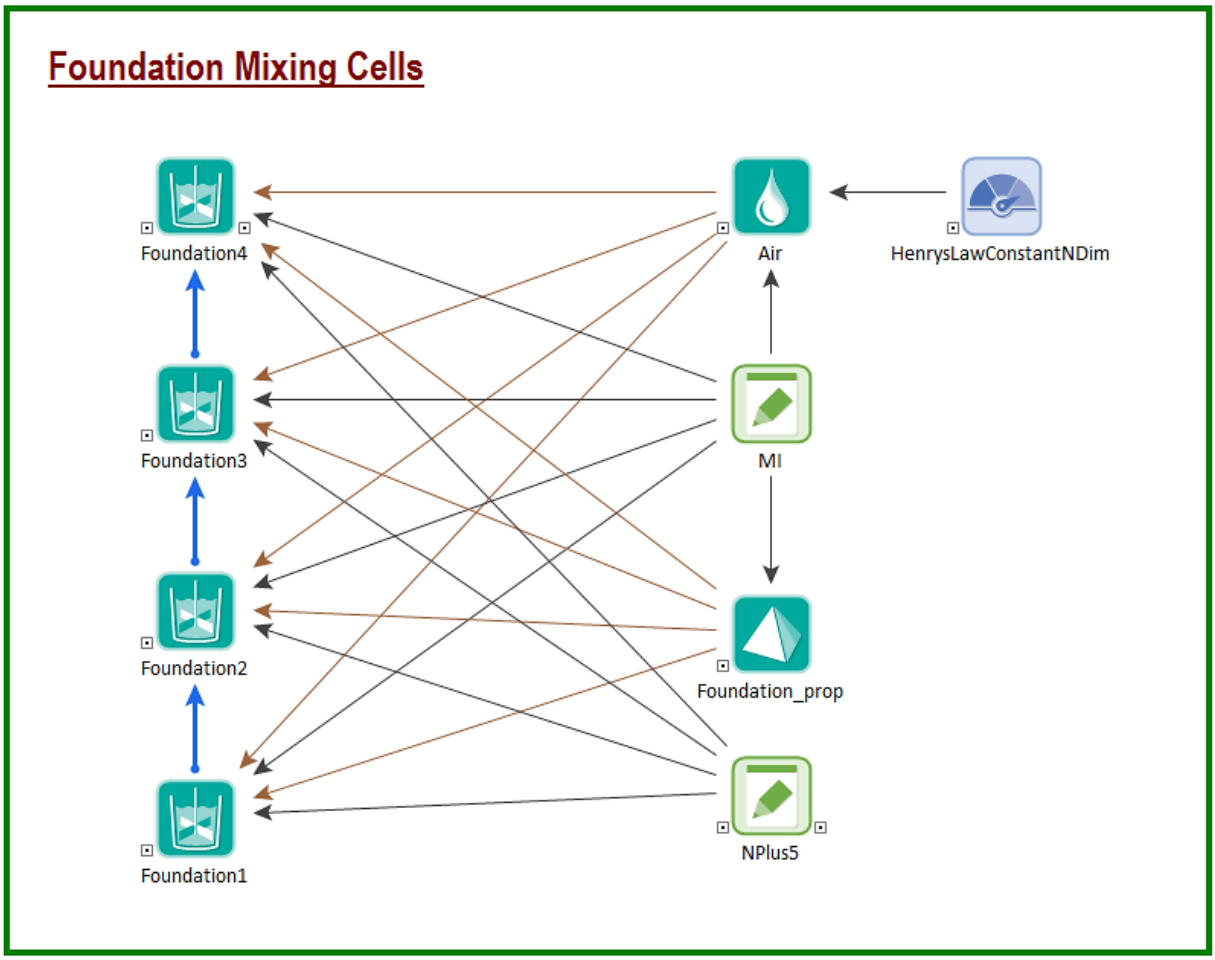

Figure 3.3-11: Upper Drainage Layer Mixing Cells for 150-Foot Diameter SDUs

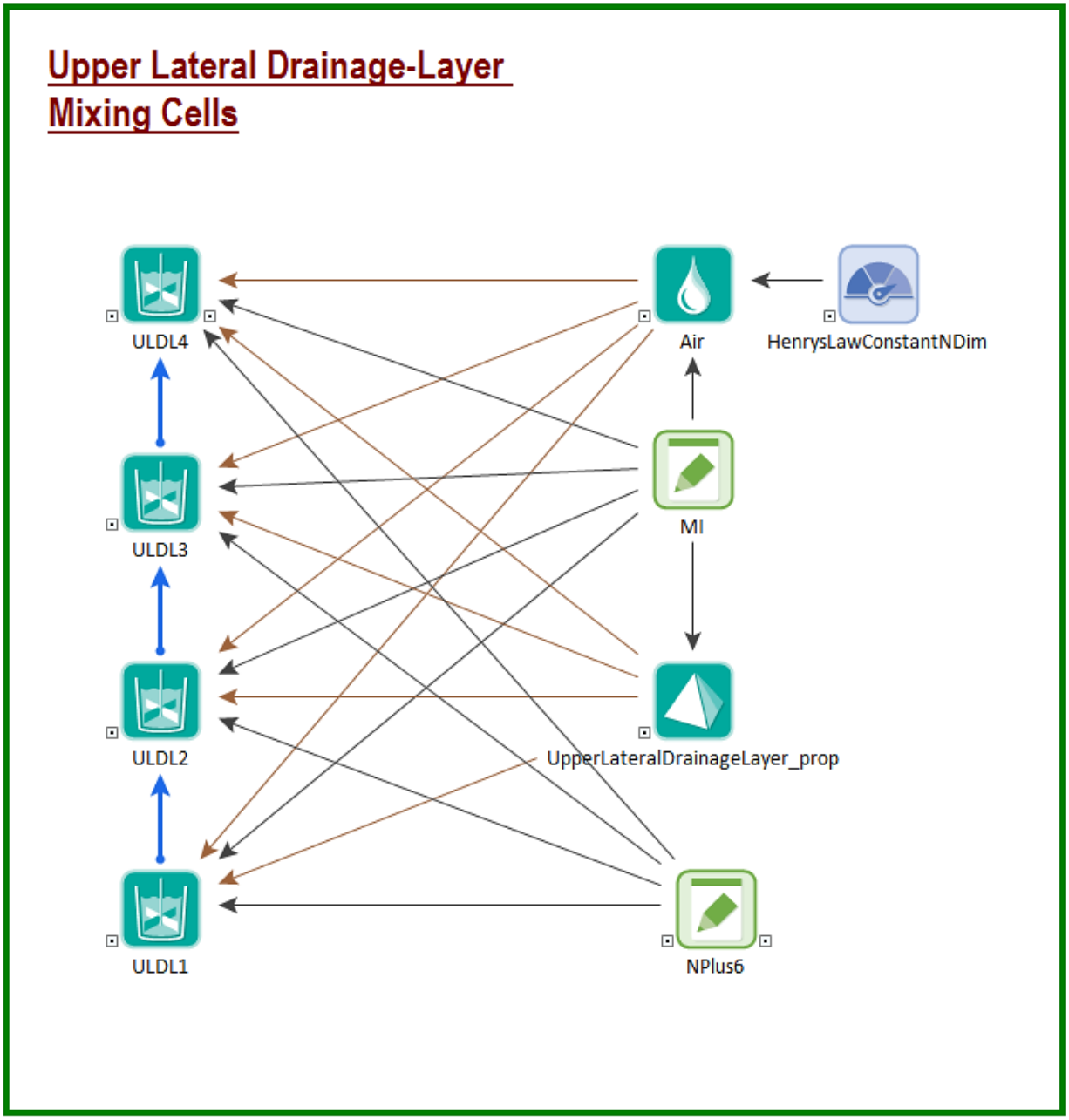

Figure 3.3-12: Middle Backfill Layer Mixing Cells for 150-Foot Diameter SDUs

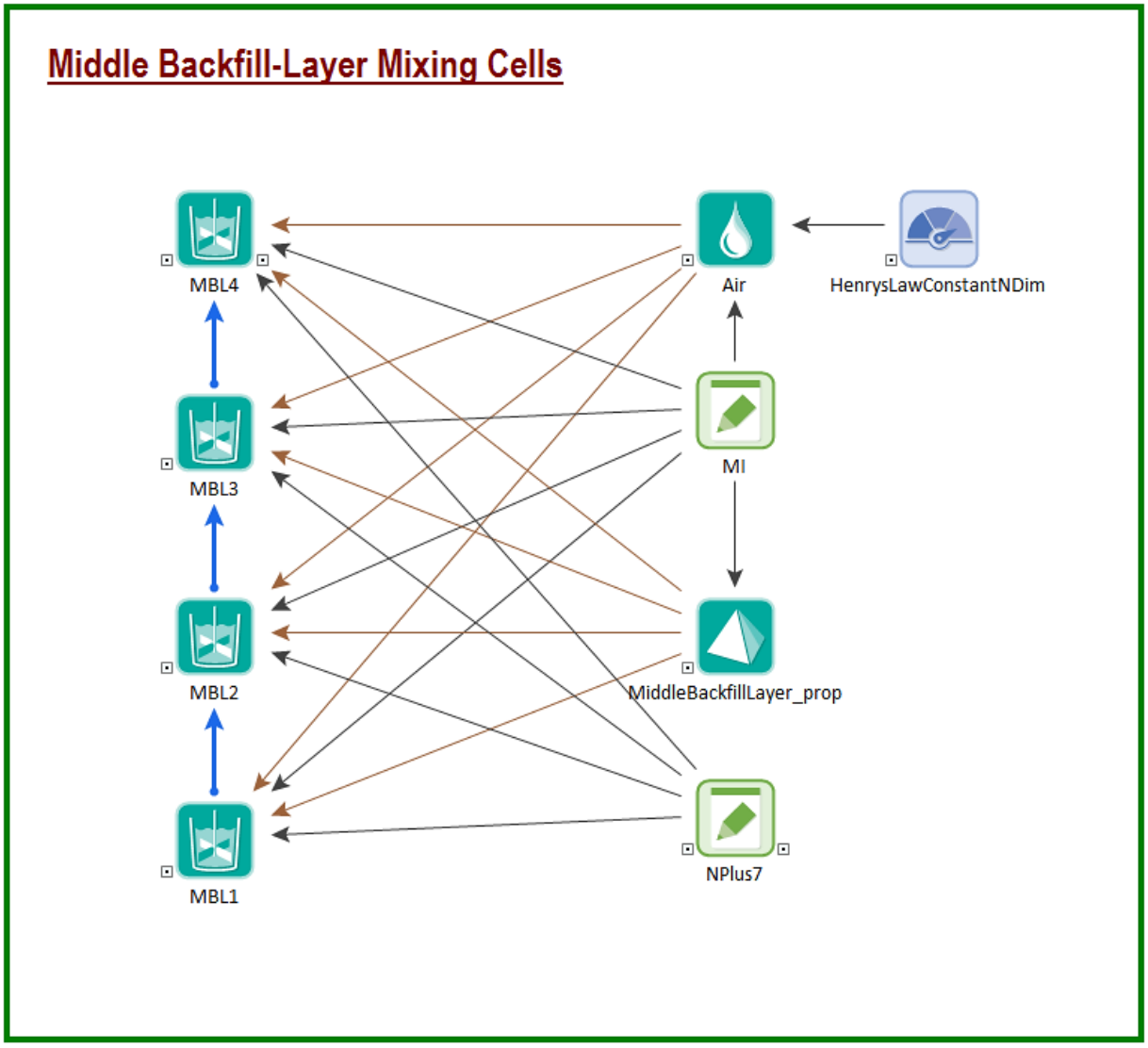

4.0 SAMPLE RUNS

Model simulations were performed to evaluate the peak fluxes of the gas-phase radionuclides released to the atmosphere. The sample runs reflect the peak releases resulting from each of the future SDUs for two different saturation conditions. The peak fluxes for each future SDU are the same since these units were modeled with the same inventories and physical parameters.

4.1 Model Simulations

To evaluate the influence of water-air partitioning above the source zone (the saltstone monolith), two simulations were performed. The first simulation assumed that the pore space above the saltstone was fully unsaturated, and the second assumed that the pore space above the saltstone was partially saturated. The resultant maximum atmospheric releases of radionuclides from the SDUs (in Ci/yr) for the two simulations were compared.

In the first simulation, the partitioning of the gas phase into the water phase above the saltstone monolith was disregarded to representing the desired fully-unsaturated condition. This conservative assumption allows the initial gas phase to remain stable in the various chemical environments it diffuses through. The results of the simulation are depicted in Figure 4.1-1 with the peak release data presented in Table 4.1-1. As depicted in the results presented for the initial simulation, only C-14 and H-3 releases seem to be of concern.

Figure 4.1-1: Maximum Radionuclide Releases from the SDUs for Run with Air-Filled Pore Space above the Saltstone Monolith

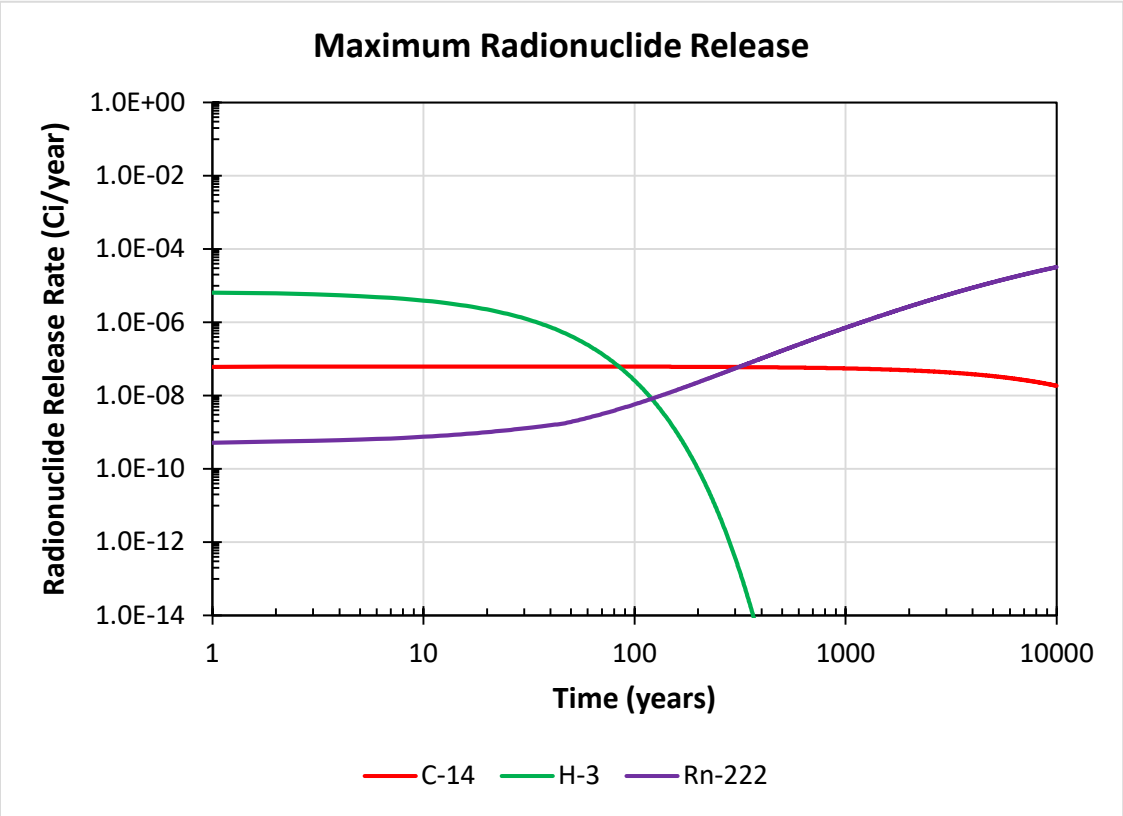

Data taken from SaltstonePA_Air&Radon_PathwayModel_V2.0e_ Full Desaturation.gsm.

Table 4.1-1: Peak Radionuclide Releases to the Atmosphere and Time of Peak Release for Run with Air-Filled Pore Space above the Saltstone Monolith

Radionuclides	Release (Ci/yr)	Peak Release Time (years)
C-14	6.3E-08	2
Cl-36	5.2E-24	2
H-3	6.4E-06	1
I-129	2.7E-26	9,998
Rn-222	3.2E-05	10,000
Sb-125	0.0E+00	N/A
Sb-126	0.0E+00	N/A
Se-79	0.0E+00	N/A
Sn-126	0.0E+00	N/A
Tc-99	0.0E+00	N/A

Data taken from SaltstonePA_Air&Radon_PathwayModel_V2.0e_ Full Desaturation.gsm.

In the second simulation, an alternative assumption, partitioning of the gas phase into the water phase above the saltstone monolith, is simulated representing partially-saturated conditions and possible changes in chemical environments. The results of the simulation are depicted in Figure 4.1-2 with the peak release data presented in Table 4.1-2.

Figure 4.1-2: Maximum Radionuclide Releases from the SDUs for Run with Partially Saturated Pore Space above the Saltstone Monolith

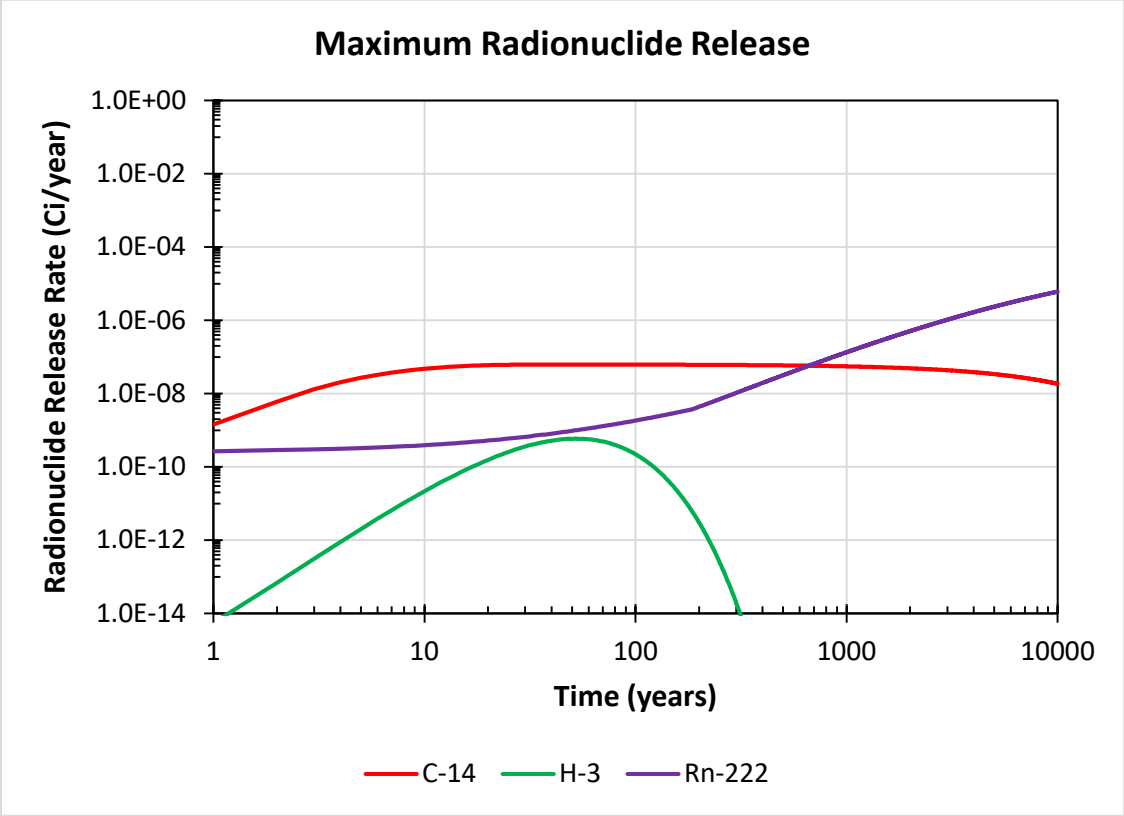

Data taken from SaltstonePA_Air&Radon_PathwayModel_V2.0e_ Partial Saturation.gsm.

Table 4.1-2: Peak Radionuclide Releases to the Atmosphere and Time of Peak Release for Run with Partially Saturated Space above the Saltstone Monolith

Radionuclides	Release (Ci/yr)	Peak Release Time (years)
C-14	6.2E-08	43
H-3	5.9E-10	52
Rn-222	6.1E-06	10,000
Cl-36	0.0E+00	N/A
I-129	0.0E+00	N/A
Sb-125	0.0E+00	N/A
Sb-126	0.0E+00	N/A
Se-79	0.0E+00	N/A
Sn-126	0.0E+00	N/A

Tc-99	0.0E+00	N/A

Data taken from SaltstonePA_Air&Radon_PathwayModel_V2.0e_ Partial Saturation.gsm.

As can be seen by comparing the results presented in Figure 4.1-3, partitioning of the gas phase into the water phase above the saltstone monolith, retards the rate of diffusive transport to the atmosphere. The Rn-222 appears to be slightly affected. The C-14 is reduced early but then shows little difference. A significant difference is observed from H-3.

Figure 4.1-3: Maximum Radionuclide Releases from the SDUs for Run with Air-Filled Pore Space above the Saltstone Monolith and Run with Partially Saturated Pore Space above the Saltstone Monolith

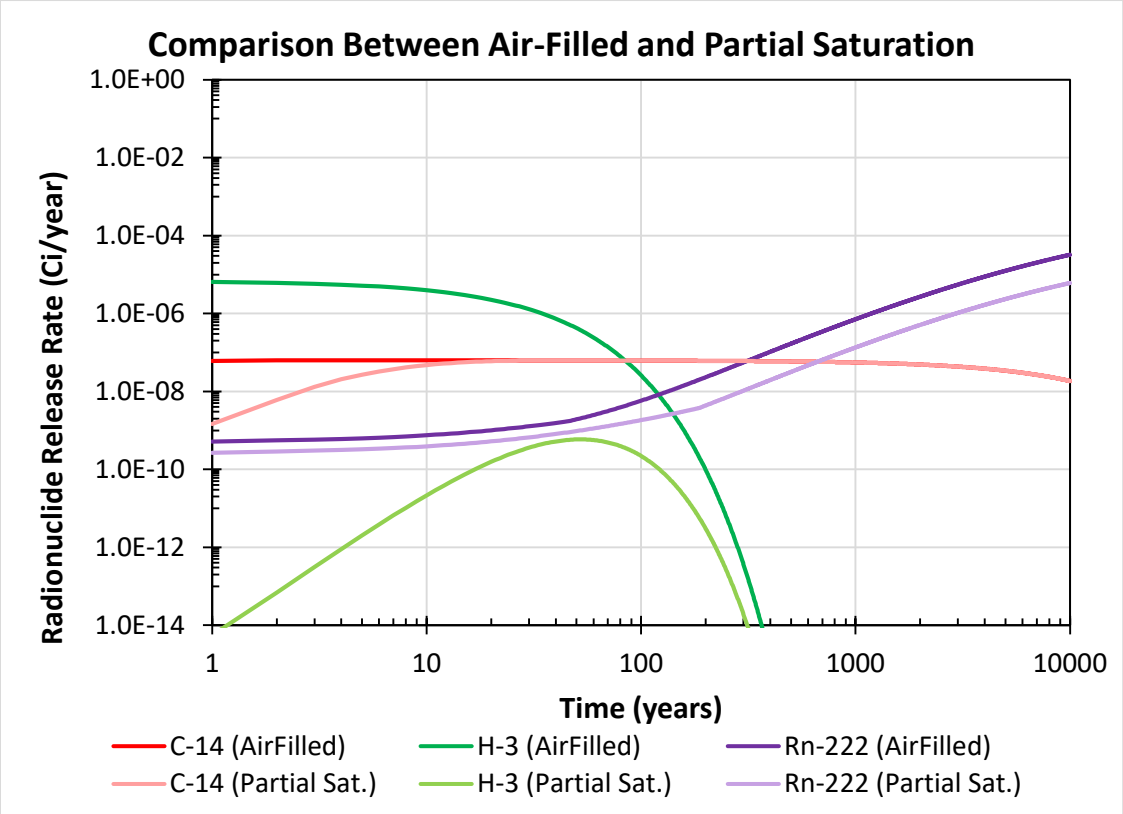

5.0 SUMMARY AND CONCLUSION

As part of the efforts to update the SDF PA, an updated model was developed to evaluate the release of radionuclides from SDUs to the atmosphere and through air pathways to the site boundary (pre-closure) and to a 100-meter compliance boundary (post-closure). The Air Pathway Release Model (SDFAPR Model) was developed using GoldSim software (GTG-2017a, GTG-2017b).
Version 1 of this SDFAPR was developed to benchmark the calculations against previous modeling work performed in PORFLOW (as documented within Appendix A). Specifically, it was designed to provide the surface flux which can be used as in input to an atmospheric transport model for evaluating the degree of attenuation associated with air-pathway transport to the site boundary and 100-meter compliance boundary.

Version 2 of this SDFAPR Model, as documented within this report, was developed to update select input values to evaluate the release of radionuclides from SDUs to the atmosphere. Peak atmospheric concentrations calculated at the site boundary and 100-meter compliance boundary will be used to evaluate peak doses at the boundaries.

For the air pathway analysis, several gaseous-phase radionuclides can be evaluated by the SDFAPR Model, including C-14, Cl-36, H-3, I-129, Rn-222, Se-79, Sb-125, Sb-126, Sn-126, and Tc-99. Note that, although Sb-125 and Sb-126 are not found in the present inventories included in the model, they are included for consistency with the earlier PORFLOW model. [SRNL-STI-2008-00447] Because the release of radon (in the form of Rn-222) from the SDUs will be strongly controlled by ingrowth of parent radionuclides found in the saltstone, parent radionuclides are included in the model. These parent radionuclides include Cm-246, Pu-242, Pu-238, U-238, U-234, Th-230, and Ra-226.

The SDFAPR Model has been designed for two purposes. First, to generate gas-phase radionuclide releases to be used in atmospheric transport and dose calculations. Secondly, to allow the PA developers to evaluate the degree of influence various processes will have on the resultant releases.

6.0 REFERENCES

Bethke, C.M., 2005, The Geochemist's Workbench® (geochemical modeling software), Release 6.0, University of Illinois.

G-AES-S-00004, Winship, G., *Future Saltstone Disposal Units Siting*, Savannah River Site, Aiken, SC, Rev. 0, May, 2018.

GTG-2017a (Copyright), *GoldSim User's Guide: Probabilistic Simulation Environment*, GoldSim Technology Group LLC, Issaquah, WA, February 2017.

GTG-2017b (Copyright), *GoldSim User's Guide: GoldSim Contaminant Transport Module*, GoldSim Technology Group LLC, Issaquah, WA, February 2017.

Rogers, V. C. and K. K. Nelson, *Correlations for Predicting Air Permeabilities and Rn-222 Diffusion Coefficients of Soil*, Health Physics Vol. 61, No. 2 (August), pp. 225-230, 1991. DOI: 10.1097/00004032-199108000-00006.

Sander, R., *Compilation of Henry's Law Constants (Version 4.0) for Water as a Solvent*, Atmos. Chem. Phys., 15, 4399-4981, 2015. DOI:10.5194/acp-15-4399-2015.

SRNL-STI-2008-00447, Dixon, K.D., Flach, G.P., Denham, M.E., and Phifer, M.A., 2008, *Air and Radon Pathway Modeling for the Saltstone Disposal Facility*, Rev. 0. Savannah River National Laboratory, Aiken, SC.

SRNL-STI-2009-00473, Kaplan, D., *Geochemical Data Package for Performance Assessment Calculations Related to the Savannah River Site*, Savannah River Site, Aiken, SC, Rev. 1, July 2016.

SRNL-STI-2017-00331, Denham, M.E., 2017, *Recommended Henry's Law Constants for Non-Groundwater Pathways Models in GoldSim*, Savannah River National Laboratory, Aiken, SC.

SRNL-STI-2017-00592, Wohlwend, J.L., 2017, *Atmospheric Release Model for the E-Area Low-Level Waste Facility: Updates and Modifications*, Savannah River National Laboratory, Aiken, SC, Rev. 0, November 2017.

SRRA107772-000009, Benson, C.H. and Benavides, J.M., *Predicting Long-Term Percolation from the SDF Closure Cap*, Report No. GENV-18-05, University of Virginia School of Engineering, April 2018.

SRR-CWDA-2009-00017, *Performance Assessment for the Saltstone Disposal Facility at the Savannah River Site*, Savannah River Site, Aiken, SC, Rev. 0, October 2009.

SRR-CWDA-2013-00058, Hommel, S., *Dose Calculation Methodology for Liquid Waste Performance Assessments at the Savannah River Site*, Savannah River Site, Aiken, SC, Rev. 1, July 2014.

SRR-CWDA-2018-00004, Hommel, S., *Recommended Values for Cementitious Degradation Modeling to Support Future SDF Modeling*, Savannah River Site, Aiken, SC, Rev. 0, August, 2018.

SRR-CWDA-2018-00012, Watkins, D., *Additional Recommended Inputs to PORFLOW Modeling for SDU 7*, Savannah River Site, Aiken, SC, Rev. 2, August 2018.

SRR-CWDA-2018-00018, Watkins, D., *Database Compilation of Radionuclides Standardized with Half-Lives in Seconds and Specific Activity in Ci/g*, Savannah River Site, Aiken, SC, Rev. 0, April 2018.

SRR-CWDA-2018-00044, Wooten, L., *Inventory Screening Methodology and Application to the FY2019 Saltstone Disposal Facility (SDF) Performance Assessment (PA) Inventory*, Savannah River Site, Aiken, SC, Rev. 0, August 2018.

SRR-CWDA-2018-00045, Hommel, S., *Iodine Kds for Simulating I-129 Releases from Saltstone SDUs*, Savannah River Site, Aiken, SC, Rev. 0, August 2018.

SRR-TR-2010-00096, Denham, M.E., 2010, *Vapor – Aqueous Solution Partition Coefficients for Radionuclides Pertinent to High Level Waste Tank Closure*, Rev. 2, Savannah River National Laboratory, Aiken, SC.

WSRC-STI-2007-00544, Denham, M.E., 2010, *Conceptual Model of Waste Release from the Contaminated Zone of Closed Radioactive Waste Tanks*, Rev. 2, Savannah River National Laboratory, Aiken, SC.

WSRC-STI-2008-00244, Jones, W.E. and Phifer, M.A., *Saltstone Disposal Facility Closure Cap Concept and Infiltration Estimates*, Savannah River National Laboratory, Aiken, SC, Rev. 0, May 2008.

APPENDIX A. BENCHMARK TESTING

The benchmarking of the SDFAPR Model was performed in the initial version of this report, Rev. 0. This was done by comparing the results of the GoldSim based model, Rev. 0, with results based on the original PORFLOW model described in SRNL-STI-2008-00447 and used in the 2009 SDF PA, SRR-CWDA-2009-00017. Given the very good comparisons between the GoldSim (SDFAPR Model Rev. 0) results and the PORFLOW model results, the SDFAPR Model is valid and is appropriate to use in support of the SDF PA.

Benchmark Test 1a and 1b

Benchmark Test 1a was based upon the PORFLOW model described in SRNL-STI-2008-00447 representing a 150-foot diameter SDU, including the saltstone monolith, clean-cap grout, concrete roof, and closure cap above. See Figure 3.2-10 and Figure 3.2-6 for the geometry of both the SDFAPR Model and the original PORFLOW Model. Using a simplified set of parameters with the saltstone source set to 1 mass-unit evenly distributed within the saltstone monolith, an air-filled porosity of 1, and an effective diffusion coefficient to 1 m^2/yr, the normalized ground-surface release of a tracer gas in units of 1/yr, was generated by each of the two models and compared in Figure A-1.

Figure A-1: Comparison of Tracer Releases from a 150-ft Diameter SDU as Simulated by the SDFAPR and PORFLOW Models (Instantly Applied Source)

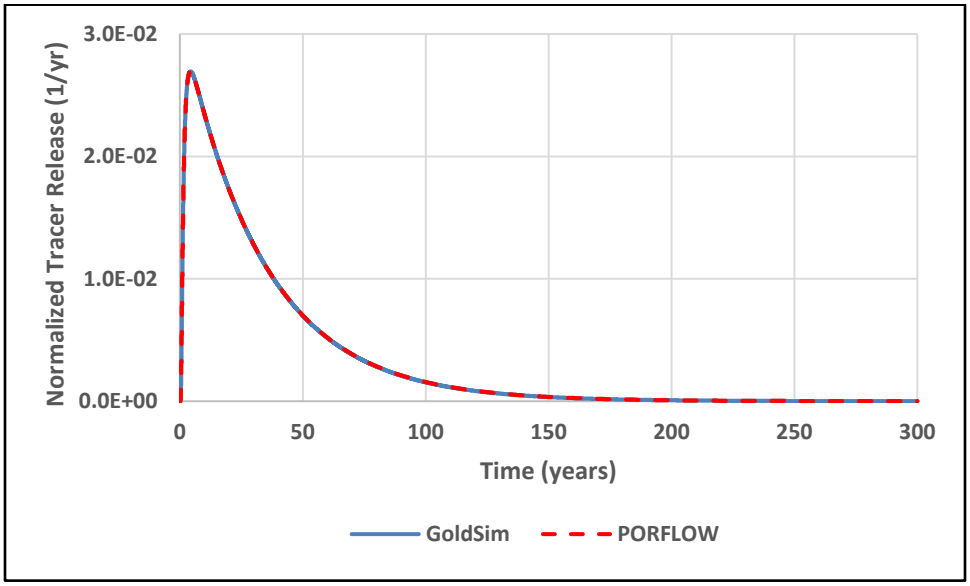

Benchmark Test 1b was similarly based upon the PORFLOW model described in SRNL-STI-2008-00447. Using the same simplified set of parameters with the instantaneously applied saltstone source replaced by a constant flux source of 1-mass unit/yr, the normalized ground-surface release of a tracer gas in units of 1/yr, was generated by each of the two models and compared in Figure A-2.

Figure A-2: Comparison of Tracer Releases from a 150-ft Diameter SDU as Simulated by the SDFAPR and PORFLOW Models (Constant Mass Flux Source)

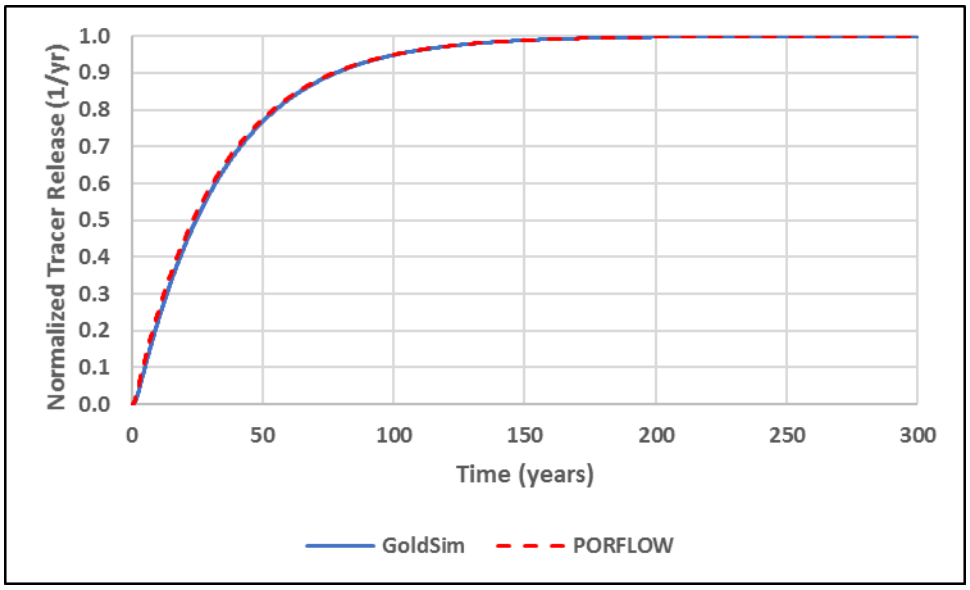

Benchmark Test 2

Benchmark Test 2 is a repeat of the air pathway model results presented in Section 3.2.4.1 of SRNL-STI-2008-00447 with a data change made to correctly apply the Henry's Law constant in conjunction with the density term in the PORFLOW model which need to be entered in consistent units in the PORFLOW model. The original simulations described in SRNL-STI-2008-00447 used a K_d (replacing the Henry's Law Constant) defined in mL/g and a particle density defined in kg/m^3 (in the PORFLOW input file). The product of the two terms results in a storage capacity for the liquid phase water, which is 1E+06 times too large. The resultant releases in the original document are therefore six orders of magnitude to small. Note that the error that is reflected in the results presented in Table 19 of SRNL-STI-2008-00447 is still of little consequence because of the small peak flux releases at the ground surface and associated dose release factors at points of compliance presented in Table 19.

Benchmark Test 2 was also based upon the PORFLOW model described in SRNL-STI-2008-00447 representing a 150-foot diameter SDU, including the saltstone monolith, clean-cap grout, concrete roof, and closure cap above (see Figure 3.2-10 and Figure 3.2-6). The particle densities, total porosities, and saturations used in Benchmark Test 2 are presented above in Table 3.2-14 and Table 3.2-15. The Henry's Law Constants are presented in Table 3.2-20. For the effective air diffusion coefficients, instead of using Equation 3-3, default effective air diffusion coefficients were specified based on the material-specific reference (Rn-222) diffusion coefficient (see values from Table 13 of SRNL-STI-2008-00447). Sorption in the solid phase was not considered. The peak results are presented in Table A-1 and the time histories of the releases for C-14, H-3, Cl-36, and Se-79 are presented in Figures A-3, A-4, A-5, and A-6, respectively. The results for all other radionuclides considered were below the GoldSim threshold for non-zero results.

Table A-1: Peak Radionuclide Releases to the Atmosphere and Time of Peak Release for Benchmark Tests 2 and 3

Radionuclides	SDFAPR Model Release (1/yr)[a]	Peak Release Time (years)	PORFLOW Model Release (1/yr)	Peak Release Time (years)
C-14	4.75E-08	144	4.27E-08	147
Cl-36	2.36E-21	217	2.12E-21	302
H-3	2.89E-07	15	2.97E-07	10
I-129	0.0E+00	N/A	0.0E+00	N/A
Rn-222[b]	4.27E-20	1.5	2.16E-20	1
Sb-125	0.0E+00	N/A	0.0E+00	N/A
Sb-126	0.0E+00	N/A	0.0E+00	N/A
Se-79	4.70E-10	311	4.24E-10	314
Sn-126	0.0E+00	N/A	0.0E+00	N/A
Tc-99	0.0E+00	N/A	0.0E+00	N/A

[a] Data taken from SaltstonePA_Air&Radon_PathwayModel_V1.005_run4PFe.gsm.

[b] Data for Rn-222 is taken from Air&Radon_PathwayModel_V1.005_run4PFdCi2Ra_work_satz_10ka.gsm.

Figure A-3: Comparison of SDFAPR and PORFLOW Model Normalized C-14 Releases from a 150-foot Diameter SDU

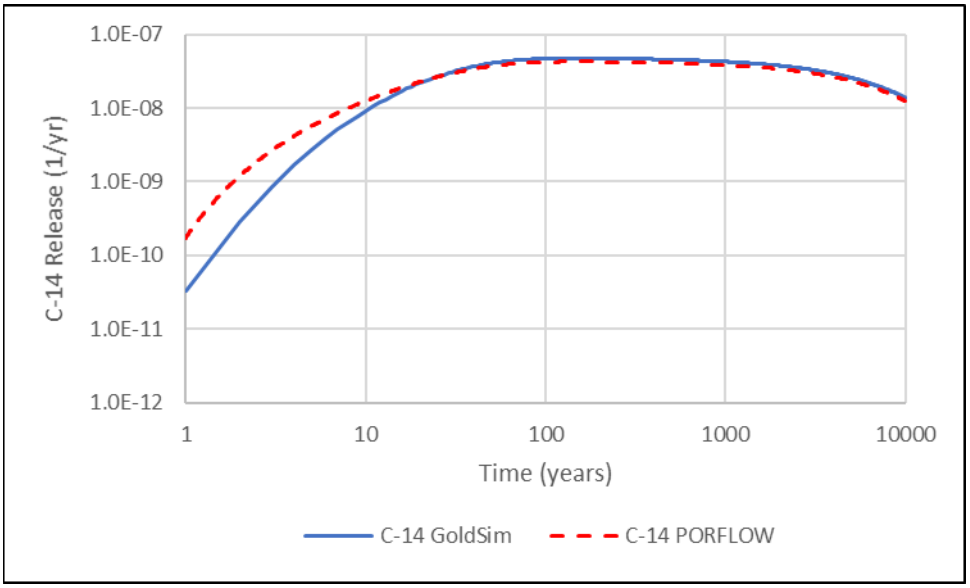

Data taken from SaltstonePA_Air&Radon_PathwayModel_V1.005_run4PFe.gsm.

Figure A-4: Comparison of SDFAPR and PORFLOW Model Normalized H-3 Releases from a 150-foot Diameter SDU

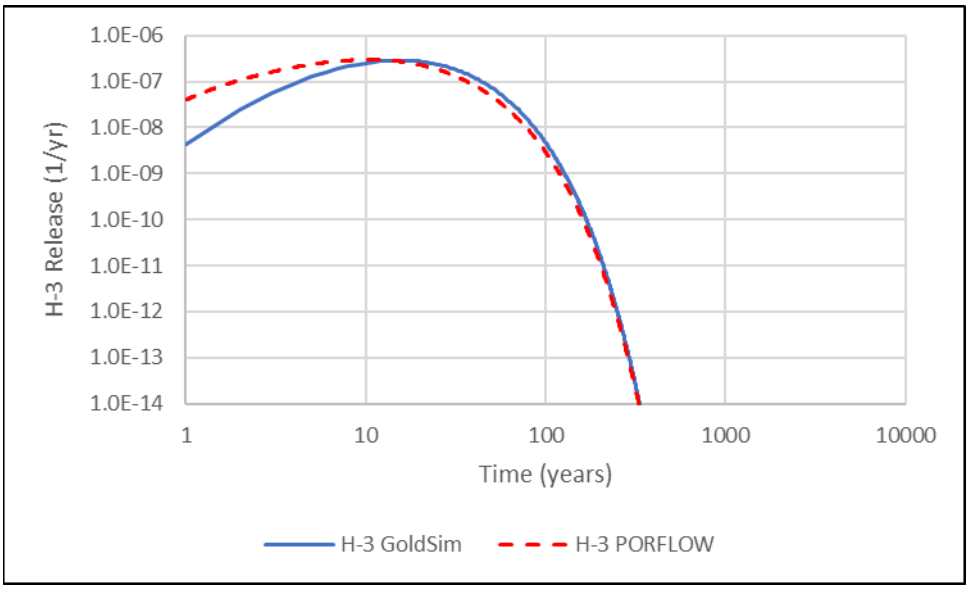

Data taken from SaltstonePA_Air&Radon_PathwayModel_V1.005_run4PFe.gsm.

Figure A-5: Comparison of SDFAPR and PORFLOW Model Normalized Cl-36 Releases from a 150-foot Diameter SDU

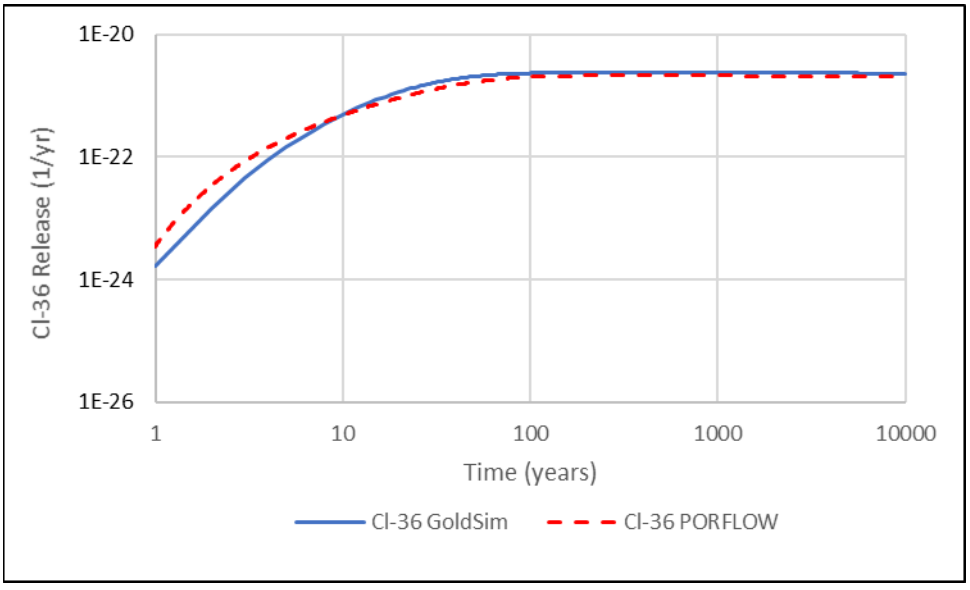

Data taken from SaltstonePA_Air&Radon_PathwayModel_V1.005_run4PFe.gsm.

Figure A-6: Comparison of SDFAPR and PORFLOW Model Normalized Se-79 Releases from a 150-foot Diameter SDU

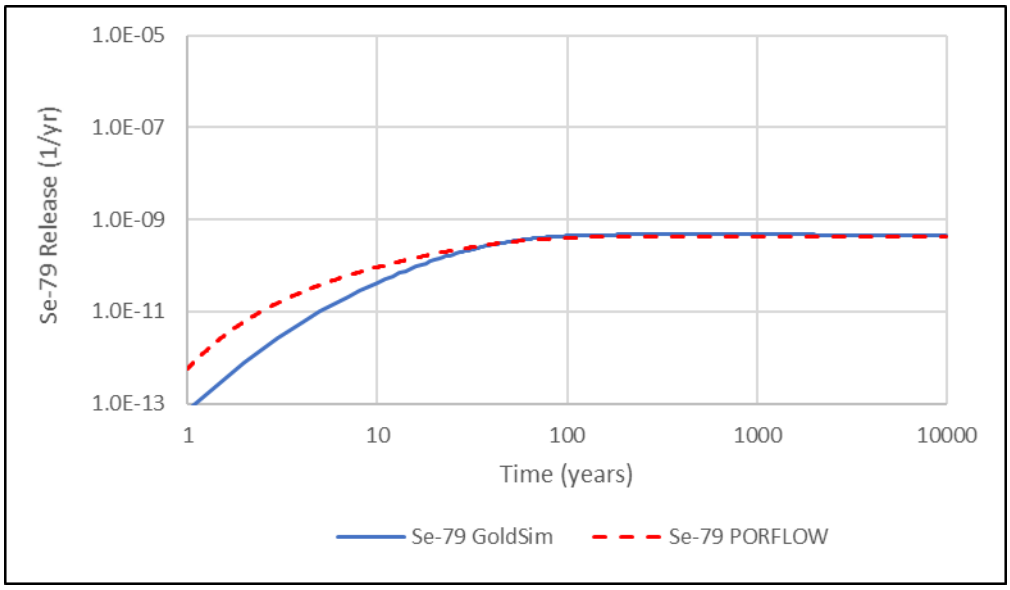

Data taken from SaltstonePA_Air&Radon_PathwayModel_V1.005_run4PFe.gsm.

Benchmark Test 3

Benchmark Test 3 is based on the air pathway model results presented in Section 3.3 of SRNL-STI-2008-00447. The original simulations described in SRNL-STI-2008-00447 assumed an emanation coefficient of 0.25 reflecting the fraction of ingrowth generated Rn-222 escaping the soil particles and entering the void (unsaturated portion of) pore space. The influence of the emanation factor is reproduced by using an initial source of 0.25 Ci for each parent product. The particle densities, total porosities, average saturations, and air-filled porosities used in Benchmark Test 3 are presented above in Table 3.2-14 and Table 3.2-15. For the effective air diffusion coefficients, instead of using Equation 3-3, default effective air diffusion coefficients were specified based on the material-specific reference (Rn-222) diffusion coefficient (see values from Table 13 of SRNL-STI-2008-00447. For consistency with the simulations described in SRNL-STI-2008-00447, the Ra-226 inventory is assumed to reside in the unsaturated portion of the saltstone monolith pore space but is not subject to diffusive transport. This simplification, which also represents a conservative assumption, negates the influence of the Henry's Law Constants. The peak results for release from Ra-226 generated ingrowth is presented in Table A-1. The time histories of the releases for Rn-222, generated by ingrowth from Ra-226, and Th-230, are presented in Figure A-7 and A-8, respectively. Note that the SDFAPR Model results are a factor of 2 times greater than the PORFLOW model results. This difference seems to reflect differences in the manner in which material parameter changes are handled at zonal boundaries in the two models.

Figure A-7: Comparison of SDFAPR and PORFLOW Model Rn-222 Releases as a Daughter Product of Ra-226

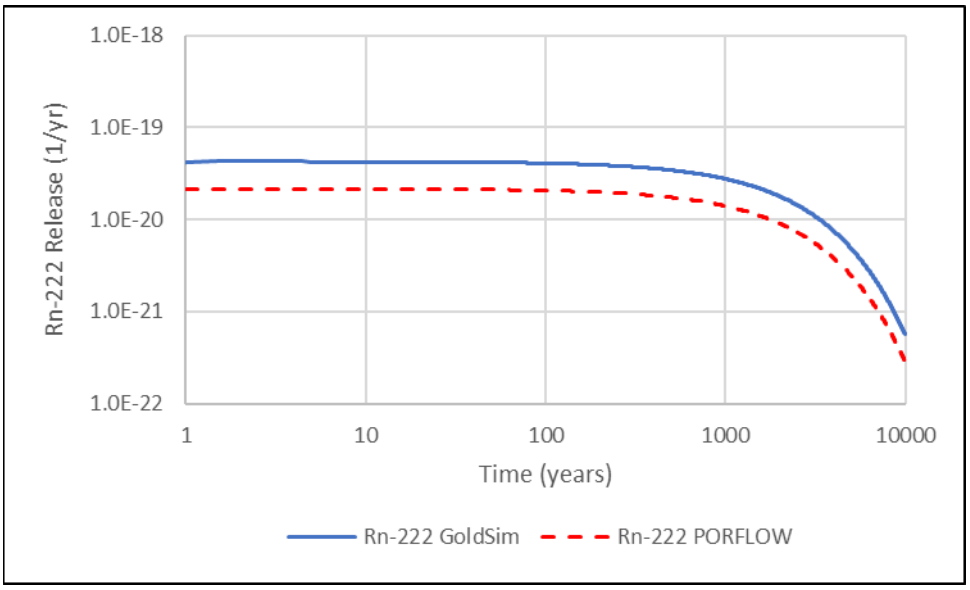

SaltstonePA_Air&Radon_PathwayModel_V1.005_run4PFdCi2Ra_work_satz_10ka.gsm.

Figure A-8: Comparison of SDFAPR and PORFLOW Model Rn-222 Releases as a Daughter Product of Th-230

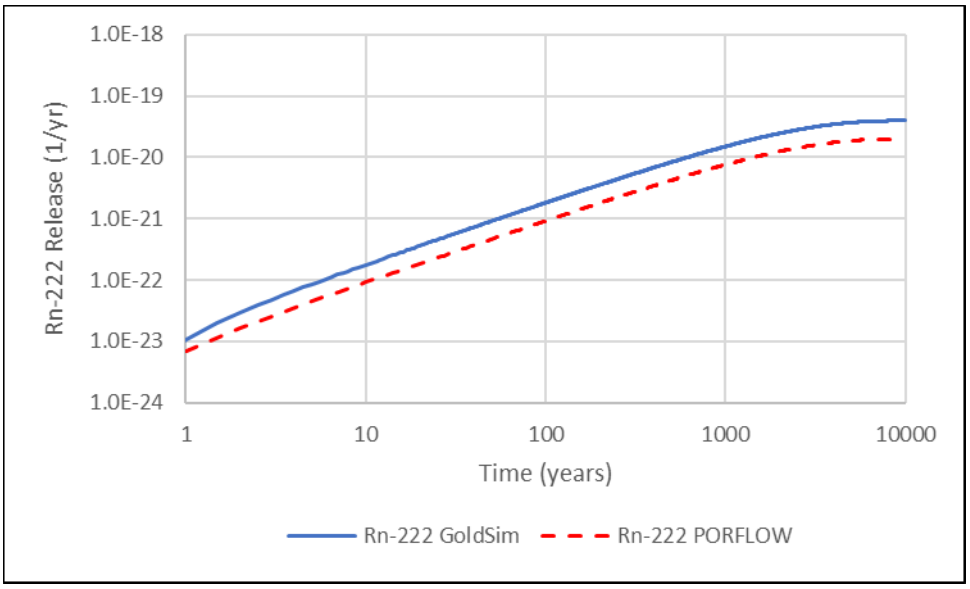

SaltstonePA_Air&Radon_PathwayModel_V1.005_run4PFdCi2Th_work_satz_10ka.gsm.